DECIPHERING THE MECHANISM OF ADULT REPRODUCTIVE DIAPAUSE IN *C. ELEGANS*

by

Jennifer Chen Hei Mak

DECIPHERING THE MECHANISM OF ADULT REPRODUCTIVE DIAPAUSE IN *C. ELEGANS*

Inaugural-Dissertation

zur

Erlangung des Doktorgrades

der Mathematisch-Naturwissenschaftlichen Fakultät

der Universität zu Köln

vorgelegt von

JENNIFER CHEN HEI MAK

aus

Birmingham, UK

Koeln, 2020

Berichterstatter: Prof. Dr. Adam Antebi

Prof. Dr. Thorsten Hoppe

Tag der mündlichen Prüfung: November 2020

1 CONTENTS

2 ABSTRACT

The discovery of novel longevity genes, through the use of model organisms has revealed different conserved molecular pathways involved in the ageing process. RNAi or mutagenesis based screens are powerful tools however both possess limitations. To ease the challenge of mutagenesis screens we incorporated ARD as tool to allow direct selection of longevity mutants. Starvation conditions encountered at the late larval stage of wild type *C. elegans* induces ARD. This delays reproduction and extends the lifespan compared to animals grown in *ad libitum* (AL) conditions, to survive more than 80 days without food. Known longevity mutants displayed additive ARD lifespan extension, therefore, we hypothesised the selection of longevity mutants through an ARD mutagenesis screen would also show longevity in AL conditions. This allowed us to directly select for longevity mutants. We performed four different screens and obtained longevity mutants through this method. However, we discovered the method requires optimisation to obtain a higher number of longevity mutants with more robust phenotypes to discover novel longevity genes.

Upon re-evaluation, we observed a high number of our mutants were long lived under ARD and decided to focus on deciphering the mechanism driving ARD longevity. Since previous work from our laboratory discovered signalling pathways known to regulate longevity are additive to ARD lifespan, this suggests an independent mechanism for survival. We discovered mutants of *upp-1*, encoding uridine phosphorylase, to extend ARD lifespan as well as improve recovery from ARD. *upp-1* is a key regulator of pyrimidine metabolism, catalysing the conversion of uridine to uracil and ribose phosphate. In *C. elegans*, *upp-1* exhibits uridine and thymine phosphorylase activity. We performed metabolomic analysis of *upp-1* mutants after 10 days of ARD and discovered elevated levels of uridine and thymine compared to wild type. Interestingly, supplementation of thymine increased ARD lifespan in wild type animals but not *upp-1* mutants, revealing that thymine enhanced ARD survival

through a similar mechanism as *upp-1* mutants. Altogether, we discovered a role for pyrimidine metabolism in regulated ARD longevity.

Our laboratory recently identified HLH-30/TFEB as a master regulator of ARD. *hlh-30* mutants drastically reduces ARD lifespan, depletes fat stores, rapidly reduces body length, reduces oxygen consumption and fails to recover from ARD upon refeeding. This reveals HLH-30 to be essential for regulating ARD survival, morphogenesis and recovery. To investigate the mechanism by which HLH-30 modulates ARD survival, we performed an unbiased suppressor screen to identify mutants rescuing *hlh-30* ARD shortevity. We discovered mutations on *daf-1* (TGF-β receptor subtype 1 of the TGF-β pathway) and *pdk-1* (phosphoinositide dependant protein kinase of the IIS pathway) to not only increase *hlh-30* ARD lifespan but also prevented the rapid body shrinkage and decreased fat content of *hlh-30* mutants in ARD. We also discovered other components of these pathways, *daf-7* (TGF-β ligand) and *daf-2* (insulin receptor) to show similar effects to *daf-1* and *pdk-1* respectively. We performed a second screen and discovered other components of the TGF-β pathway, *daf-3*, further validating our first screen, as well as some new interesting candidates such as *mxl-2*, part of the Myc superfamily, *let-363*, the *C. elegans* orthologue of mammalian mTOR, and *ceh-60*, a homeodomain transcription factor. Taken together, these results suggest a role of the TGF-β pathway in regulating *hlh-30* ARD longevity and survival.

3 ABBREVIATIONS

ADPr	polyADP-ribose
AL	ad libitum
AMPK	adenosine monophosphate kinase
ARD	adult reproductive diapause
ASI	amphid neurons, single
BODIPY	DIPYrromethene BOron Difluoride
CGC	C. elegans genomic centre
cGMP	cyclic guanosine monophosphate
CR	calorie restriction
CRISPR	clustered regularly interspace short palindromic repeats
CYP450	cytochrome P450
DA	dafachronic acid
DAF	abnormal dauer formation
DEGs	differentially expressed genes
DNA	deoxyribonucleic acid
ER	endoplasmic reticulum
EMS	ethyl methanesulfonate
FOXO	forkhead box class O
5-FU	5-fluorouracil
FUDR	5-fluorodeoxyuridine
GFP	green fluorescent protein
GO	gene ontology
GPCR	G-protein couple receptor
HIF	hypoxia inducible factor
HLH-30	helix-loop-helix-30
IGF-1	Insulin-like growth factor 1
IIS	insulin/insulin-like growth factor 1 signalling
ILPs	insulin like peptides
InR	insulin receptor
KEGG	Kyoto Encyclopedia of Genes and Genomes
LBD	ligand binding domain
MML	Myc and Mondo-Like
MXL	max-like
NAD	nicotinamide adenine dinucleotide
NGM	nematode growth media
NHR	nuclear hormone receptor
NMN	nicotinamide mononucleotide
NPC	Niemann-Pick C
NR	nicotinamide riboside
PAR	poly (ADR-ribose)
PARP	PAR polymerases

PC	principle component
PCR	polymerase chain reaction
PI3K	phosphoinositide 3-kinase
PIP3	phosphatidylinositol 3,4,5-trisphosphate
PTEN	phosphatase and tensin homologue
qPCR	quantitative polymerase chain reaction
RAGA	(RAs-related GTP-binding protein A
RNA	ribonucleic acid
RNAi	RNA interference
S6K	S6 kinase
SNP	single nucleotide polymorphism
TFEB	Transcription factor EB
TGF-β	transforming growth factor-β
TOR	target of rapamycin
7TM	7 transmembrane
WT	wild type

4 INTRODUCTION

Hallmarks of ageing

Ageing is the time dependant decline of physiological functions vital for survival leading to diseases, such as cancer, neurodegenerative diseases and cardiovascular disorders. The curiosity in ageing has baffled the scientific community, however research within the field has excelled since the isolation of the first long-lived strains in *Caenorhabditis elegans* (*C. elegans*) (Klass, 1983). This research has led to the discovery that the rate of ageing is determined, to some extent, by conserved genetic pathways and biological processes.

Nine cellular and molecular hallmarks of ageing have been categorised that contribute to an ageing phenotype: genomic instability, telomere attrition, epigenetic alterations, loss of proteostasis, deregulated nutrient sensing, mitochondrial dysfunction, cellular senescence, stem cell exhaustion and altered intercellular communication (López-Otín et al., 2013). López-Otín et al clusters the hallmarks into three different groups: primary hallmarks, antagonised hallmarks and integrative hallmarks. The primary hallmarks determine negative factors leading to cellular damage, including genomic instability and telomere attrition. Antagonistic hallmarks of ageing at low levels alleviate damage, however at higher levels, become detrimental to the organism. These include mitochondrial dysfunction and cellular senescence. Integrative hallmarks are responsible for the functional decline in ageing, directly affecting tissue homeostasis and function. These comprise of stem cell exhaustion and altered intercellular communication.

Improved understanding of the molecular pathways involved in the ageing process will aid to establish better interventions for age related diseases where the main challenge is to discover pharmacological targets with minimal side effects to improve human health during ageing. Ageing research has been conducted in many different model organisms from yeast to apes however; the small nematode *C. elegans* has proven to be a powerful model organism in ageing research.

4.2 *C. elegans* as a model organism for ageing research

Since the introduction of the nematode, *C. elegans*, for genetic studies in 1965 by Sydney Brenner, the model has become a beneficial tool in diverse fields of research, ranging from neuroscience to ecotoxicology to ageing (Brenner, 1974). The ease and versatility of *C. elegans* has led to several breakthroughs in biomedical science, including the use of green fluorescent protein as a protein marker and the discovery of RNA interference, which has aided the discovery of characterised genes and signalling pathways that regulate longevity. Their small size, short lifespan (~3 weeks) when cultured at 20^{o}C and well-established genetic tools, makes *C. elegans* an ideal model organism for ageing research.

Furthermore, this transparent nematode, made up of 959 somatic cells gives them an advantage towards extensive microscopic studies. The annotation of the *C. elegans* genome (*C. elegans* sequencing consortium, 1998) has also revealed 35% homology with *Homo Sapiens* making them ideal for studying conserved pathways.

This free-living, self-fertilising hermaphrodite nematode is optimal for chemical mutagenesis screens to identify candidate genes in an unbiased manner. This method was used in *C. elegans* to isolate the first long lived mutants, mostly associated with reduced calorie intake (Klass, 1983). Mutants from this screen underwent further experimentation to identify the long-lived mutant *age-1* (Friedman & Thomas, 1987). Subsequent genetic studies then defined the insulin/insulin-like growth factor 1 signalling (IIS) pathway as the first lifespan regulating pathway (C. Kenyon, 2011).

Another major advantage of using *C. elegans* is the well-established RNAi library, where knockdown of a specific gene by feeding double stranded RNA expressing bacteria (Boutros & Ahringer, 2008), making *C. elegans* the ideal tool to conduct large scale RNAi screens. Additionally, they are a suitable model for drug screenings to identify lifespan-extending compounds, and for external interventions such as stress resistance and caloric restriction. The low cost and ease of maintenance and handling, allow these animals to be propagated on a

large scale. Another advantage is the ability to freeze *C. elegans* in glycerol, aiding large scale storage (Brenner, 1974) which has led to a large, valuable library of mutant strains (CGC, NBRP). To summarise, the short lifespan, highly conserved genome and the availability for easy genetic and external manipulations, has allowed *C. elegans* to become a valuable organism to study ageing and age-related diseases.

4.3 Lifespan regulating genes and pathways in *C elegans*

Research in different model organisms have highlighted a number of genetics factors, vital for regulating the ageing process, which integrate into different conserved molecular pathways influencing longevity. These include the insulin/IGF-1, TOR and germ line signalling pathways, which control many crucial processes such as development, metabolism, reproduction and stress resistance.

4.3.1 Insulin/IGF-1 signalling (IIS)

Genes involved in this pathway were the first to be implicated in lifespan regulation in *C. elegans*, with the identification of *age-1* and *daf-2* genes, the orthologues of mammalian phosphoinositide 3-kinase (PI3K) and the insulin/IGF-1 receptor (InR) respectively, where mutations in these genes doubles the lifespan (Friedman & Thomas, 1987; C. Kenyon et al., 1993). Subsequent studies in *Drosophila melanogaster* (Tatar 2001) and *Mus musculus* (Selman 2008) have shown conserved functions of this pathway in regulating longevity. Human studies researching genetic variations in centenarians may also link insulin signalling and longevity in humans (Flachsbart et al., 2009; Willcox et al., 2008).

Ligand binding to the DAF-2 initiates the canonical pathway, activating a series of phosphorylation events triggering several kinases such as AGE-1/PI3K, 3-phosphatidyinositide-dependant kinase 1(PDK-1), AKT-1/2 and serine/threonine-protein kinase (SGK-1). This cascade ultimately leads to the phosphorylation and inactivation of DAF-16, a FOXO transcription factor, preventing its nuclear translocation and blocking the transcription of target

genes (R. Y. N. Lee et al., 2001; K. Lin et al., 2001; Paradis et al., 1999; Paradis & Ruvkun, 1998). Reduced insulin signalling, for example by mutations in *daf-2*, relieves the phosphorylation of *daf-16* allowing translocation into the nucleus thereby inducing the expression of downstream target genes, promoting stress resistance and longevity (C. T. Murphy et al., 2003). Evidence has shown *daf-16* plays a central role in lifespan extension, however evidence suggests it does not act alone. Firstly, sole overexpression of DAF-16 in wild type animals only leads to a mild lifespan extension (Henderson & Johnson, 2001). Furthermore, inducing nuclear localisation of DAF-16 is also not sufficient to extend lifespan (K. Lin et al., 2001). Lastly, the DAF-16-binding element (Furuyama et al., 2000) is present in the 5kb upstream region of 78% of C. elegans genes, however only few of these genes are activated in young adult animals (C. T. Murphy et al., 2003). Therefore, other factors must be involved with DAF-16 for lifespan extension. There are several mechanisms encouraging DAF-16 nuclear localisation. The overexpression of kinases, JNK-1 (the *C. elegans* homolog of c-Jun N-terminal kinase) and CST-1 (the *C. elegans* homolog of mammalian ste20-like kinase (MST)) have shown *daf-16* dependent lifespan extension (Lehtinen et al., 2006; Oh et al., 2005), suggesting their influence with *daf-16* activity. Components of the ubiquitin proteasome system has also shown to regulate DAF-16 activity. RLE-1, a E3 ubiquitin ligase, catalyses ubiquitination of DAF-16/FOXO to target it for degradation (Wensheng Li et al., 2007). The *rle-1* loss of function mutant extends lifespan (Wensheng Li et al., 2007) while the gene encoding deubiquitylase, *math-33*, suppresses *daf-2* lifespan extension (Heimbucher et al., 2015). Mutations on the gene encoding the ligand for the transforming growth factor-β (TGF-β) family, *daf-7*, leading to lifespan extension, is dependent on DAF-16, suggesting the TGF-β pathway operates as an upstream regulator of IIS pathway activity (Shaw et al., 2007). Mutations in other transcription factors such as, *hsf-1* (*C. elegans* homolog of heat-shock transcription factor) and *skn-1* (*C. elegans* homolog of nuclear respiration factor 2 (Nrf2)) suppresses *daf-2* lifespan extension suggesting a co-regulatory function with *daf-16* (Hsu et al., 2003; Tullet et al., 2008). Reduced insulin

signalling triggers SKN-1 nuclear localisation, allowing activation of target genes required for stress resistance and longevity independent of *daf-16* (Tullet et al., 2008). Identification of *daf-16* target genes have highlighted genes involved in several cellular processes such as immunity, proteostasis, metabolism and oxidative stress (Halaschek-Wiener et al., 2005; McElwee et al., 2003; C. T. Murphy et al., 2003). Examples of these genes are heat shock proteins, cytochrome P450 enzymes and superoxide dismutase. IIS in specific tissues has also been implicated in regulating lifespan. Intestinal or neuronal expression of *daf-16* can extend the lifespan of the short lived mutant *daf-2;daf-16* suggesting *daf-16* acts cell non-autonomous to modulate intercellular signals (C. T. Murphy et al., 2003).

A recent study has shown *daf-16* acts in combination with *hlh-30*/TFEB, forming a complex under harmful conditions to promote longevity and resistance to oxidative stress. Under stress conditions, both transcription factors translocate to the nucleus, forming a complex to co-regulate specific target gene sets, promoting optimal survival (X. X. Lin et al., 2018).

4.3.2 TOR signalling and Calorie Restriction

TOR (target of rapamycin), a serine/threonine kinase, is part of a nutrient sensing pathway which regulates growth, reproduction, motility and survival in response to nutrient availability (Wullschleger et al., 2006). TOR inhibition extends lifespan across a wide range of species from yeast, to mice (Harrison et al., 2009; Kaeberlein et al., 2005; Kapahi et al., 2004; Sheaffer et al., 2008; Tibor Vellai et al., 2003). Under sufficient nutrient conditions, TOR is activated leading to growth stimulation and inhibition of salvage pathways, such as autophagy (Wullschleger et al., 2006). Therefore, reducing TOR activity is speculated to mirror the effects of dietary restriction conditions. Following this, reducing TOR activity by RNAi of mTOR/*let-363* or *daf-15/raptor* (mTORC1 component) leads also to longevity which is independent of *daf-16* (Jia et al., 2004; Tibor Vellai et al., 2003). Reduced TOR signalling leads to reduced phosphorylation of S6 kinase (S6K) or activation of the translational inhibitor, 4E BP, resulting in decreased protein translation (Meijer & Codogno, 2008; T.

Vellai, 2009). The longevity effect is mediated by PHA-4 (a FOXA transcription factor), which is a regulator of autophagy (Sheaffer et al., 2008). Lifespan extension by rapamycin, a TOR inhibitor, is also dependent on autophagy genes (Bjedov et al., 2010).

Lifespan extension by rapamycin is not the only intervention that spans across many species. Longevity by calorie restriction (CR) also extends throughout many model organisms from *C. elegans* to *Drosophilia melanogaster* and *Mus Musculus* (R. M. Anderson et al., 2009; Lakowski & Hekimi, 1998; Pletcher et al., 2002). Evidence suggest these interventions are comparable since they display similar physiological effects, plus, TOR inhibition fails to increase the lifespan extension from CR (Kaeberlein & Kapahi, 2009) . Additionally, the genetic CR model in *C. elegans*, *eat-2* mutants, which displays lower pharyngeal pumping, extends lifespan by reducing TOR signalling (Lakowski & Hekimi, 1998). Moreover, lifespan extension of *eat-2* mutants was not further increased by inhibiting TOR. Lifespan extension in *eat-2* mutants is also dependent on the transcription factor *pha-4*, which is also essential for the longevity demonstrated by TOR inhibition as previously described (Panowski et al., 2007).

A transcriptional factor connecting TOR and CR is the hypoxia inducible factor, HIF-1. Studies in mammalian and Drosophila cells have implicated HIF-1 as a target of the TOR pathway (Bernardi et al., 2006; Dekanty et al., 2005; Hui et al., 2006; Treins et al., 2002). In *C. elegans*, HIF-1 normally functions in response to oxygen deprivation; however, it also plays a role in modulating lifespan extension by CR in *C. elegans* (D. Chen et al., 2009). Animals deficient in HIF-1 exhibit a longevity phenotype under nutrient rich conditions, where genetic epistasis experiments have proven it operates downstream of RSKS-1/S6 kinase to modulate lifespan (D. Chen et al., 2009). Under normoxia, HIF-1 is hydrolated by the PH superfamily of dioxygenase encoded by *egl-9*. Mutations in *egl-9* increases HIF-1 activity and reduces the lifespan extension under CR (D. Chen et al., 2009).

Another factor linking longevity by TOR and CR is AMP-activated protein kinase (AMPK). Activation of AMPK occurs under low energy availability, such as starvation or CR conditions, and senses the ratio of AMP to ATP. Genetically overexpressing AMPK, mirrors starvation conditions, which leads to lifespan extension in *C. elegans* (Apfeld et al., 2004). Pharmacologically activating AMPK by the drug metformin has also shown a similar longevity effect (Onken & Driscoll, 2010).

Knockdown of several ribosomal protein genes and translation initiation factors results in lifespan extension, as well as, mutations on the ribosomal protein S6 kinase/RSKS-1. In *C. elegans*, *rsks-1* mutants displayed increased AAK-2 phosphorylation, implying, similar to mice studies, loss of S6 kinases increased AMPK activity (Selman et al., 2009). This further solidifies similar mechanisms between TOR and CR for lifespan extension. Furthermore, AMPK modulates longevity through the post-translational modification of CRTC-1, the worm homologue of CREB- regulated transcriptional coactivators (Mair et al., 2011).

4.3.3 Germline signalling

In *C. elegans*, germline signalling is another pathway modulating ageing. Laser ablation to remove the germline cells increases lifespan by 60%, however complete removal of the gonad (both the germline and somatic gonad) abolishes this longevity suggesting opposing signals from the germline and somatic gonad (Hsin & Kenyon, 1999). This longevity can also be achieved genetically in glp-1/Notch receptor mutants, resulting in the lack of germ cells (Arantes-Oliveira et al., 2002).

Components of the steroid hormone-signalling pathway are closely associated with germline longevity. The nuclear hormone receptor, DAF-12, which responds to a steroid hormone called dafachronic acid (DA), is a key regulator of germline-less longevity (Hsin & Kenyon, 1999). DAF-9/cytochrome P450 and DAF-36/Rieske oxygenase, regulates DAF-12 activity and are also both essential for the lifespan extension of germline absent animals (Birgit Gerisch et al., 2001, 2007; Wollam et al., 2011). Interestingly, supplementation of DA to

animals lacking both the germline and somatic gonad, restored the expression of DAF-12 and their lifespan was increased, suggesting a role of the somatic gonad to promote longevity through the steroid signalling pathway (Yamawaki et al., 2010). However, tissue specific production of DA is not vital for the longevity since DAF-9 overexpression in other tissues was able to increase the lifespan in animals lacking a full gonad (Yamawaki et al., 2010).

DAF-16, a key component of the IIS, is a regulator of germline-less induced longevity, linking these two longevity pathways. *daf-12* and *daf-9* regulates the nuclear localisation of DAF-16 in germline-deficient animals (Berman & Kenyon, 2006; Birgit Gerisch et al., 2007). DAF-12 target genes include *mir-84* and *mir-241*, where increased expression of these genes stimulates DAF-16 nuclear localisation and activation by downregulating two inhibitors of DAF-16, AKT-1 and LIN-14 (Shen et al., 2012).

Other transcription factors in addition of DAF-12 and DAF-16 are required for germline-less longevity, including NHR-80 and PHA-4 (Goudeau et al., 2011; Lapierre et al., 2011). Lifespan extension occurs overexpressing *nhr-80* in germline-less animals in a DAF-16 independent manner, however relies on the presence of DAF-12 (Goudeau et al., 2011). A key target of NHR-80 is FAT-6, a gene encoding an acyl-CoA desaturase, which is vital to promote germline-deficient longevity, linking fatty acid desaturation and longevity in germline-less animals (Goudeau et al., 2011). Germline-loss induces autophagy through PHA-4, which is required to extend lifespan. TOR expression in reduced in *glp-1* mutants, inducing *lipl-4* (a gene encoding a triglyceride lipase) expression, which is dependent on PHA-4 and other autophagy genes. Reciprocally, *lipl-4* is essential for autophagy induction (Lapierre et al., 2011). This implies TOR may function upstream of autophagy and *lipl-4* in germline-less animals to regulate lifespan, as well as, underlining a potential role of fatty acids in modulating ageing.

4.3.4 Convergent mechanisms for longevity

The signalling pathways regulating longevity highlighted above operate independent of each other, however recent reports have underlined several factors involved in the crosstalk between these pathways (Figure 1). One such factor is the mammalian transcription factor EB (TFEB), shown to regulate multiple genes in the autophagy process (Settembre et al., 2011). The predicted TFEB orthologue in *C. elegans* is HLH-30, which regulates the expression of multiple autophagy-related and lysosomal genes (Settembre et al., 2011). It has been implicated as a key player for lifespan extension across several longevity models, such as, TOR inhibition, germline removal, reduced IIS and dietary restriction (Lapierre et al., 2013), suggesting a central role for HLH-30 in determining lifespan in *C. elegans*. HLH-30 becomes nuclear localised across these longevity models to drive the expression of its downstream targets for autophagy and lysosomal processes. It was also shown that overexpression of HLH-30 can also extend the lifespan of *C. elegans* (Lapierre et al., 2013). The Myc-like HLH transcription factor network consisting of Mondo/Max-like complex is another factor involved in the convergent mechanisms regulating *C. elegans* lifespan. A suppressor screen to identify factors regulating germline-mediated longevity identified the Myc superfamily members MML-1(Myc/Mondo-like) and MXL-2(Max,Max-like) as novel regulators of the gonadal longevity pathway, as well as, mediating longevity in other known pathways, such as, reduced TOR, IIS, mitochondrial function and calorie restriction (Nakamura et al., 2016). MML-1 and MXL-2 function to reduce TOR signalling, stimulating autophagy and HLH-30 activity in the nucleus (Nakamura et al., 2016).

The nucleolus is another convergent point of regulating major longevity pathways across species. A suppressor screen to unravel the regulators of longevity induced by dietary restriction identified the nucleolar factor NCL-1 (Tiku et al., 2016). NCL-1 also mediates lifespan of other known longevity models such as reduced IIS, TOR, mitochondrial and gonadal longevity, where overexpression in a wild type background was also sufficient to increase lifespan

(Tiku et al., 2016). NCL-1 regulates nucleolar size, where *ncl-1* mutants have enlarged nucleoi compared to wild type (Tiku et al., 2016). Strikingly, multiple longevity mutants displayed reduced nucleolar size compared to wild type, reduced ribosomal biogenesis and decreased levels of the nucleolar marker, FIB-1, a protein involved in regulation and maturation of rRNA (Tiku et al., 2016). Intriguingly, the effects from the loss of NCL-1 can be reversed further enhancing the use of nucleolar size as a predictive marker for longevity. This marker also hold true as a predictor for life expectancy in higher model organisms (Tiku et al., 2016), further validating the role of convergent factors regulating lifespan across species.

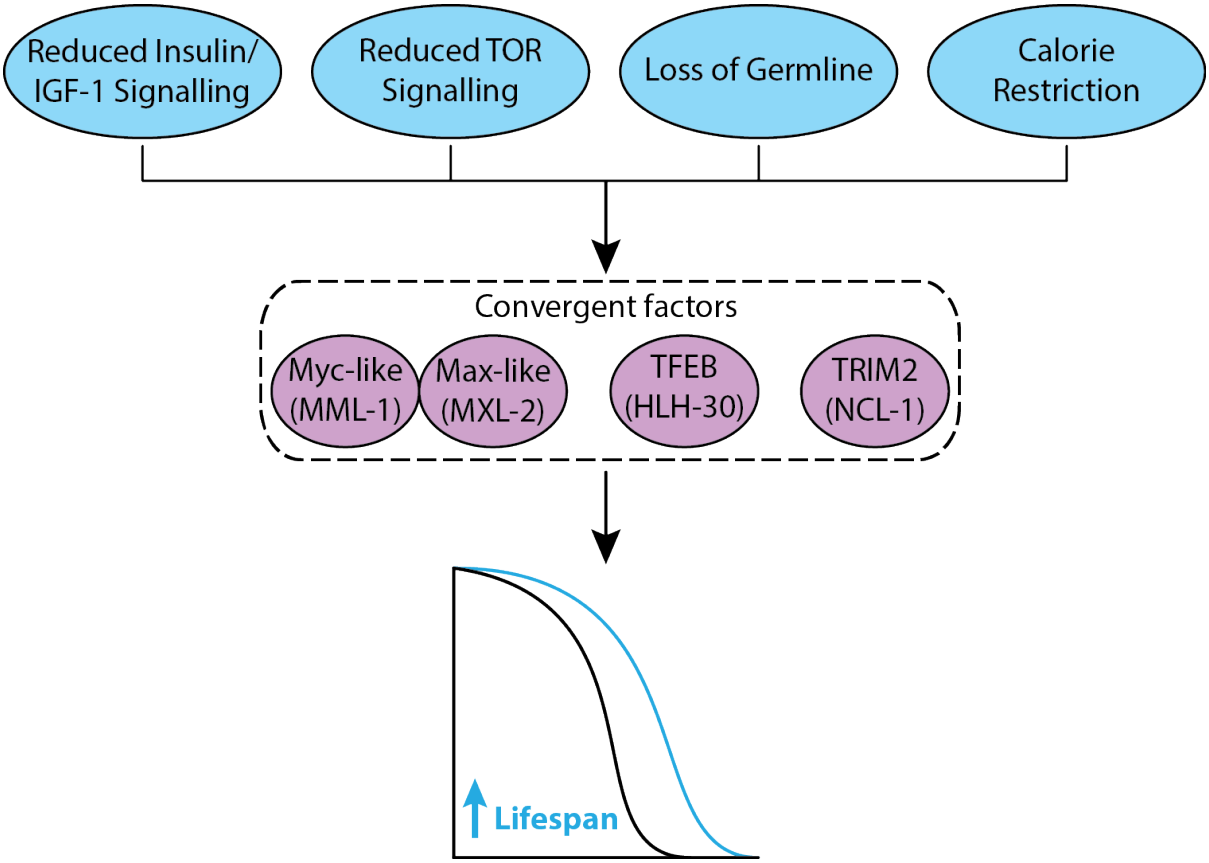

Figure 1. Lifespan regulating signalling pathways and convergent mechanisms of ageing. Several molecular interventions have been discovered to regulate longevity in *C. elegans* including insulin/IGF-1 signalling, TOR signalling, germline and calorie restriction, which converge on factors such as the Mondo/Max-like complex (MML-1/MXL-2), TFEB (HLH-30) and the nucleolar factor, NCL-1, to modulate ageing. Adapted from (Lapierre & Hansen, 2012; Uno & Nishida, 2016).

4.4 Effect of starvation on development

The natural habitat for *C. elegans* is a microbe-rich environment, especially from decomposing plant matter, including rotting fruit and stems (Schulenburg & Félix, 2017). This species-rich microbial community can be the worm's food, become part of the gut microbiome, parasites and pathogens, or even competitors. This nematode often experiences periods of over-population because of the short generation time and rapid growth, limiting the availability of food. This induces the worm's robust response to starvation, involving complex and dynamic processes, dependent on the developmental stage of nutrient deprivation. Other than dauer diapause, the most characterised response, *C. elegans* can also enter L1 arrest, late-larval arrest and adult reproductive diapause (ARD) in times of low nutrient availability (Figure 2).

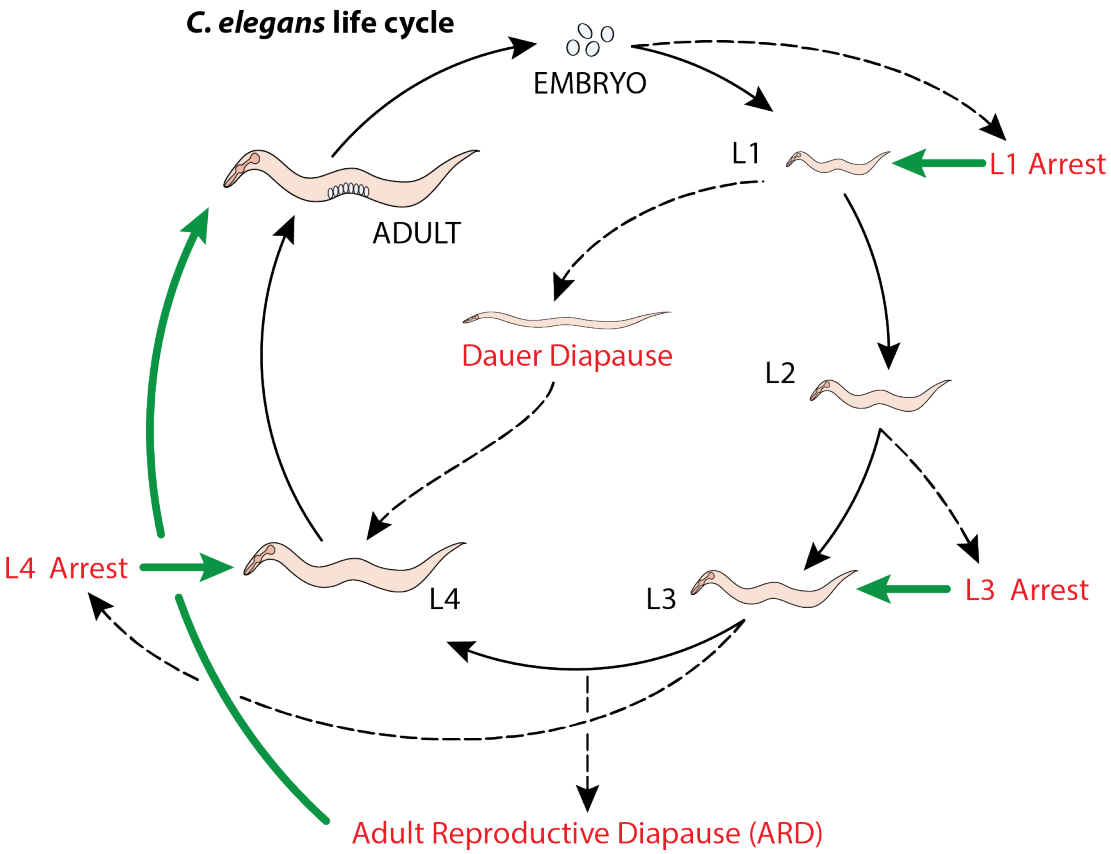

(Figure 2: refer to page 22 for legend)

Figure 2. *C. elegans* starvation response at different developmental time-points. Differential arrest outcomes are dependent upon encountering unfavourable conditions at different larval stages. Under favourable conditions, *C. elegans* develop from eggs through L1 to L4 larval stages before developing into mature adults. Eggs hatching in starvation undergo L1 arrest (Baugh, 2013), while high population density and low nutrient availability in young larvae (L1) induces dauer diapause (Cassada & Russell, 1975). Starvation conditions at the L2 and L3 stages results in late larval arrest (Schindler et al., 2014), while acute starvation in the mid L3 stage induces adult reproductive diapause (ARD) (B. Gerisch et al., 2020). Solid black arrows indicate larval development in favourable (*ad libitum*) conditions. Dotted black arrows indicate induction of diapause in unfavourable conditions with the developmental arrest stage in red. Solid green arrows indicate recovery from the arrest stage by re-introduction to food. Adapted from (Altun & Hall, 2009).

4.4.1 Dauer diapause

R. Cassada and R. Russell first observed the dauer larvae in 1975. They described an arrested developmental stage that forms when young larvae encounter environmental stresses such as overpopulation or starvation (Cassada & Russell, 1975). Dauer larvae are morphologically different to *C. elegans* grown in optimal conditions where they adopt a thicker protective cuticle, a constricted pharynx that ceases to pump, the germline is developmentally arrested and shrinkage of muscle, intestine and hypodermal cells that allows for radial constriction. These changes allow *C elegans* to become increasingly resistance to starvation and other stressors, which aids survival for several months. Specialised behaviours, such as nictation where dauer larvae stand on its tail and waves its head, is exhibited to allow attachment to other animals to promote dispersal (Yang et al., 2020). Encountering a favourable environment, *C. elegans* exit dauer diapause and become reproductive adults.

This reversible alternative stage has since been extensively studied for the regulatory mechanisms governing morphological changes during development. Recently, the identification of genes involved in dauer arrest were discovered in mutants exhibiting abnormal dauer formation (*daf* mutants). They revealed the evolutionarily conversed pathways in insulin signalling, transforming growth

factor-β (TGF-β), guanylyl cyclase and hormonal signalling to be critical in the regulation of dauer arrest.

4.4.1.1 Molecular pathways regulating dauer formation

The molecular mechanisms governing the formation of dauer is understood to operate through four distinct pathways. Firstly, environmental conditions are sensed through the secretion of ascarosides (also known as the dauer pheromone) which indicate population density (A. Ludewig & Schroeder, 2013). This information is conveyed through the conserved DAF-7/TGF-β and DAF-2 insulin-like growth factor receptor pathways (Fielenbach & Antebi, 2008; Hu, 2007; Riddle & Albert, 1997). The outputs from these two signalling pathways converge on the steroid hormonal signalling pathway for bile acid hormone (dafachronic acid (DA)) production to activate the nuclear hormone receptor, DAF-12 (Fielenbach & Antebi, 2008; Hu, 2007). Unfavourable conditions will ultimately results in an unliganded form of DAF-12 to promote dauer development (Schaedel et al., 2012) (Figure 3).

The four distinct pathways regulating dauer formation, guanylyl cyclase pathway, insulin-like signalling, transforming growth factor-β (TGF-β), and steroid hormonal signalling will be explained in more detail below.

4.4.1.1a Guanylyl cyclase pathway

The receptor guanylyl cyclases are vital for sensory processing in *C. elegans*, catalysing the conversion of GTP to cGMP. In *C. elegans*, *daf-11*, encodes the transmembrane guanylyl cyclase (GCY) (Birnby et al., 2000) and *tax-2* and *tax-4* encodes the subunits of a cGMP-gated ion channel (Coburn & Bargmann, 1996; Komatsu et al., 1996). cGMP acts as a second messenger for several chemosensory seven-transmembrane G protein-coupled receptors (7TM GPCRs), to sense environmental conditions for regulating the decision to enter dauer or continue in reproductive development. Sensing of the dauer pheromone is a well-studied example of chemosensory 7TM GPCRs in regulating development through cGMP (A. Ludewig & Schroeder, 2013). *C elegans* constitutively secretes dauer pheromone, consisting of different

ascarosides, allowing *C. elegans* to sense population density, where high concentrations of the pheromone induces dauer formation (Golden & Riddle, 1982). There are several 7TM GPCRs which senses different combinations of dauer inducing ascarosides including SRBC-64, SRBC-66, SRG-36, SRG-37, DAF-37 and DAF-38 (K. Kim et al., 2009; McGrath et al., 2011; Park et al., 2012), which signal through the G_{α} subunits, GPA-2 and GPA-3 (K. Kim et al., 2009). In high dauer pheromone levels, DAF-11 is inhibited by GPA-2 and GPA-3, causing decreased concentrations of cGMP (K. Kim et al., 2009). Mutations inactivating GPA-2 and GPA-3 results in a dauer-defective (Daf-d) phenotype (Zwaal et al., 1997)

Loss of function *daf-11* mutants are dauer-constitutive (Daf-c) and displays defects in chemosensation and olfaction (Vowels & Thomas, 1994). Supplementation of the cGMP analogue 8-bromo-cGMP rescues the Daf-c phenotype of *daf-11* mutants suggesting the Daf-c phenotype is due to reduced cGMP synthesis (Birnby et al., 2000). However, it fails to rescue dauer arrest seen in *tax-4* mutants (Birnby et al., 2000) suggesting TAX-4 is a target of cGMP signalling through DAF-11. Additionally, the transcript levels of antagonistic insulin like peptides in the IIS pathway, *ins-7* and *daf-28*, increases with the supplementation of 8-bromo-cGMP (Hahm et al., 2009)

The weak Daf-c phenotype observed in *tax-4* mutants compared to *daf-11* (Coburn et al., 1998), indicates activation of several downstream modulators by DAF-11 to inhibit dauer arrest. Interestingly, a gain of function mutation on *daf-21*, a gene encoding a HSP90 homolog, has similar phenotypes and patterns of epistasis to *daf-11* (Birnby et al., 2000), proposing an unknown role for Hsp90 in regulating cGMP levels.

Previous reports have indicated that cGMP signalling is upstream of IIS and TGF-β signalling. Firstly, Daf-d mutants, *daf-5* and *daf-16*, part of the TGF-β and IIS signalling respectively, partially suppress the Daf-c phenotype of *daf-11* mutants. (Thomas et al., 1993; Vowels & Thomas, 1992). Secondly, exogenous cGMP rescues the Daf-c phenotype of *daf-11* mutant unlike mutants from the

TGF-β and IIS signalling pathways. Lastly, *daf-11* mutants are defective in expressing *daf-7* in ASI neurons (Murakami et al., 2001) and the insulin-like peptide, *daf-28*, expressed in ASI and ASJ neurons, is downregulated in dauer conditions in *daf-11* mutants (Weiqing Li et al., 2003).

4.4.1.1b Insulin-like signalling pathway

Daf-c and Daf-d mutants were originally isolated from genetic screens performed by the Riddle lab. These mutants defined the Daf-c genes, *daf-2* and *age-1*, and Daf-d gene, *daf-16*. Characterisation of these genes has led the discovery of a conserved insulin-like pathway inhibiting dauer arrest by the activation of DAF-2, the insulin receptor homolog. As previously described, unfavourable conditions decreased IIS signalling leading to DAF-16 nuclear localisation turning on genes for stress resistance, longevity and dauer formation. Additionally, DAF-18/PTEN phosphatase counteracts the activity of AGE-1/PI3K, downregulating the pathway (Gil et al., 1999; Mihaylova et al., 1999; Ogg & Ruvkun, 1998; Rouault et al., 1999). Mosaic and specific tissue rescue studies have shown the non-autonomous function of DAF-2 and AGE-1 to inhibit dauer formation and DAF-2 functions predominately in the nervous system to regulate lifespan and dauer arrest (Apfeld & Kenyon, 1998; Wolkow et al., 2000). However, similar studies have suggested DAF-16, the major target of IIS, displays tissue specific regulation of dauer arrest and lifespan. Intestinal DAF-16 activity has a greater influence on lifespan whereas DAF-16 activity in neurons exhibits stronger control over dauer arrest (Libina et al., 2003).

Additionally, IIS functions temporally to influence the outcome out the pathway. IIS during adulthood has a greater influence on ageing, while during larval development, the pathways regulates dauer arrest (Dillin, Crawford, et al., 2002).

Additional signalling through insulin-like peptides (ILPs) may also regulate dauer arrest. There are 40 ILPs, primarily expressed in neurons, and exhibit functional diversity towards IIS. The most similar to human insulin among these peptides is INS-1. Expressed in ASI neurons, INS-1 is antagonist towards DAF-2 and is

potentially involved in sensing the environmental cues for dauer formation (Fernandes de Abreu et al., 2014; Matsunaga et al., 2012; Pierce et al., 2001). *ins-7* is an agonist of DAF-2, whose activity is repressed by DAF-16, suggesting positive feedback (C. T. Murphy et al., 2003, 2007). Interestingly, mutations on *daf-28*, encoding an insulin-like protein, results in dauer arrest and downregulation of DAF-2 signalling. A *daf-28* GFP transgene, was downregulated upon exposed to dauer pheromone and starvation implying the expression of *daf-28* is regulated by the environmental cues which normally promote dauer formation (Weiqing Li et al., 2003).

Insulin-like molecules can activate components of the TOR pathway to trigger reproductive development (Oldham & Hafen, 2003). *let-363*/TOR and *daf-15*/Raptor mutants show dauer-like larval arrest, implying regulation of dauer diapause by TOR signalling (Jia et al., 2004). Mutants of *let-363* and *daf-15* causes increase fat accumulation and increased lifespan. These phenotypes are epistatic to *daf-16* suggesting LET-363 and DAF-15 function downstream or parallel of DAF-16 to control *C. elegans* development and metabolism (Jia et al., 2004).

4.4.1.1c Transforming Growth Factor-β Signalling Pathway

The TGF-β pathway operate downstream of the guanylyl cyclase pathway to regulate dauer formation. Components of the pathway include DAF-7, a TGF-β homolog (Ren et al., 1996) and DAF-1 and DAF-4 as the type I and type II serine/threonine kinase TGF-β receptors respectively (Estevez et al., 1993; Georgi et al., 1990). DAF-3, DAF-8 and DAF-14 are SMAD transcription factors (Inoue & Thomas, 2000; Patterson et al., 1997); and lastly DAF-5 is a SNO/SKI oncoprotein that binds to DAF-3/SMAD (da Graca et al., 2004; Tewari et al., 2004). Expression of DAF-7/TGF-β is primarily in the ASI amphid neurons (Ren et al., 1996; Schackwitz et al., 1996), while other components of the pathway are widely expressed (da Graca et al., 2004; Gunther et al., 2000; Inoue & Thomas, 2000; Patterson et al., 1997). The dauer pheromone and high temperature inhibits the expression of *daf-7* and promotes dauer formation, while the presence of food reactivates *daf-7* expression and induces recovery

from dauer arrest, suggesting a clear connection with environmental cues (Neal et al., 2015; Ren et al., 1996).

Under favourable conditions, high levels of DAF-7/TGF-β are secreted and bind to the type I and type II receptor kinases, DAF-1 and DAF-4. Receptor activation induces phosphorylation of SMADs, DAF-8 and DAF-14 resulting in their nuclear localisation, where they inhibit the function of DAF-3 and DAF-5, which promote dauer formation. This signalling cascade is downregulated under unfavourable conditions due to reduced DAF-7/TGF-β binding, allowing the DAF-3/DAF-5 complex to induce dauer induction. Several studies have also identified modulators of this pathway outside of its core components (Aoyama et al., 2004; Daniels et al., 2000; Morita et al., 2001; Y. Wang & Levy, 2006).

Interestingly, expressed primarily in the nervous system, *daf-4* and *daf-5* can rescue phenotypes throughout the body indicating downstream components determine dauer induction (da Graca et al., 2004; Inoue & Thomas, 2000). Further evidence has revealed a strong link between the IIS and TGF-β pathways. Gene expression research comparing wild type and TGF-β mutants revealed regulation of genes involved in the IIS and steroid hormone pathway (Liu et al., 2004). The expression profiling also showed regulation in a large group of genes with putative binding sites for DAF-16 (Liu et al., 2004). In addition, *daf-16* mutants partially suppresses the Daf-c phenotype of *daf-7* mutants (Thomas et al., 1993) and becomes nuclear localised (R. Y. N. Lee et al., 2001). The cross talk between TGF-β and IIS also spans further than dauer formation. The life span extension observed in Daf-c TGF-β mutants is dependent on DAF-16, in the presence of 5-fluorodeoxyuridine (FUDR) to decreased premature death by egg retention (Shaw et al., 2007), suggesting TGF-β converges on IIS for survival.

4.4.4.1d Steroid Hormone Pathway

Previous reports through genetic epistasis experiments have shown the insulin-like, TGF-β and cyclic GMP pathways converge on the nuclear hormone receptor, DAF-12, to control the regulation of dauer (Riddle et al., 1981; Thomas

et al., 1993; Vowels & Thomas, 1992). Among dauer formation, DAF-12 is also associated with fat metabolism, developmental timing, gonadal maturation and longevity. Suitable environmental conditions, conveyed through high levels of DAF-2/insulin receptor or DAF-7/TGF-β signalling, stimulate the production of dafachronic acids (DAs). They are synthesised by the cytochrome P450 enzyme, DAF-9, and bind to DAF-12 to promote reproductive development (Butcher, 2017; Fielenbach & Antebi, 2008; Motola et al., 2006; Riddle & Albert, 1997). Unfavourable conditions would leave DAF-12 in the unliganded form, promoting dauer arrest.

Further evidence has implemented DAF-9 and DAF-12 in the regulation of dauer arrest through a steroid hormone pathway. Sterols may act as a substrate of *daf-9* and a ligand of *daf-12* since cholesterol deprivation phenocopies *daf-9* and *daf-12* mutants (Birgit Gerisch et al., 2001). Also since DAF-9 functions in a cell non-autonomous manner to inhibit dauer arrest provides further evidence of a hormonal function (Birgit Gerisch & Antebi, 2004; Mak & Ruvkun, 2004). As previously described above, *daf-9* encodes a cytochrome P450, with similarity to steroid hydroxylases (Birgit Gerisch et al., 2001; Jia et al., 2002), and *daf-12* encodes a nuclear hormone receptor containing a DNA and ligand binding domain with close relationship to vertebrate vitamin D and pregnane-X receptors (Antebi et al., 2000). Null mutants of *daf-9* exhibit a Daf-c phenotype; however recover to sterile, stress resistance and long-lived adults. Mutants of *daf-12* suppresses these phenotypes, suggesting DAF-9 inhibits DAF-12 activity (Birgit Gerisch et al., 2001; Jia et al., 2002). Mutations on the ligand-binding domain of DAF-12 express a Daf-c phenotype, implying insensitivity of these mutants to DAF-9 inhibition, because of their inability for ligand binding (Antebi et al., 2000). Supplementation of DA successfully rescues the dauer and longevity phenotypes observed in *daf-9* mutants, as well as, the Daf-c phenotypes of upstream IIS and TGF-β mutants; however has no effect on the downstream ligand binding domain (LBD) mutants of *daf-12* (Motola et al., 2006). Interactions between co-regulators and DAF-12 aid to mediate the decision for dauer arrest. The homolog of mammalian SHARP corepressor, DIN-1, forms a

complex with DAF-12 to regulate lipid metabolism, longevity and dauer diapause (A. H. Ludewig et al., 2004).

Mutants with enhanced Daf-c phenotypes by cholesterol deprivation may highlight other components of this pathway (J. Li et al., 2004; Ohkura et al., 2003). Another hormone biosynthetic enzyme, DAF-36, a Rieske oxygenase, operates upstream of DAF-9 to synthesise DA (Rottiers et al., 2006). DAF-9 expression occurs in the hypodermis, somatic gonad and the endocrine XXX cells (Birgit Gerisch et al., 2001; Jia et al., 2002; Ohkura et al., 2003), however, expression of DAF-36 is primarily intestinal and is not in the XXX cells (Rottiers et al., 2006) implying transportation of sterol metabolites from tissue and cells expressing DAF-36 to the hypodermis. Niemann-Pick C (NPC) proteins, NCR-1,2, are predicted to be involved in intracellular cholesterol trafficking (Chang et al., 2005). Single mutants of *ncr-1* and *ncr-2* exhibit a weak Daf-c phenotype while the double mutant, *ncr-1;ncr-2* displays a strong Daf-c phenotype (J. Li et al., 2004; Sym et al., 2000) which is rescued by the supplementation of DA (Motola et al., 2006). Cholesterol deprivation also triggers a Daf-c phenotype, cementing a link between dietary sterols and dauer signalling (Birgit Gerisch et al., 2001).

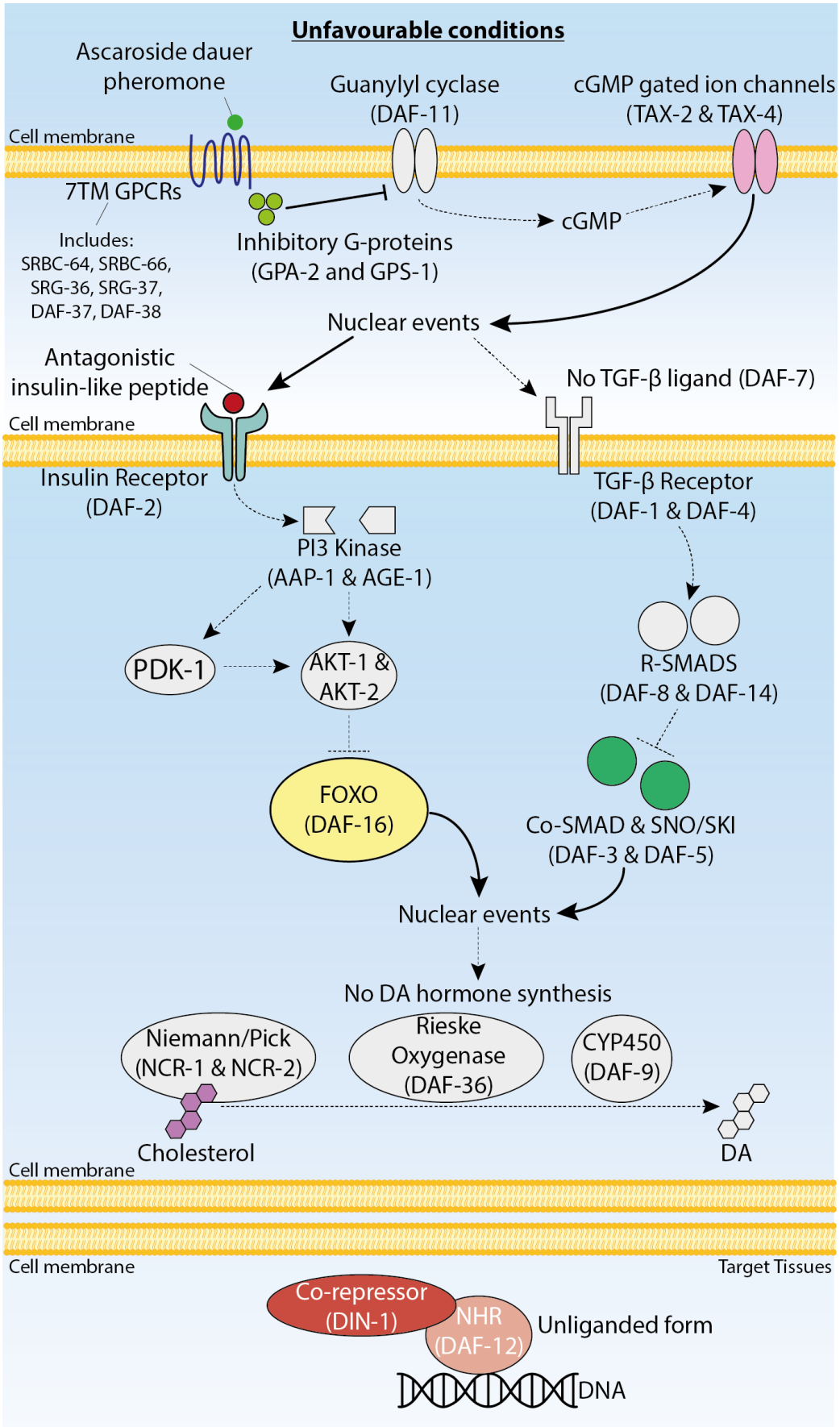

(Figure 3: refer to page 31 for legend)

Figure 3. Schematic overview of the cellular signalling pathways involved in regulation of dauer formation. The process of dauer formation is regulated by four signalling pathways: guanylyl cyclase pathway, insulin/IGF-1 signalling (IIS) pathway, dauer TGF-β pathway and the steroid hormone pathway. In unfavourable conditions, dauer induction is stimulated by decreased cGMP production leading to increased antagonistic insulin-like peptide production and decreased expression of the TGF-β ligand, resulting in down-regulation of both IIS and TGF-β pathways respectively, which ultimately inhibits production of DAs. Dotted lines represent down-regulated signalling and black lines represent up-regulated signalling. Coloured proteins are active and greyed out proteins are inactive. Adapted from (Fielenbach & Antebi, 2008; Stoltzfus et al., 2014).

4.4.2 L1 Arrest

Larvae hatching in compete starvation conditions arrest in a non-morphological modified, stress resistant stage termed L1 arrest/diapause (Baugh, 2013) exercising their ability to arrest development as an acute starvation response. Animals are able to survive for weeks in this state and upon refeeding, are able to recover to resume development. Mutations in *daf-2* cause constitutive L1 arrest under nutrient conditions at a high temperature (Gems et al., 1998). However low temperatures reverses this effect to produce reproductive adults (Baugh & Sternberg, 2006). They also survive longer in L1 arrest compared to wild type, suggesting resistance to starvation by the regulation of L1 arrest by IIS. Disrupting insulin-like peptide secretion also leads to constitutive L1 arrest providing further evidence that IIS regulates L1 arrest (Kao et al., 2007). The FOXO transcription factor, DAF-16 is required for L1 arrest (Baugh & Sternberg, 2006), are sensitive to starvation, and die quickly (Muñoz & Riddle, 2003). Nuclear localisation of DAF-16 occurs during L1 arrest to regulate gene expression (Weinkove et al., 2006). Cell divisions, migrations and fusions occurs normally in *daf-16* mutant L1 arrest-defective phenotype, however at a slower rate than normal development in well-fed larvae. DAF-18/PTEN, a negative regulator of the insulin-like pathway, regulates L1 arrest in the germline, which is dependent on AGE-1 and AKT-1, but not DAF-16 (Baugh & Sternberg, 2006; Fukuyama et al., 2006). The L1 arrest phenotypes of *daf-2* and *daf-16* mutants

suggest the role of IIS in the regulation of L1 development in a nutrient dependent manner.

Downstream of IIS for L1 arrest and development is the cyclin-dependent kinase inhibitor, *cki-1*, and the microRNA (miRNA), *lin-4* (Baugh & Sternberg, 2006; Hong et al., 1998). CKI-1 activity is required to suspend division of blast cells during L1 arrest and cease cell cycling at G1/S transition (Hong et al., 1998). Expression of *cki-1* is upregulated in blast cells during L1 arrest, which requires *daf-16* suggesting a connection between IIS and cell cycle arrest (Baugh & Sternberg, 2006). Expression of *lin-4* occurs during mid-late L1 stage, where the timing of accumulation determines postembryonic development timing (Feinbaum & Ambros, 1999). The expression is supressed by *daf-16*, placing IIS upstream of developmental timing (Baugh & Sternberg, 2006). Another microRNA, *mir-235* (the orthologue of mammalian miR-92), is a vital modulator for L1 arrest (Kasuga et al., 2013). During L1 arrest, expression of *mir-235* is upregulated and decreases upon exit from the diapause state in a *daf-16* dependent manner (Kasuga et al., 2013). Upregulation of the *mir-235* target, *nhr-91* (encoding the mammalian germ cell nuclear factor), is epistatic to *mir-235* for the arrest defective phenotype of *mir-235* mutants (Kasuga et al., 2013).

The germ cells, Z2 and Z3, arrest at different points of the cell cycle to the somatic gonad via different mechanisms during L1 arrest, which is dependent on *daf-18*/PTEN (Fukuyama et al., 2006; Ogg & Ruvkun, 1998). Likewise, the α-subunits of AMPK, *aak-1* and *aak-2*, are also required for germ cell arrest (Fukuyama et al., 2012; I. Lee et al., 2012). Although functioning independently for germ cell regulation, DAF-18 and AMPK, both converge on inhibition of TOR complex 1, which is required for aberrant germ cell proliferation during L1 arrest (Fukuyama et al., 2012).

There is evidence revealing IIS may function in a cell-nonautonomous manner to regulate L1 arrest and recovery. Genetic mosaic analysis and tissue specific transgenic rescue of IIS components have revealed cell-nonautonomous regulation of lifespan (Apfeld & Kenyon, 1998; Libina et al., 2003; Wolkow et al.,

2000). Tissue specific transgenic rescue of *daf-16* in a *daf-2* mutant background showed the constitutive developmental arrest phenotype observed in *daf-2* mutants can result from *daf-16* activity in different somatic tissues (Libina et al., 2003). Furthermore, tissue specific expression of *daf-16* in the intestine, epidermis and neurons have revealed cell non-autonomous regulation of L1 arrest by *daf-16* (Kaplan et al., 2015).

As mentioned above, the TGF-β and steroid hormone signalling pathways regulated dauer development in addition to IIS (Hu, 2007). As well as DAF-7, another known TGF-β ligand is DBL-1. The *dbl-1*/TGF-β pathway is distinct from the *daf-7*/TGF-β pathway, and regulates body size and male tail development and acts through the Sma/Mab pathway (Savage-Dunn, 2005). Mutants of *daf-16* in L1 arrest were upregulated for *dbl-1*, *daf-12* and *daf-36* (Kaplan et al., 2015), suggesting the repression of these genes by *daf-16* (Kaplan et al., 2015). Genetic epistasis analysis also showed the *dbl-1*/TGF-β and *daf-12*/NHR steroid hormone signalling pathways are required for the arrest-defective phenotype of *daf-16* mutants (Kaplan et al., 2015). Altogether, this implies the *daf-16* regulated induction of L1 arrest by inhibiting other pathways involved in promoting development.

The widespread feedback regulation of IIS is likely to influence homeostasis. The transcription for the DAF-2 agonist, *ins-7*, is repressed by *daf-16* (C. T. Murphy et al., 2003, 2007), while transcription is activated for the antagonist *ins-18* (Matsunaga et al., 2012; C. T. Murphy et al., 2003), suggesting positive feedback for IIS. Integrated analysis of insulin like peptides (ILPs) identified an ILP-to-ILP signalling network, predicted for feedback regulation (Fernandes de Abreu et al., 2014). Gene expression analysis for insulin-like mRNAs in *daf-2* and *daf-16* mutants in L1 arrest to feeding, illustrated positive and negative feedback for a majority of the ILPs (Kaplan et al., 2019). Cross talk between tissues presumably occurs to support organismal homeostasis. As previously mentioned, dauer development involves IIS between the intestine and neurons (Hung et al., 2014). External and internal conditions are likely to be processed through chemosensory neurons and the intestine respectively, with feedback

incorporating these inputs by broadcasting signalling throughout the animal to achieve organisation of postembryonic development (Kaplan & Baugh, 2016). Food or polypeptide perception, without ingestion, significantly alters gene expression and lipid metabolism to activate IIS in a *daf-28* dependent manner in starved L1 larvae (Kaplan et al., 2018).

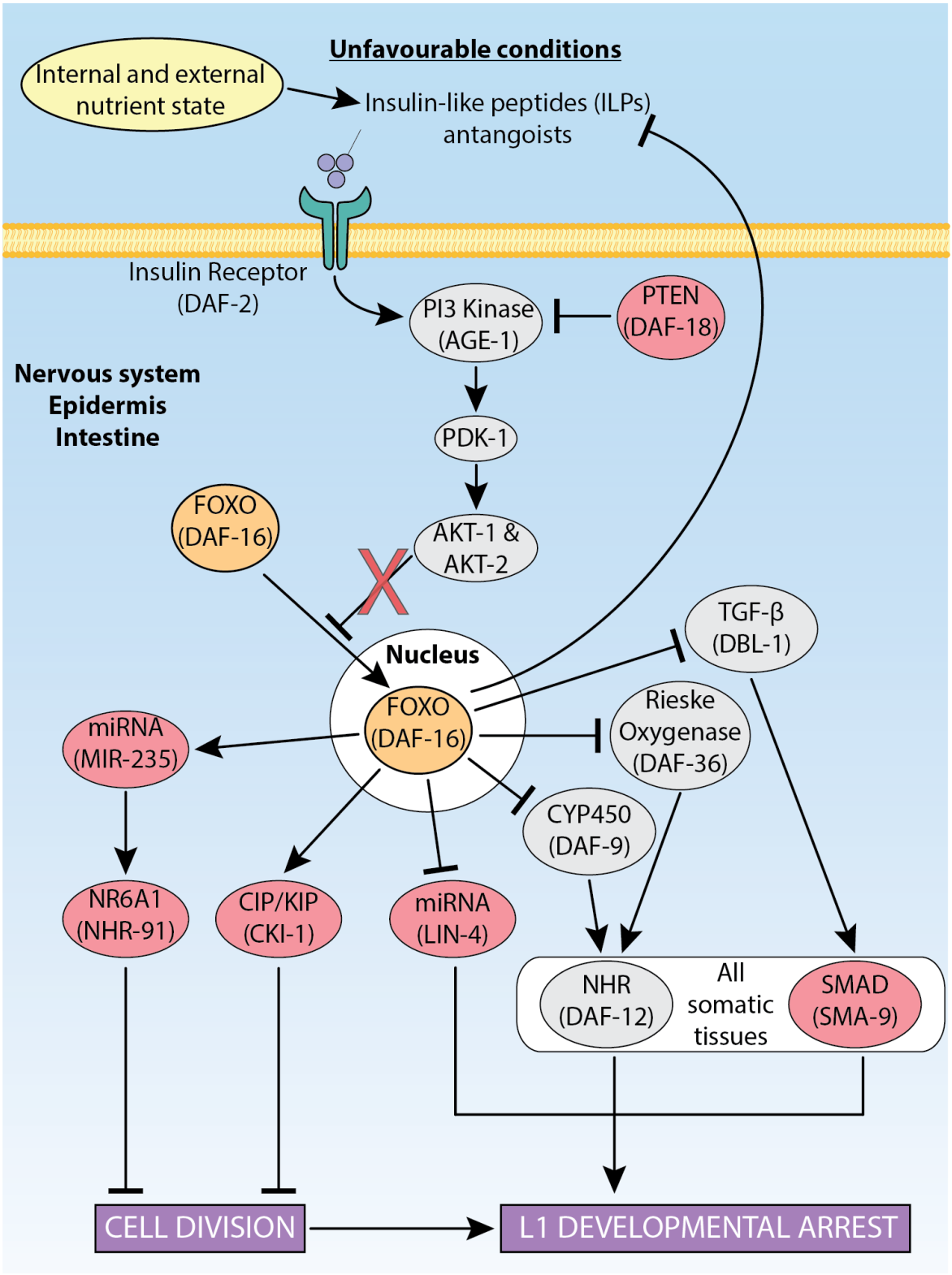

Figure 4. Schematic diagram representing the mechanisms involved in L1 arrest. Unfavourable conditions during hatching disrupts ILP secretion, decreasing DAF-2 activity and preventing the inhibition of DAF-16 nuclear localisation, allowing DAF-16 to promote stress resistance during starvation. Nuclear DAF-16 stimulates expression of MIR-235, required for arresting cell division, and the cyclin-dependant kinase inhibitor, CKI-1, but inhibits LIN-4,

required for the regulation of post-embryonic development. Dafachronic acid synthesis and TGF-β/DBL-1 signalling is also inhibited encouraging L1 arrest. DAF-16 produces positive and negative feedback by repressing and activating different ILPs. DAF-18 is a negative regulator of IIS and is required for L1 arrest. Red proteins are active and greyed out proteins are inactive. Adapted from (Baugh & Sternberg, 2006; Kaplan & Baugh, 2016; Kasuga et al., 2013).

4.4.3 Late larval arrest

The ability for larvae to induce an acute response to starvation is not limited to the L1 stage. Starved L2 or L3 larvae initially complete a molt cycle before arresting at the beginning of the next developmental stage, uncovering developmental checkpoints before the molt cycle of L3 and L4 larvae (Schindler et al., 2014). Similar to L1 diapause, L3 and L4 arrested larvae lack morphological modifications, with L3 arrested larvae absent in dauer specific features (Schindler et al., 2014). The lifespan duration of late larval arrest lasts for weeks rather than months, similar to L1 arrest, although L3 larvae are more resistant to starvation than L1 larvae (Hibshman et al., 2018).

In line with L1 arrest and dauer diapause, insulin signalling also regulates late larval arrest (Schindler et al., 2014). The absence of *daf-16* in starved larvae during L2 and L3 causes animals to bypass the arrest checkpoint, with the majority of animals progressing to adulthood (Schindler et al., 2014). Shifting temperature-sensitive *daf-2* mutants from the permissive to the restrictive temperature at the mid L2 stage (bypassing dauer formation), leads to a developmental delay at the L3 and L4 checkpoints in fed larvae, which was shown to be dependent on *daf-16* (Schindler et al., 2014). Additionally, *daf-16* functions cell-nonautonomously to regulate L3 and L4 development (Schindler et al., 2014).

It is probable that IIS also regulates steroid hormone signalling in late larval development. The reduction in *daf-9/CYP2* expression partially suppresses the late larval arrest defective phenotype of *daf-16* mutants. Furthermore, overexpression of *daf-9* promotes continued development of L2 and L3, bypassing the checkpoints, in the absence of food, revealing a more robust effect than loss of *daf-16* (Schindler et al., 2014). Interestingly, *daf-12*/NHR

mutants do not bypass the L3 checkpoint during starvation, and failed to suppress the arrest-defective phenotype of *daf-16* mutants and *daf-9* overexpression animals (Schindler et al., 2014). Taken together, these results suggest *daf-16* promotes L3 and L4 arrest during starvation by inhibiting *daf-9*, similar to L1 and dauer diapauses, however not through the effector *daf-12*/NHR. The *C. elegans* genome encodes 284 nuclear hormone receptors (Antebi, 2006), therefore it is speculated DAF-9 functions through an uncharacterised steroid hormone pathway to modulate the effects of starvation through late larval development.

4.4.4 Adult Reproductive Diapause

Adult reproductive diapause (ARD) is an alternative stress-resistant stage in the life cycle of *C. elegans* where by developmentally mature adults facing starvation conditions induces ARD. Removal of the bacterial food source during the mid L3 stage of *C. elegans* larval development establishes an ARD (B. Gerisch et al., 2020). During ARD, reproduction is delayed with the inhibition of embryo production, atrophy of the intestine, tissue and cellular ageing progresses over several weeks and the appearance of dead embryos can be observed in the uterus (Angelo & Van Gilst, 2009). Germline cells in the gonad decreases to a small population as ARD progresses, which is maintained throughout the duration of ARD, suggesting their protection from mechanisms inducing cell death to the rest of the germline (Angelo & Van Gilst, 2009). ARD animals have a longer lifespan up to 80 days in 20°C compared to animals in *ad libitum* (AL) conditions (22 days) (B. Gerisch et al., 2020). ARD animals maintained at 15°C showed even greater resilience, living past 200 days, more than 5 times the normal AL lifespan at this temperature. Due to metabolic remodeling, they are able to survive for long periods of starvation.

Induction of diapause occurs to increase the survivability of *C. elegans* under unfavourable conditions. The ability of the arrested worms to exit the diapause, search for nutrients and produce progeny can determine the effectiveness of the diapause. The regeneration of the germline and lifespan upon exit from this diapause demonstrates the robust survivability of *C. elegans* in ARD. The

reintroduction of food triggers ARD exit, marked by drastic morphological changes which allows for a normal adult lifespan equivalent to animals under *ad libitum* conditions, and the ability to produce progeny even after 80 days of starvation, comparable to worms starved for shorter periods (B. Gerisch et al., 2020). ARD animals differ greatly from dauer diapause in environmental inputs, physiology, timing, stress resistance and behaviour (Fielenbach & Antebi, 2008).

Unlike dauer diapause, a pheromone controlling the entry and exit from ARD has not been discovered. ARD animals are partially dependant on population density since high densities of worms were require for successful induction into ARD. Isolation of individual ARD animals led to exit from ARD, supporting evidence of a potential ARD pheromone (Angelo & Van Gilst, 2009).

The reduction of TOR signalling leads to longevity across several species (C. J. Kenyon, 2010), however both reducing and increasing TOR signalling led to a decreased ARD lifespan (B. Gerisch et al., 2020), suggesting a precise signalling output for longevity. The upstream regulator of TOR activity, AMP-kinase, was required for ARD longevity, while loss of downstream TOR targets, such as S6K and factors promoting protein synthesis such as RAGA extended AL lifespan but reduced ARD lifespan (B. Gerisch et al., 2020). The nucleolar regulator, NCL-1, inhibits ribogenesis and is required for multiple longevity pathways (Tiku et al., 2016). Mutants of *ncl-1* have increased nucleolar size and upregulated rRNA (Frank & Roth, 1998), which also reduced ARD lifespan (B. Gerisch et al., 2020). In line with this, activation of ribosomal RNA synthesis is essential for recovery from ARD (Burnaevskiy et al., 2018).

The HLH transcription factor, TFEB, previously associated for its requirement in major known longevity pathways (Lapierre et al., 2013) is vital for ARD longevity. The loss of *hlh-30*, the orthologue of TFEB in *C. elegans*, dramatically reduces the lifespan of ARD animals by 88% which is companied by drastic phenotypic changes: body shrinkage, loss of neutral lipids and failure to recover after 24hr of ARD (B. Gerisch et al., 2020), highlighting the importance of *hlh-30* for ARD

survival, recovery and metabolic remodelling. Rapid nuclear translocation of HLH-30 occurred upon ARD entry, accompanied with major transcriptional changes to suppress growth, morphogenesis and reproduction (B. Gerisch et al., 2020). TFEB/HLH-30 is a master regulator of autophagy and lipid biogenesis (Napolitano & Ballabio, 2016), however the reduction of autophagy via mutations in *pha-4* and *unc-51* and impaired lipid metabolism (*nhr-80, fat-6, fat-7*) did not reduce ARD lifespan (B. Gerisch et al., 2020), suggesting a different requirement for *hlh-30* for ARD longevity. The HLH-30 transcriptional outputs Max-like HLH factors, MXL-2 and MXL-3, reduced ARD lifespan (B. Gerisch et al., 2020) suggesting an extended HLH network for promoting ARD longevity. Another HLH-30 target vital for ARD survival is AMPK, previously implicated in L1 and dauer diapause (Fukuyama et al., 2012), AMPK and TOR are crucial modulators of mitochondrial dynamics (López-Lluch et al., 2018), which also plays a role in ARD survival.

To maintain integrity under stressful conditions, mitochondria continuously undergo fission and fusion events (Gomes & Scorrano, 2011). Mutations of *fzo-1*, encoding mitofusin which is involved in mitochondrial fusion, decreased ARD longevity, consistent with the mitochondrial fragmentation and reduced oxygen consumption observed in *hlh-30* mutants in ARD. Mutations in the gene *drp-1*, involved in mitochondrial fission, modestly increases ARD lifespan (B. Gerisch et al., 2020) signifying a role of mitochondrial signalling for ARD longevity.

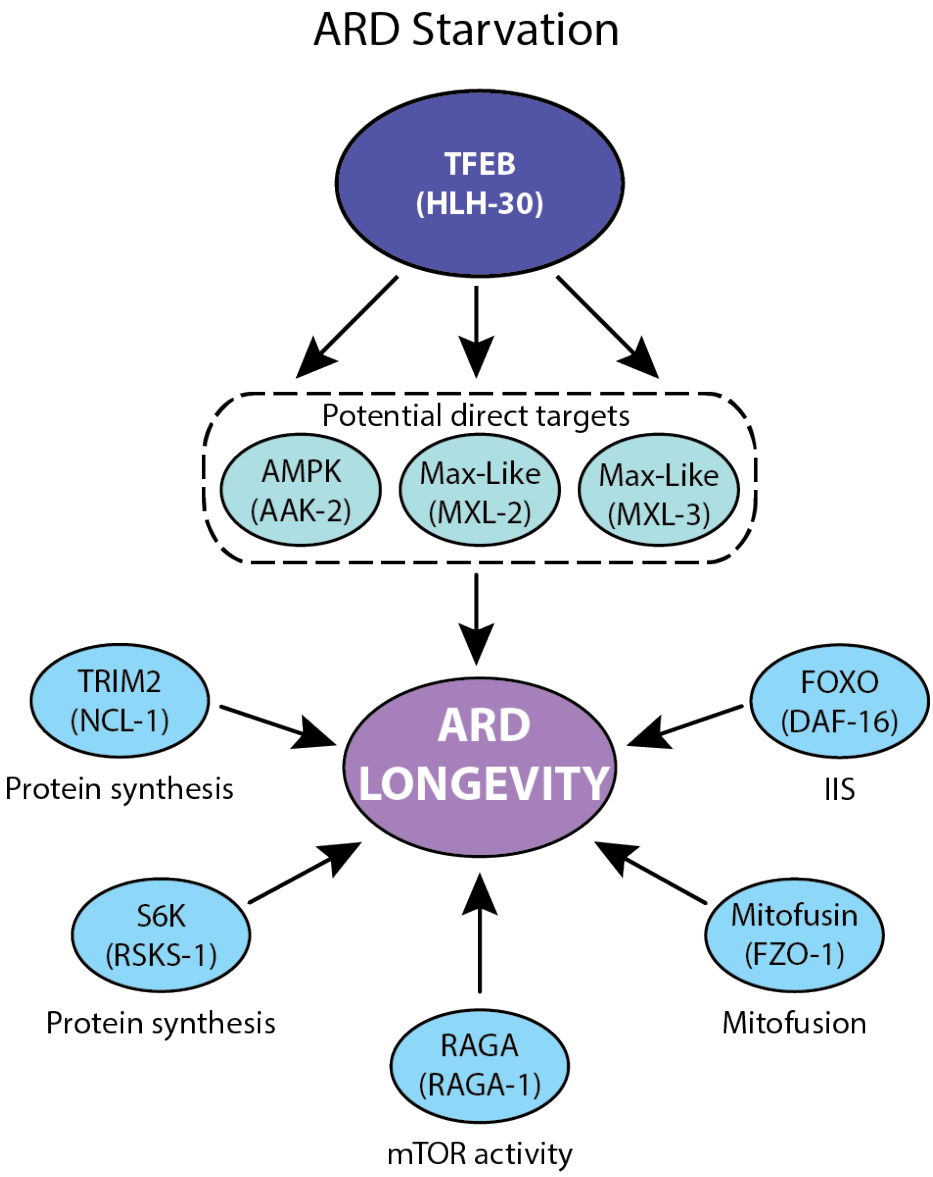

Figure 5. Overview of the factors regulating ARD longevity. Under ARD starvation conditions TFEB/HLH-30 functions through the potential direct targets of AAK-2, MXL-2 and MXl-3 to regulate ARD longevity. Active FOXO/DAF-16 is also partially required for ARD survival as well as other processes including TOR activity (RAGA-1), protein synthesis (NCL-1 and RSKS-1) and mitochondrial function (FZO-1). Adapted from (B. Gerisch et al., 2020).

4.5 Previous longevity screens in *C. elegans*

The progression of ageing research has identified many genetic and environmental factors that influence longevity across several species (Fontana et al., 2010; Kaeberlein, 2007; C. J. Kenyon, 2010). *C. elegans* has become an invaluable model system for investigating the molecular mechanisms of ageing,

where the development of modern laboratory techniques utilising *C. elegans* can largely be attributed to the pioneering research performed by Sydney Brenner and John Sulston (Brenner, 1974; Sulston & Brenner, 1974).

Ageing research using *C. elegans* became fashionable since the seminal work of Michael Klass, by employing mutagenesis techniques to isolate long-lived mutants. This led to the first identified and described *C. elegans* longevity gene *age-1* (Klass, 1983). A decade later with the enhancement of methods and technologies to advance beyond the identification of single genes, began the classification of genetic and molecular pathways regulating ageing. This led to the discovery of *daf-2* and its dependence on *daf-16* for lifespan extension (C. Kenyon et al., 1993; Larsen et al., 1995). The formally discovered longevity gene, *age-1*, was then implicated to operate within the same genetic pathway as *daf-2* and *daf-16*, defining the insulin /IGF-1-like signalling pathway to modulate ageing in *C. elegans*. Several factors modulating lifespan have since been characterised including germline signalling, calorie restriction and mitochondrial respiration.

A unique feature of using *C. elegans* is the common genetic background, wild type N2, used in a majority of studies for ageing research. Therefore, it is often assumed that experimental methodology between laboratories is relatively consistent. However, subtle differences in methodologies can have a substantial effect on the outcome, such as the use of live verses dead *E.coli*, the temperature at which the experiment was performed; and the use of 5-fluorodeoxyuridine (FUDR) to prevent progeny from hatching.

Before the development of RNAi technology in *C. elegans*, ageing research was limited to a ‘forward’ genetics approach, whereby the induction of random mutations leading to a longevity phenotype were identified and validated. The discovery of RNA interference (RNAi) has allowed extensive forward and reverse genetic screens for genes modulating lifespan. Injecting *C. elegans* with double-stranded RNA was an effective method for genetic interference (Fire et al., 1998). Soaking and feeding worms dsRNA (Tabara et al., 1998; Timmons &

Fire, 1998) was later recognised to be equally effective as injecting methods to induce RNAi knockdown. The development of the bacterial feeding RNAi method led to the construction of extensive RNAi libraries comprising approximately 80% of the genes in the *C. elegans* genome, becoming an extremely useful systematic tool for *C. elegans* ageing research. This unlocked the direct measurement of how knocking down individual genes effected lifespan. It also allowed other age-related phenotypes, such as, developmental rate, fecundity and lipofuscin accumulation to be measure on a larger scale. Several laboratories have utilised this technology to perform genome wide RNAi screens for longevity to discover the importance of mitochondria, signal transduction, stress responses, protein translation, gene expression and metabolism in regulating lifespan in *C. elegans* (Dillin, Hsu, et al., 2002; Hamilton et al., 2005; Hansen et al., 2005, 2007; S. S. Lee et al., 2003). The overlap of longevity genes discovered between the major genome wide RNAi studies was surprisingly low. Several factors including differences in temperature, strain background and the use of FUDR may have contributed to this lack of replication. Although high throughput, RNAi screens to identify longevity genes has technical limitations. For instance, depending on the time of RNAi induction, genes required for development capable of modulating lifespan could be overlooked. Subsequent studies focussing on this particular gene set revealed new genes influencing longevity, which was not identified in the initial RNAi screens (Curran & Ruvkun, 2007).

Known longevity genes have established roles in stress tolerance and development. Mutations in genes modulating lifespan also exhibited stress resistance and therefore implicated in stress response pathways (T. E. Johnson et al., 2002; Thomas E. Johnson et al., 2001). Several studies have screened for altered stress resistance as a primary phenotype before testing for longevity. Many studies used either forward (mutagenesis) or reverse (RNAi) genetics prior to screening for stress phenotypes, for example, related to oxidative stress (Y. Kim & Sun, 2007), heat resistance (Muñoz & Riddle, 2003), the hypoxic

response (Mehta et al., 2009) and ER stress (Denzel et al., 2014) before examining the longevity effect.

Network biology is another approach to gain insight into known longevity genes and to identify novel regulator of lifespan, providing vital information about complex interactions between biological systems. Networks can be constructed from protein-protein interactions, transcriptional co–regulation, putative microRNA targets and annotated biological pathways (De Magalhães & Toussaint, 2004; S. K. Kim et al., 2001; Tacutu, Budovsky, Wolfson, et al., 2010). Databases for such interactions exist for many species from yeast to flies to humans (Rohl et al., 2006). Previous network analysis studies have demonstrated longevity genes to have more protein-protein interactions with other proteins than non-longevity genes in the interactome (Tacutu, Budovsky, & Fraifeld, 2010). Other studies have used these networks to construct longevity networks in both humans and *C. elegans* to predict novel longevity regulators (Tacutu et al., 2012).

C. elegans is an optimal organism to study drugs that influence ageing. It has proven to be a worthy pharmacological tool to identify small molecules with pro-longevity effects (Lucanic et al., 2013). As previously described, screening following resistance to acute stress has also become a strategy to identify potential pharmacological agents that extend lifespan based on their ability to enhance resistance to oxygen radicals or other stressors (Gill et al., 2003). Several small compound screens using drugs already known to have effects on human physiology identified pro-longevity effects of anticonvulsant drugs (Evason et al., 2005) and antidepressants (Petrascheck et al., 2007). High throughput methodology and the use of FUDR allowed follow up screens to identify 115 small molecules (Petrascheck et al., 2009) and 60 compounds of known mammalian pharmacology (Ye et al., 2014) to extend the lifespan of *C. elegans*. Recent screens combining manual and automated assays (Lucanic et al., 2016) and the development of microfluidic devices (Xian et al., 2013) has identified new lifespan extending chemicals and interventions.

Although there have been several studies to determine the mechanisms of ageing there is still plenty to learn regarding this process. Mutagenesis screens can produce subtle genetic changes in the genome to manipulate longevity, which can highlight novel longevity genes. Here we show that this high maintenance method can be simplified by using ARD as a tool.

5 AIMS OF THE STUDY

AIM 1: Assessing ARD as a tool to screen for novel regulators of longevity

The use of model organisms to study ageing has revealed different conserved molecular pathways in regulating longevity. RNAi screens to find new loci have helped illuminate new activities, but are limited to gene knockdown and loss of function. The discovery of long-lived mutants through mutagenesis screens has the advantage of identifying point mutations that more subtly alter gene function. However, this approach is hindered by the challenge of finding mutants through post-reproductive clonal screens. Notably, longevity is a post reproductive phenotype, and therefore selection of longevity mutants is only possible if there are thousands of clonal lines to go back to. To overcome these limitations, we took advantage of the diapause stage, adult reproductive diapause (ARD). As previously mentioned starvation in the late larval stage of wild type *C. elegans* induces ARD, delays reproduction and triples the lifespan, compared to animals in *ad libitum* (AL) conditions. The re-introduction to food regenerates the germ line tissues capable of producing progeny. This then allows the direct selection of strains that exceed the normal survival times, and the subsequent recovery of progeny. The discovery that known longevity interventions are additive to ARD lifespans suggests longevity mutants obtained through ARD selection would display similar lifespan extension in AL conditions. We induced ARD in a mutagenised population and screened for ARD longevity. Long-lived mutants under ARD were selected, reintroduced to food to induce recovery, and analysed further to isolate the causative gene for longevity.

AIM 2: Identify novel factors regulating ARD longevity

The screen to identify novel regulators of longevity yielded several mutants with ARD specific longevity. Research in our laboratory has characterised this relatively unknown diapause stage and discovered that regulators of known longevity pathways are additive to ARD lifespan. Therefore, it is curious to understand the mechanism driving ARD longevity. We further analysed the ARD longevity mutants, looking for alleleism, to highlight a causative gene or pathway

inducing ARD longevity. To ARD specific longevity mutants, may provide insights into regeneration and rejuvenation processes after long periods of starvation.

AIM 3: Decipher the role of HLH-30 in regulating ARD survival

Our research into ARD has uncovered HLH-30/TFEB to be essential to ARD survival. The loss of this HLH transcription factor, previously implicated to be required in known major longevity pathways, completely abolished ARD lifespan extension. HLH-30 mutants in ARD exhibit adult features but lacked embryos, as well as, a dumpy morphology, vacuolisation of tissues, germline pathology, depleted fat stores and failure to recover upon refeeding. This reveals HLH-30 to be vital for metabolic remodelling, ARD morphogenesis and recovery. To decipher the role of *hlh-30* in ARD, we performed a suppressor screen by inducing ARD in a mutagenised *hlh-30* mutant population and screening for mutants rescuing *hlh-30* ARD shortevity. Mutants surpassing *hlh-30* mutant lifespan under ARD were collected and analysed to help understand the critical role of HLH-30 for ARD survival.

6 RESULTS

6.1 Using extended ARD survivorship to select for longevity mutants

6.1.1 Selecting for longevity mutants using extended ARD survivorship

The discovery of novel longevity genes through RNAi and mutagenesis based approaches have greatly aided in illuminating new activities involved in the ageing process (Ailion et al., 1999; E. Yanos et al., 2012; Klass, 1983; Larsen et al., 1995). However, each method possesses its own limitations. The advantage of mutagenesis screens is that they allow for identification of point mutations that subtly alter gene function, but are hindered by the challenge of finding mutants through post-reproductive clonal screens, since longevity is a post reproductive phenotype, and therefore selection of longevity mutants can only be performed if there are thousands of clonal lines to go back to. To overcome these challenges, we used ARD as a tool to aid in selecting long-lived mutants. Wild type animals in ARD exhibit an extended lifespan compare to animals grown in AL conditions and often survive more than 80 days without food (B. Gerisch et al., 2020) yet can recover to produce progeny. Known longevity interventions through reduced insulin signalling, reduced reproductive signalling and reduced mitochondrial function further extended ARD lifespan (B. Gerisch et al., 2020) revealing that ARD lifespan is additive with these longevity mutants. Therefore, we hypothesised that long-lived mutants obtained through ARD selection and recovery, would also show lifespan extension in AL conditions. This approach allows one to select rather than screen for long lived mutants, and recover individual mutants and their progeny, and does not require a F3 clonal screen.

We performed ethyl methanesulfonate (EMS) mutagenesis to induce random germline point mutations before ARD induction in the F2 generation and selected for mutants surpassing wild type ARD lifespan (Figure 6A).

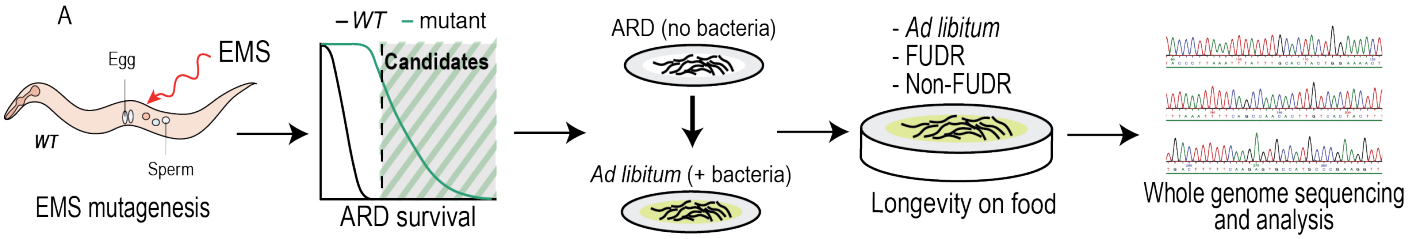

B

EMS Screen	EMS concentration (%)	Time in ARD (Days)	Number of long-lived mutants		
			ARD	*Ad Libitum*	
				FUDR	Non-FUDR
ARD 1 (Wild type)	0.3	120	52/100	12	3
ARD 2 (*daf-16 (mgDf50)*)	0.15	40	43/51	12	1
ARD 3 (Wild type)	0.15	100	70/73	8	3
ARD 4 (Wild type)	0.15	100	58/100	13	1
		Total:	179/324	45	8

Figure 6. Using extended ARD survivorship to identify longevity mutants. A) Mutagenesis screen workflow used to select for long-lived mutants. ARD is induced in a mutagenised WT population and surviving animals picked after a fixed number of days beyond the maximal wild type survivorship of 80 days. Re-introduction to food initiates recovery and progeny production to retrieve mutant strains for sequencing and analysis. **B)** Table summarising the screens conducted and the number of mutants obtained for each screen. Screen 2 was performed using *daf-16(mgDf50),* whose maximal survivorship is 40 days in ARD, in order to discover mutants downstream or independent of *daf-16.*

Four different screens were carried out as summarised in (Figure 6B). To obtain mutants with a robust longevity phenotype, we initially induced ARD for 120 days in the wild type background, greatly surpassing the survival of N2 in ARD (80 days). In addition, we carried out screens in the *daf-16* mutant background. DAF-16/FOXO is a transcription factor implicated as the key downstream regulator to several signalling pathways involved in longevity, including the insulin/IGF-1 pathway, mTOR signalling, AMPK pathway and germline signalling (Sun et al., 2017). *daf-16* mutants are shorter lived in ARD (maximal survival of 40 days). To discover longevity mutants independent of DAF-16/FOXO, we selected for mutants exceeding *daf-16* ARD lifespan. For these screens, we decreased the concentration of EMS to limit the number of background mutations. We also altered the duration of time in ARD to increase the spectrum of potential longevity mutants.

We washed the selected mutants onto bacteria to induce recovery from ARD and allowed them to produce progeny. From the four screens, we obtained 223 mutants, which were long lived in ARD. We next examined if these mutants were also long lived under AL conditions, therefore we analysed their lifespan using the DNA synthesis inhibitor, 5-flurodeoxyuridine (FUDR), to block progeny production, allowing simultaneous lifespan analysis of many mutants without transferring the mothers. FUDR also helps circumvent the issue of internal hatching seen in several long-lived mutants (Pickett & Kornfeld, 2013). After the FUDR ageing analysis under AL conditions, 44 of the original 223 mutants showed longevity (Figure 7A-D).

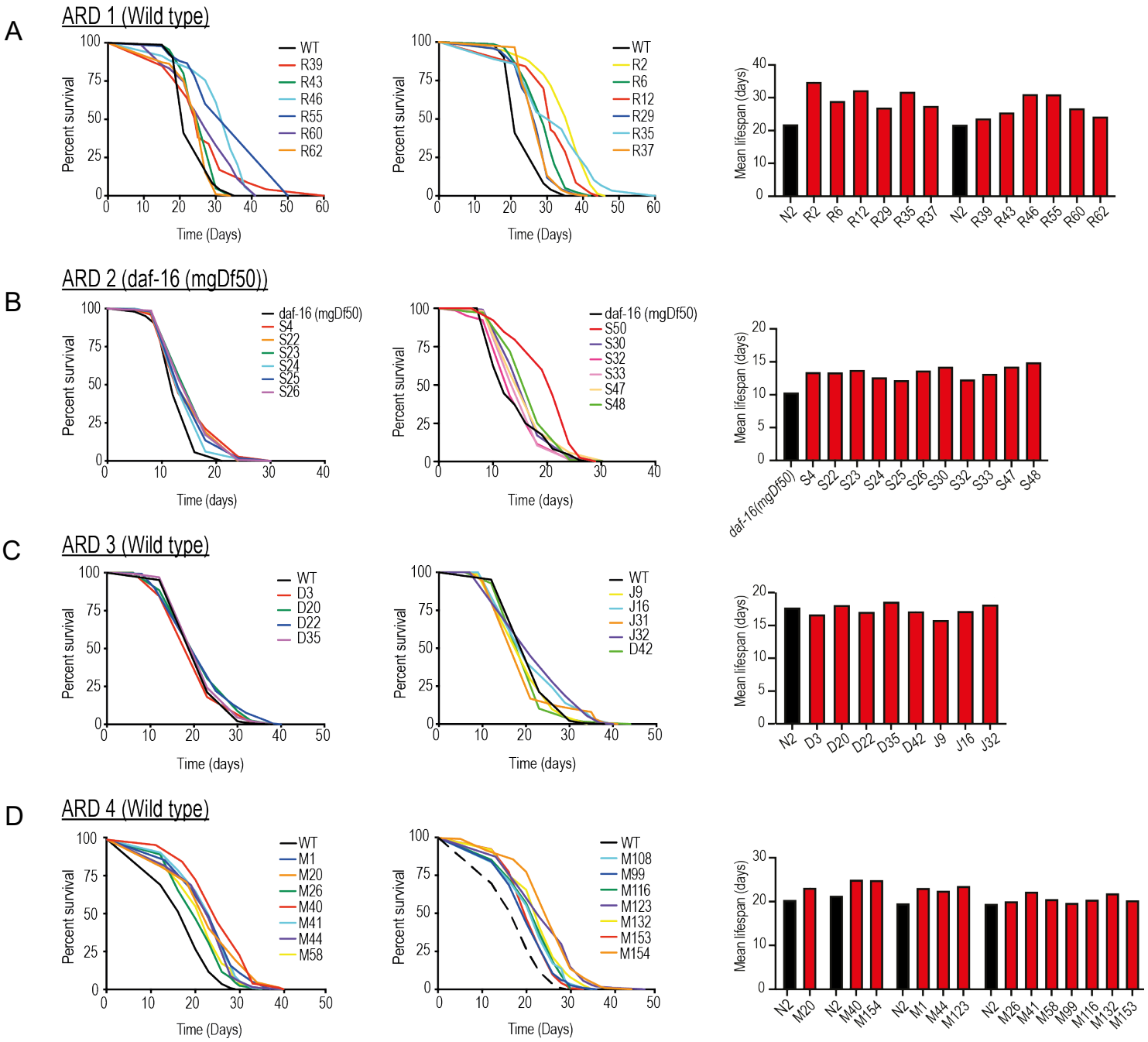

Figure 7. FUDR ageings of ARD longevity candidates. *Ad libitum* (AL) lifespan analysis in the presence of FUDR of the isolated long-lived mutants from **A)** screen 1 (WT background) **B)** screen 2 (*daf-16 (mgDf50)* background) **C)** screen 3 (WT background) and **D)** screen 4 (WT background), showing the 44 potential mutants to further validate and characterise. (n=1). Bar charts show the mean lifespans of the mutants.

In recent years, many laboratories have observed various effects of FUDR on longevity in certain mutants of *C. elegans* (Aitlhadj & Stürzenbaum, 2010; E. N. Anderson et al., 2016; Burnaevskiy et al., 2018; van Raamsdonk & Hekimi, 2011). Therefore, to address this issue we next analysed the positive mutants

in the absence of FUDR. Of the 44 mutants from the secondary FUDR screening, 8 mutants continued to show longevity in the absence of FUDR (Figure 8A & B)

A

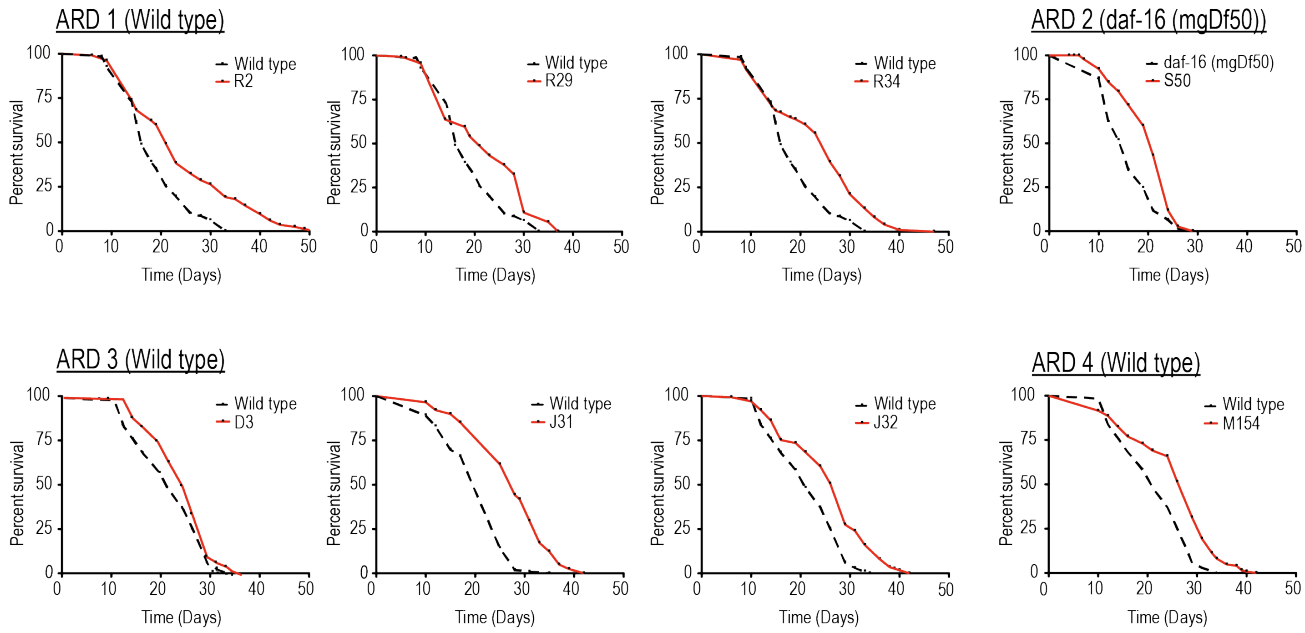

B

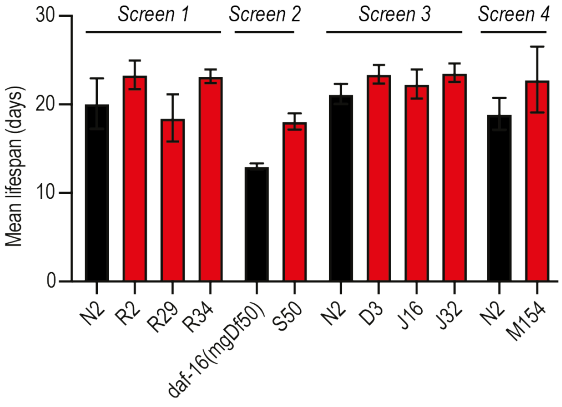

Figure 8. Mutant lines giving longevity in the absence of FUDR. A) Lifespan analysis of the long-lived candidate mutants in ARD and *ad* libitum (FUDR conditions) yielded 8 mutants that exhibit longevity compared to wild type in AL conditions in the absence of FUDR (Mantel-Cox Log Rank test, n=3). **B)** Mean lifespans of the mutants.

6.1.2 Identifying the causative mutations leading to longevity

To pinpoint the causative gene or pathway for longevity, we obtained whole genome sequencing and analysed the data using the Galaxy platform (usegalaxy.eu) to generate single nucleotide polymorphism (SNP) tables for each mutant. Notably, one of the limitations of our approach is that we could not

readily outcross the long-lived candidates, and therefore the number of candidate loci was high. To narrow down the candidates, we selected genes harbouring mutations within a coding region, residing in a conserved domain, which were evolutionarily conserved with higher organisms totalling 27 genes (Figure 9A). We also prioritised nonsense and missense mutations as these mutations are prone to disrupt gene function. To further narrow down the list of candidates, I assumed that most mutations would represent loss of function, and performed an RNAi longevity screen to measure lifespan extension. Of the RNAi clones, knockdown of 4 genes, *eplc*-2, *marc-6*, *png-1* and *ogdh-1*, showed modest lifespan extension (Figure 9B). We then used CRISPR-Cas9 to generate the exact SNP mutation and performed lifespan analysis. Unfortunately, none of the four CRISPR generated mutations elicited lifespan extension (Figure 9D), leading us to re-evaluate the screen.

Taken together, these results suggest that ARD can be used a tool to select for long-lived mutants; however, the screen requires optimisation to yield higher numbers of longevity mutants with more robust phenotypes to discover novel genes in regulating lifespan.

A

RNAi candidates			
aakg-2i	*ceh-20i*	F13B12.2i	*rsr-2i*
aars-2i	*che-3i*	F39C12.1i	*sdc-2i*
B0495i	*cogc-1i*	*fat-3i*	T24H7.2i
C27A12.9i	*egl-8i*	*kcc-3i*	*twk-31i*
C30A5.3i	*elpc-2i*	*marc-6i*	*unc-52i*
cdc-25.4i	*emb-9i*	*ogdh-1i*	Y8A9A.2i
cdh-3i	*epg-6i*	*png-1i*	

B

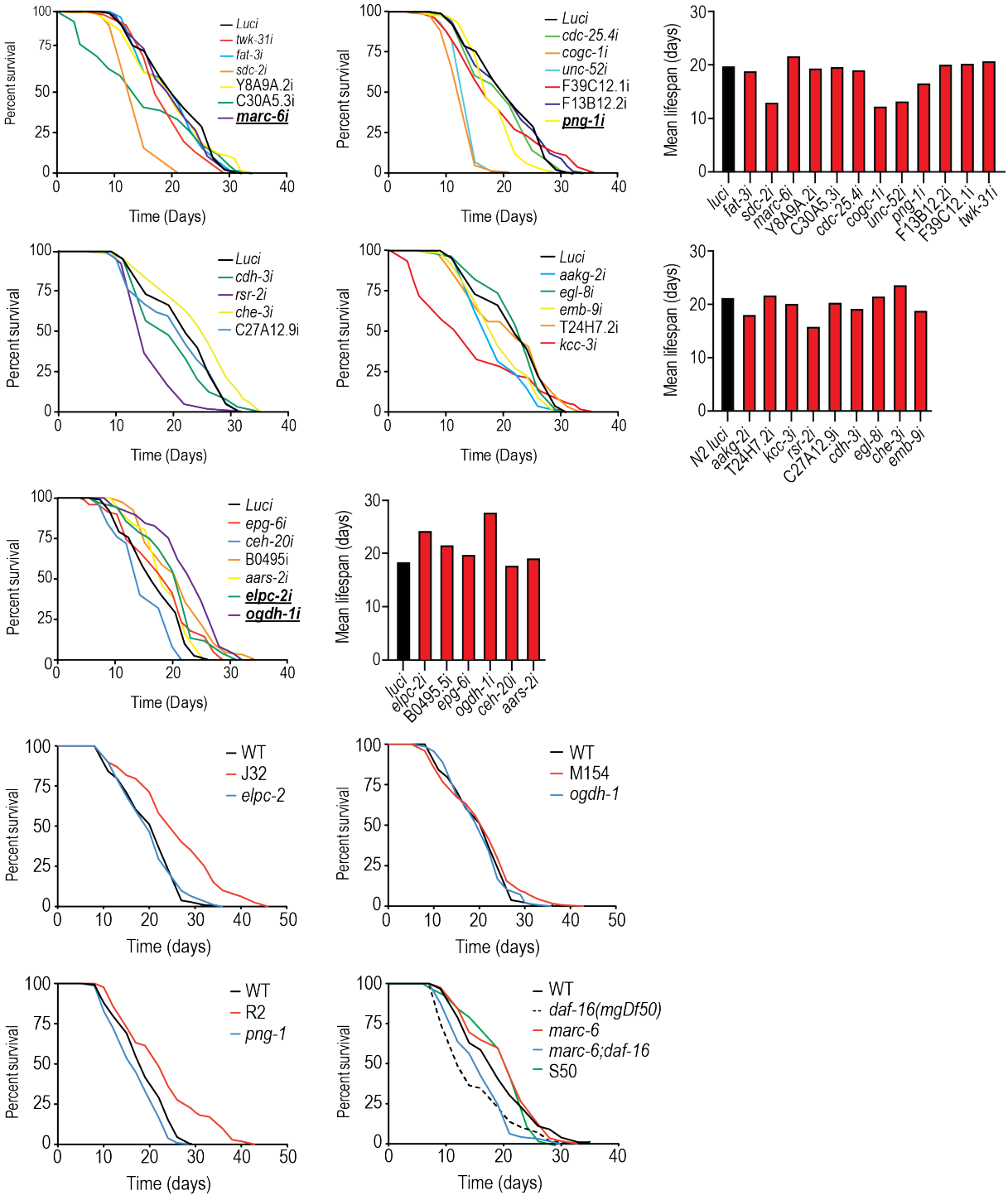

(Figure 9: Refer to page 55 for legend)

C

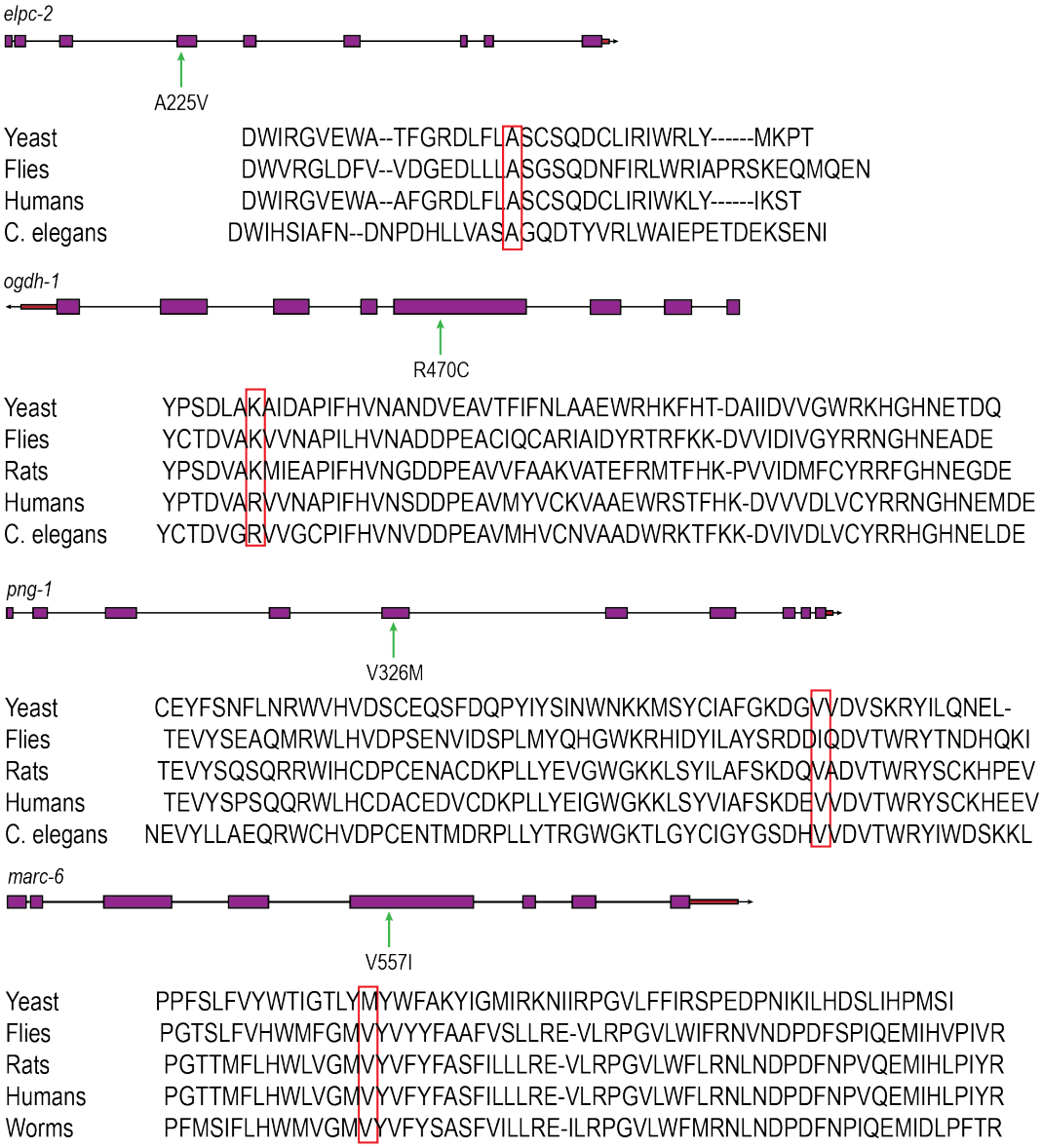

D

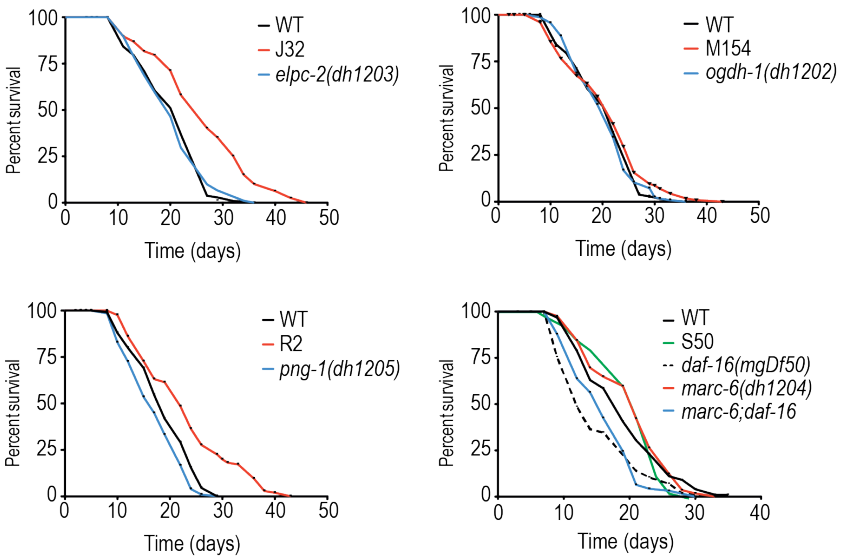

(Figure 9: Refer to page 55 for legend)

Figure 9. Analysis of RNAi screen candidates. A) Table summarising the RNAi clones tested for longevity **B)** Lifespan analysis of 27 RNAi candidate genes chosen from the whole genome sequencing analysis of the long-lived mutants, of which knockdown of 4 genes (highlighted in bold) showed lifespan extension compared to luciferase control. (Mantel-Cox Log Rank test, n=2, refer to appendix table 4 for statistics). **C)** Genomic position showing the location of the exact amino acid change obtained from the original mutagenesis screen and sequence alignments of wild type showing the conserved location of the amino acid change. **D)** Mutants of the 4 candidate genes from the RNAi screen, were created holding the exact SNP from the mutagenesis and analysed for longevity against wild type, however the mutants failed to show lifespan extension against wild type (Mantel-Cox Log Rank test, n=2, refer to appendix table 4 for statistics).

6.2 Deciphering the mechanism behind ARD longevity

6.2.1 Identification of factors regulating ARD longevity

Upon re-evaluation, we decided to focus on the 179 mutants that showed longevity more specifically under ARD conditions in order to decipher mechanisms driving longevity in this newly characterised diapause state (B. Gerisch et al., 2020) (Figure 6B). Notably, signalling pathways known to regulate longevity (insulin/IGF-1 signalling, germline signalling, reduced mitochondrial activity) are mostly additive with ARD longevity (B. Gerisch et al., 2020), suggesting an independent mechanism to survival. We prepared 25 mutants from the first (WT background) and second (*daf-16 (mgDf50)* background) screens for whole genome sequencing and analysed the data using the Galaxy platform (usegalaxy.eu) to generate SNP tables for each of the mutants. In this case, we searched for alleleism to help narrow down the candidates. We generated a list of 11 potential candidates based on two or more independent mutations in the same gene and, if the SNP resided within conserved between higher organisms and within a conserved domain in an evolutionarily conserved residue (Figure 10A). Using the CRISPR-Cas9 method, we obtained individual lines (from SunyBiotech) containing the mutation from the gene of interest to examine the ARD lifespan. Among the 11 mutants tested for ARD longevity, 4 mutants exhibited promising lifespan extension in ARD (Figure 10B). Further validating the longevity through a secondary ARD lifespan, we identified the

gene encoding uridine phosphorylase, *upp-1*, and to a lesser extent, the splicing factor, *prp-21*, to exhibit max lifespan extension in ARD by 0.7 fold compared to wild type (Figure 10D). We performed AL lifespan analysis in parallel and, interestingly, *upp-1(syb659)* and *prp-21(syn755)* mutants also demonstrated modest longevity in AL conditions (Figure 10E).

A

Gene	Function
alg-1	Argonaute ortholog, invovled in RNAi
alg-4	Argonaute protein involved in Argoclade of Argonaute small RNAi binding proteins
anoh-1	Ortholog of memebers of the human ANO (Anoctamins) family
piki-1	Encodes a class of II phosphatidylinositol 3-kinase (PI3K)
prp-21	Splicing factor
ptr-10	Non-receptor tyrosine phosphatase
upp-1	Uridine phosphorylase
vps-18	Vacuolar sorting protein
xbp-1	Excision repair protein
Y55F3BR.1	Deadbox helicase
ZC581.7	Ortholog of human FES (FES proto-onogene, tyrosine kinase) and FER (FER tyrosine kinase)

B

Day	30	40	50	60	70	80	100	110	120	130
N2	90%	50-70%	40%	10%	5%	2%	Day 85 - 0%			
alg-1	90%	80%	40%	20-30%	0%					
alg-4	90%	80%	40%	10-20%	5%	1%	Day 85 - 0%			
anoh-1	90%	70%	50%	40%	10%	5%	3%	1%	Day 115 - 0%	
piki-1	90%	50%	30%	10%	2%	0%				
prp-21	90%	50%	40%	20%	10%	5%	2%	2%	Day 115 - 0%	
ptr-10	80%	70%	30%	20%	5%	0%				
upp-1	90%	80-90%	50%	40%	20%	5%	3%	2%	1%	Day 128 - 0%
vps-18	90%	80%	50%	40%	10%	5%	Day 95 - 0%			
xpb-1	80%	70%	30%	10-20%	0%					
Y55F3BR.1	90%	80-90%	60%	40%	20%	2%	2%	1%	Day 115 - 0%	
ZC581.7	90%	70%	20%	10%	5%	1%	Day 85 - 0%			

C

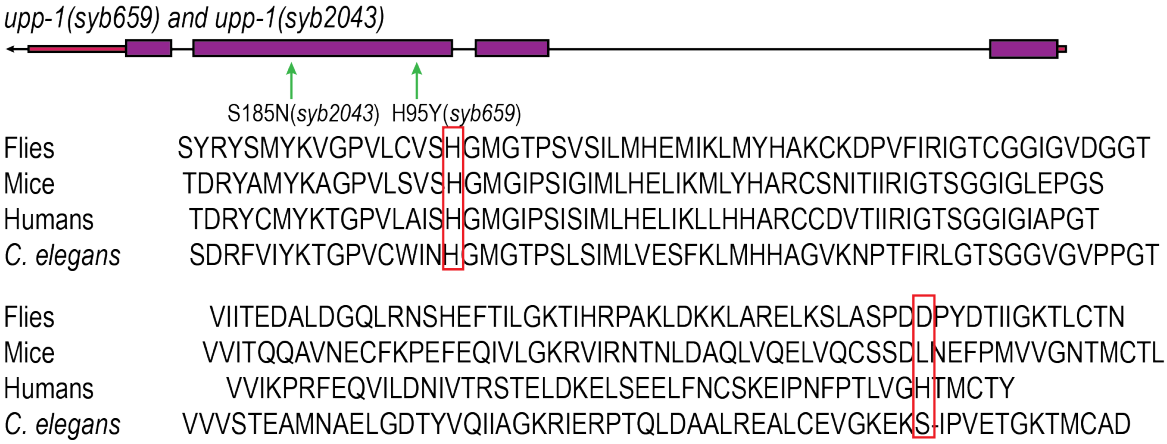

(Figure 10: Refer to page 57 for legend)

C continued

D

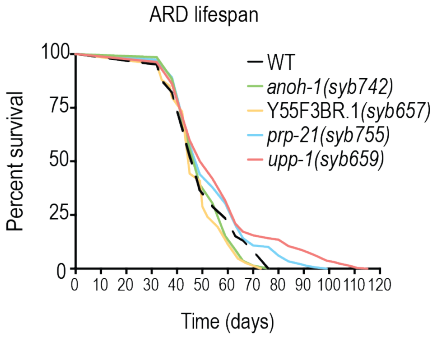

E

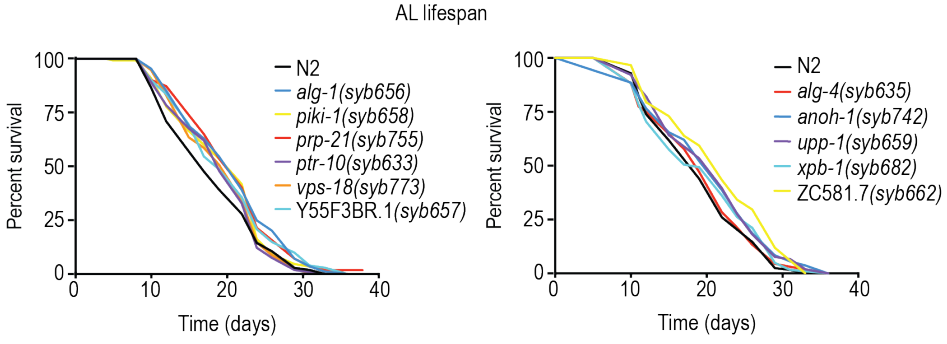

Figure 10. Identification of *upp-1* as a modulator of ARD longevity. A) Table representing the 11 candidate genes identified from whole genome sequencing and analysis of 50 ARD longevity mutants. **B)** ARD lifespan analysis of the 11 candidates showed 4 potential genes with ARD longevity to be further validated, n=1. **C)** Genomic position showing the location of the exact amino acid change

obtained from the original mutagenesis screen and sequence alignments of wild type showing the conserved location of the amino acid change. **D)** *upp-1(syb659)* and *prp-21 (syb755)* are potential regulators of ARD longevity since the mutants showed lifespan extension compared to wild type in ARD (Mantel-Cox Log Rank test, n=3, refer to appendix table 4 for statistics). **E)** *upp-1(syb659)* and *prp-21 (syb755)* also exhibited lifespan extension under AL conditions (Mantel-Cox Log Rank test, n=2, refer to appendix table 4 for statistics).

6.2.2 Characterisation of *upp-1* as a regulator of ARD longevity

UPP-1 is a uridine phosphorylase enzyme, a key regulator of pyrimidine metabolism, which catalyses the conversion of uridine to uracil and ribose phosphate (Yan et al., 2006). The *C. elegans* enzyme exhibits both uridine and thymidine phosphorylase activity (S. Kim et al., 2009) (Figure 11A & F) . The original *upp-1(syb659)* mutation resides in a conserved residue, causing H95Y change. We also obtained an independent allele of this gene from our screen that causes a S185N change in a conserved residue. We generated this other mutation, *upp-1(syb2043),* via CRISPR-Cas9 and measured ARD lifespan. As expected, I also observed robust extension of ARD lifespan with *upp-1(syb2043)*, further extending max lifespan by 0.7 fold compared to wild type, which was comparable to the first allele of *upp-1(syb659)* (Figure 11B), further validating the role of *upp-1* in ARD longevity. While this work was in progress, a study came out demonstrating how intermediates of pyrimidine metabolism, including uridine and thymine, can increase the lifespan of *C. elegans*, and knockdown of *upp-1* via RNAi leads to lifespan extension under AL conditions (Wan et al., 2019).

I next asked if *upp-1(syb569)* would affect the ability to emerge from ARD by recovering worms at day 30, 60 and 90 and measuring their brood size. The splicing factor*, prp-21*, was also included since it also displayed ARD longevity. Even after 90 days of starvation, 10% of recovered *upp-1* mutants were still able to produce progeny, suggesting not only increased ARD survival but enhance recovery (Figure 11C). Surprisingly, *prp-21* mutants survived but did not recover after 60 days of ARD to produce progeny, suggesting a role of this splicing factor for ARD longevity but not recovery. As ARD lifespan progresses, wild type

worms exhibit age related physiological changes such as muscle deterioration, body shrinkage and cuticle wrinkling. Mutation in *upp-1* appeared to delay these morphological changes compared to wild type even after 60 days of ARD. Deterioration of pharyngeal tissue is slower in *upp-1* mutants and appears less degraded compared to wild type (Figure 11D).

To understand the effect of our *upp-1* mutant in regulating ARD longevity, we performed metabolomic analysis of *upp-1* mutant animals after 10 days of ARD. Strikingly, the levels of uridine and thymine were significantly increased >10 fold in *upp-1* mutants compared to wild type in ARD (Figure 11E) suggesting a loss of function mutation of *upp-1*.

Given the accumulation of thymine and uridine in the mutant background, I next asked whether the supplementation of these compounds could mimic the effect of *upp-1* mutation and extend ARD longevity. I therefore performed ARD ageing analysis with supplemented uridine and thymine at concentrations of 0mM, 0.5mM and 1mM. Supplementation of 1mM thymine increased wild type but not *upp-1* mutant lifespan (Figure 11G) revealing that thymine enhances ARD survival and functions through the same pathway as the *upp-1* mutant to regulate ARD longevity. Uridine also had a similar but smaller effect.

Altogether, these results suggest a role for pyrimidine metabolism in regulating ARD longevity, which can be manipulated genetically, via the *upp-1* mutant, and supplementation of pyrimidine intermediates. Since *upp-1(syb659)* mutants also displayed decreased levels of uracil and thymidine (Figure 11E), it would be important to test if supplementation of these metabolites would decrease *upp-1* or WT ARD lifespan. Interestingly, we also observed that several other metabolites were altered in the *upp-1* background, including elevated NAD levels and related metabolites.

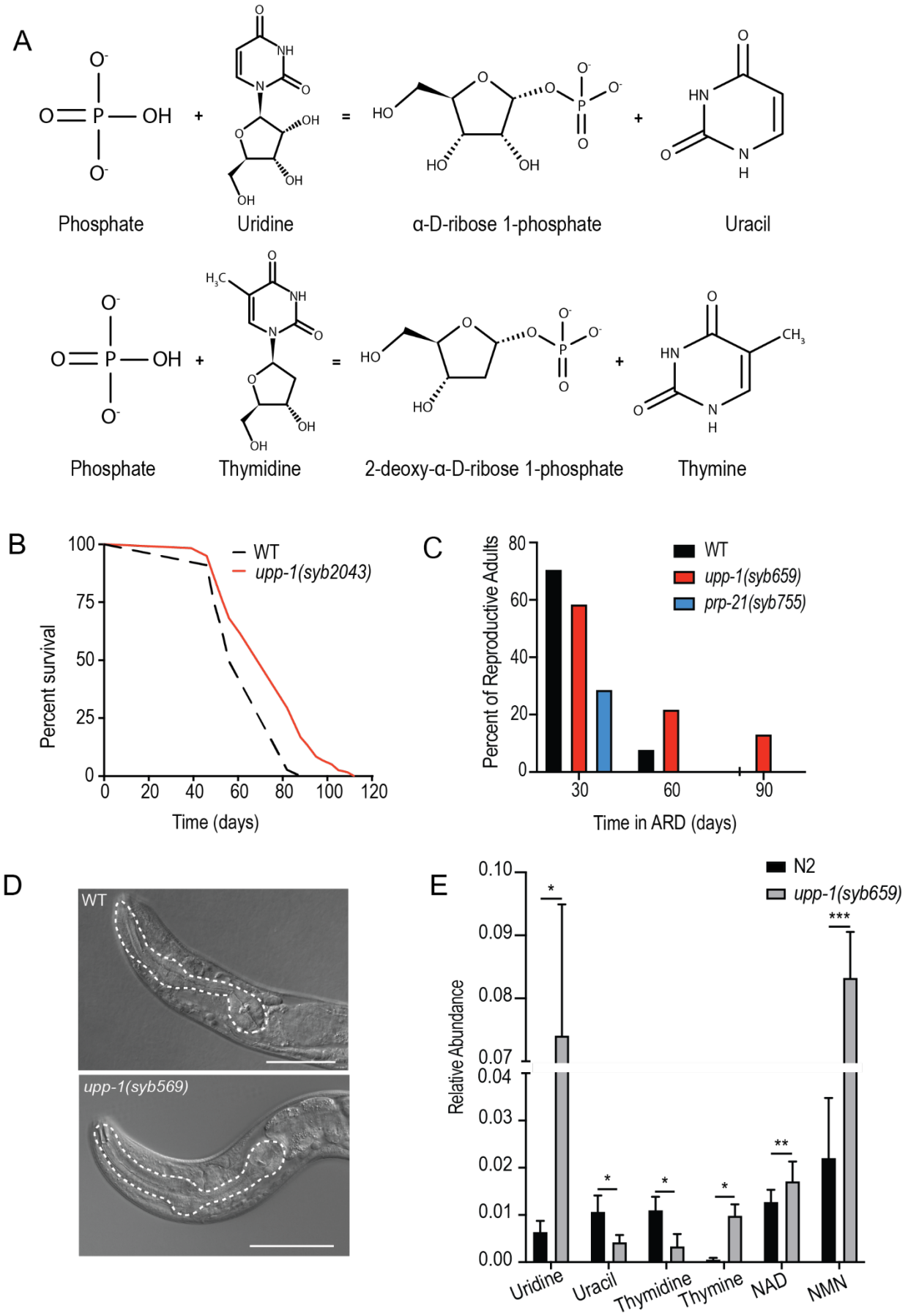

(Figure 11: refer to page 61 for legend)

F

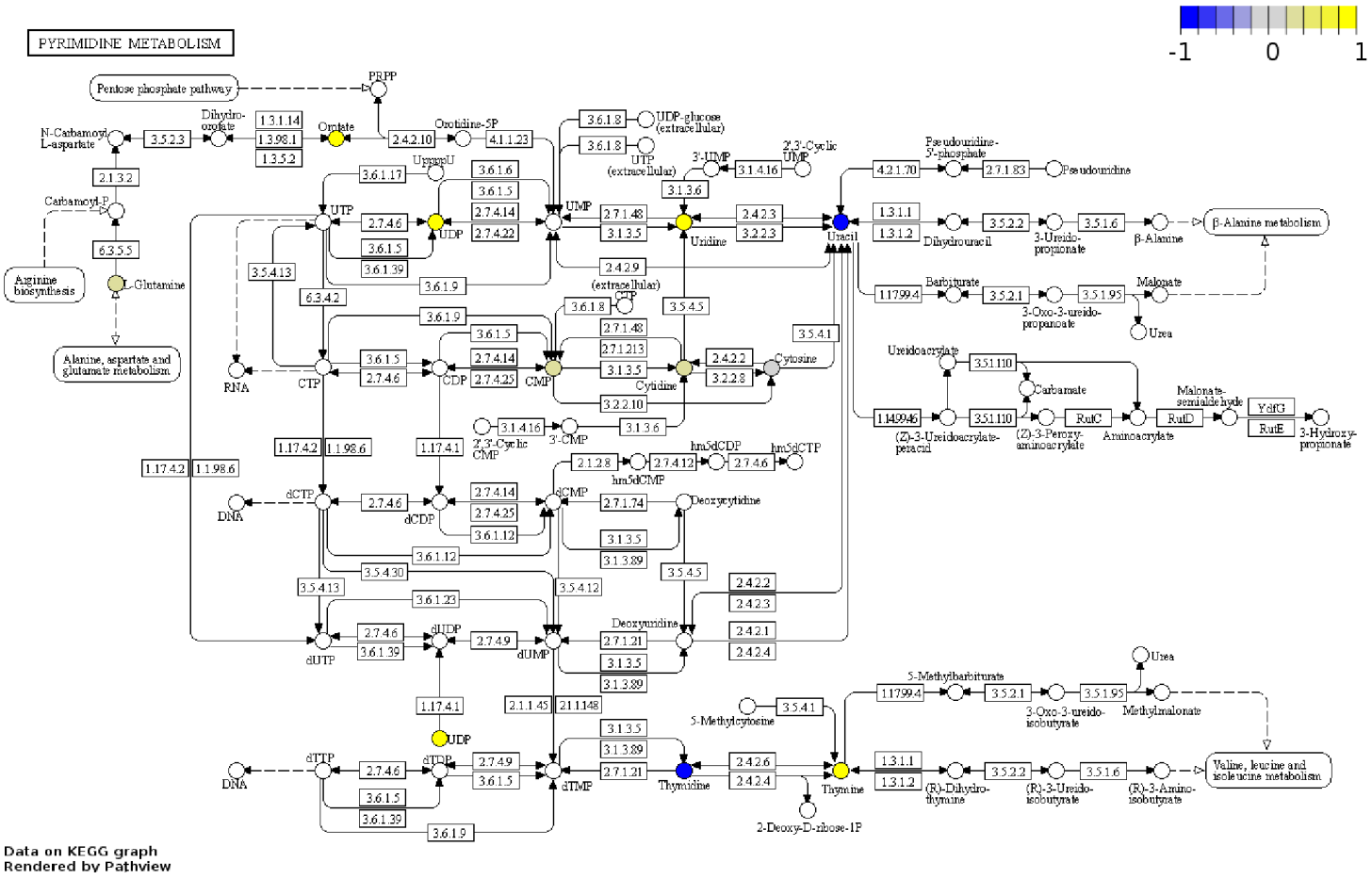

G

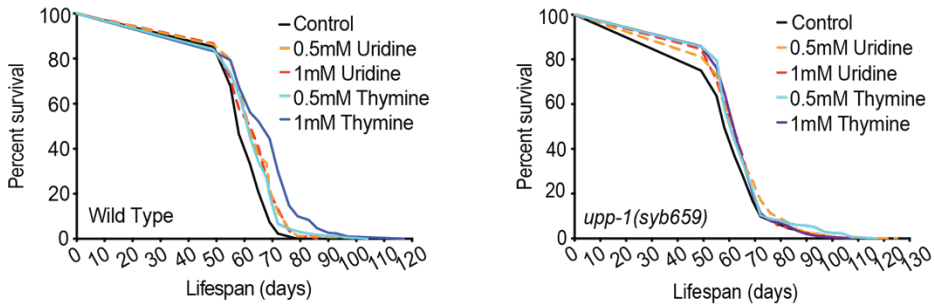

Figure 11. Characterisation of *upp-1* as a regulator of ARD survival. A) *upp-1* in *C. elegans* exhibits both uridine and thymidine phosphorylase activity, catalysing the conversion of uridine to uracil and ribose phosphate, and thymidine to thymine and ribose phosphate respectively. **B)** The second *upp-1* allele obtained from the mutagenesis screen, *upp-1(syb2043)*, showed ARD lifespan extension compared to wild type (Mantel-Cox Log Rank test, n=2, refer to appendix table 4 for statistics). **C)** Brood size measurement showed *upp-1(syb659)* but not *prp-21 (syb755)* had improved progeny production upon exit from ARD in comparison to WT (n=1). **D)** Representative photos of the pharynx of *upp-1(syb659)* (right) in ARD compared to WT (left) after 60 days of ARD using 63X DIC microscopy. Scale bars 50 μm. **E)** Comparison of metabolomics profiles of *upp-1(syb659)* versus WT after 10 days of ARD showed increased levels of uridine, thymine, NAD and NMN, and decreased levels of uracil and

thymidine. Significance was assessed using t-test * p<0.5, **p<0.01, ***p<0.001 (n=5). **F)** KEGG pathway analysis performed using Pathview showing the complete pyrimidine metabolism. Coloured circle represents changes in *upp-1* mutants compared to wild type. **G)** Supplementation of thymine increased WT lifespan but failed to further increase *upp-1(syb659)* lifespan (Mantel-Cox Log Rank test, n=2, refer to appendix table 4 for statistics).

6.3 Mechanism of *hlh-30* in regulating ARD survival

6.3.1 Suppressor screen to identify factors involved in *hlh-30* ARD survival

HLH-30/TFEB is a conserved regulator of autophagy, lysosome biogenesis, and fat metabolism (Lapierre et al., 2013; O'Rourke & Ruvkun, 2013; Settembre et al., 2011) that integrates signalling from multiple longevity pathways (Lapierre et al., 2013). Our laboratory recently identified HLH-30 as a master regulator of ARD. Mutants of *hlh-30* exhibited a dramatic reduction of mean lifespan, rapid reduction in body length, loss of body fat, reduced oxygen consumption and the inability to recover from ARD and produce progeny. These findings suggests an essential role of HLH-30 in regulating ARD survival, morphogenesis and recovery (B. Gerisch et al., 2020). To explore the mechanism by which HLH-30 modulates ARD survival, we took advantage of the short ARD lifespan of *hlh-30* mutants and performed an unbiased suppressor screen to identify mutants rescuing the shortevity. Similar to the longevity screen described above, we performed EMS mutagenesis in a *hlh-30(tm1978)* mutant background before ARD induction and screened for mutants surpassing the ARD lifespan of *hlh-30* mutants (Figure 12A). After isolating mutants rescuing *hlh-30(tm1978)* ARD shortevity, we performed whole genome sequencing and galaxy analysis to identify putative lesions, including stop codons and frameshift mutations. We cross referenced the different point mutants for the appearance of allelic hits within the same genes. We validated the candidate genes by generating double mutants with *hlh-30(tm1978)* and examining the rescue of *hlh-30(tm1978)* phenotypes in ARD.

In the initial screen, we found that several of the mutants exhibited a Daf-c phenotype in ad libitum conditions at 25°C. Therefore, we concentrated on Daf-

c genes in the sequencing analysis. This identified singleton mutations in *daf-1* (TGF-β receptor subtype 1 of the TGF-β pathway) and *pdk-1* (phosphoinositide dependant protein kinase of the IIS pathway) as potential candidate suppressors of *hlh-30* in ARD (Figure 12B & C) In *daf-1*, we obtained a G203E change, a non-conserved residue of the extracellular domain. In *pdk-1*, we found a R85STOP located near to the N-terminus that is presumed null. In a second genetic screen, we obtained another mutation in *daf-1* (R631W) confirming this locus as important for survival.

A

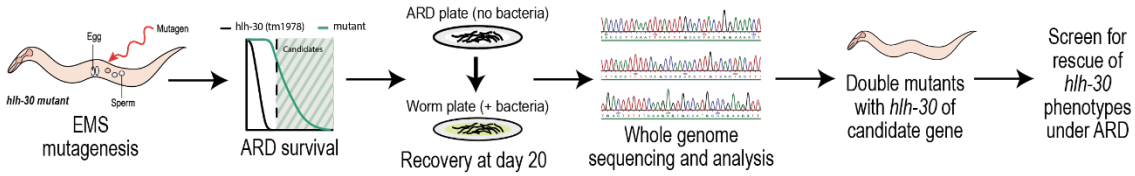

B

Chromosome	Gene ID	Gene Name	Effect	Old AA/New AA	Nucleotide Change
IV	F29C4.1	*daf-1*	Non-synonomous	G203E	G>A
IV	H42K12.1	*pdk-1*	Stop Gained	R156STOP	C>T

C

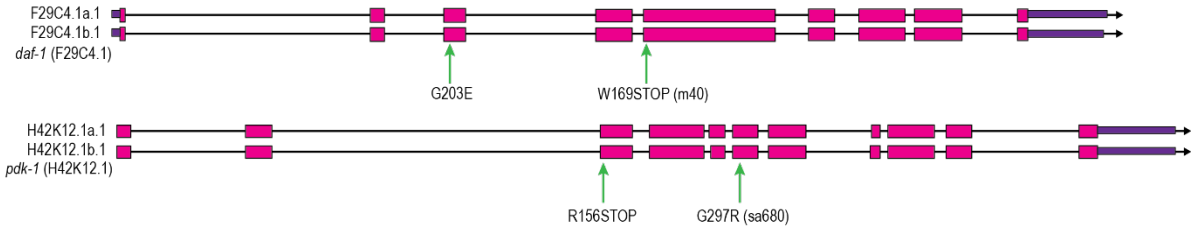

Figure 12. Identification of *daf-1* and *pdk-1* as factors modulating *hlh-30* ARD lifespan. A) EMS screen workflow to identify mutations that extends *hlh-30* ARD lifespan. **B)** Table summarising the mutations of *daf-1* and *pdk-1* obtained from the *hlh-30* suppressor screen. **C)** Schematic overview showing *daf-1* and *pdk-1* loci of the SNPs obtained from the screen reference alleles of *daf-1(m40)* and *pdk-1(sa680)* which were mainly used for this thesis.

A second suppressor screen was conducted to gain further insight into the mechanism of *hlh-30* in ARD. From this screen we isolated 213 mutants with longevity against *hlh-30(tm1978)*. After validating the rescue of the *hlh-30* short lived phenotype, 14 of the 213 mutants were shown to extend the lifespan of *hlh-30* in ARD. We tested these mutants for a Daf-c phenotype, performed whole genome sequencing and SNP analysis, concentrating on SNPs inducing missense, nonsense, frame shift and stop gained mutations, which were also

conserved and within a conserved domain to identified potential factors that suppress *hlh-30* in ARD (Figure 13A & B).

A

Name	% Survival (Day 20)	Daf-c?	Other Phenotypes
37-2.1	50	N	
39-2.2	50-60	Y	Slow growing
40-2.1	80	N	
43.3	90	Y	
51.2	50	Y	
51.3	60-70	Y	
67.2	60	N	Slow growing
70.3	50	N	
71-2.2	60	N	
87.3	60	Y	Egg-laying defect
104.B	80	N	
109.3	60	N	
A1.1	50	Y	
I4	60	N	

B

Chromosome	Gene name	Effect	Old AA/New AA	Function
V	C09H5.7	Non-synonomous	S/F	Protein serine/threonine phosphatase activity
X	*ceh-60*	Non-synonomous	G/E	Homeodomain containing transcription factor
X	*daf-3*	Non-synonomous	E/K	Co-Smad
IV	*lep-2*	Non-synonomous	G/E	Ortholog of the Makorin (Mkrn) family of proteins
I	*let-363*	Non-synonomous	D/N	Ortholog of the human mTOR
III	*tax-4*	Stop Gained	W/*	Subunit of the cGMP-gated ion channel
III	*mxl-2*	Non-synonomous	G/R	Ortholog of human Mlx
III	*pde-2*	Non-synonomous	S/G, A/P	Ortholog of human PDE2A (phosphodiesterase 2A)
X	*cgt-2*	Non-synonomous	M/I	Ortholog of human UDP-glucose ceramide glucosyltransferase
II	*fgt-1*	Non-synonomous	E/K	Ortholog of human SLC2A3 (solute carrier family 2 member 3)

Figure 13. Second *hlh-30* suppressor screen identifies additional candidates for *hlh-30* ARD regulation. A) Mutants obtained from the second *hlh-30* suppressor screen. **B)** Potential candidates identified after whole genome sequencing, to be tested for supressing *hlh-30* ARD shortevity.

6.3.2 Components of TGF-β and IIS signalling rescues *hlh-30* ARD phenotypes

To test if *daf-1* and *pdk-1* were causal for *hlh-30* suppression, we generated double mutants of *daf-1(m40);hlh-30(tm1978)* and *pdk-1(sa680);hlh-30(tm1978)* using the canonical reference alleles, and examined if they rescued the specific phenotypes of *hlh-30* in ARD. We first analysed the ARD lifespan and found that mutations of *daf-1* and *pdk-1* significantly increased *hlh-30(tm1978)* lifespan in ARD, from 10 days to 50 days, representing a 5 fold increase (Figure 14A) though not to the level of wild type. *hlh-30(tm1978)* mutants also show significant loss of neutral lipids after 48hr of ARD (B. Gerisch et al., 2020). We therefore performed BODIPY staining in the double mutants and saw that *daf-1* and *pdk-1* rescued the loss of fat in *hlh-30(tm1978)* almost back to WT levels (Figure 14B). *hlh-30* mutants also exhibit a dramatic shrinkage in body size, mutation of *daf-1* and *pdk-1* partially rescued this phenotype as well (Figure 14C). Lastly, *hlh-30(tm1978)* mutants fail to recover from ARD and produce progeny. Surprisingly, *daf-1* mutants but not *pdk-1* mutants restored the brood size of *hlh-30(tm1978)* animals recovered from ARD (Figure 14D). Altogether these results show that both *daf-1* and *pdk-1* enhance survival of *hlh-30* in ARD but that *daf-1* appears to play a greater role in recovery and progeny production upon ARD exit in *hlh-30(tm1978)* mutants.

DAF-1 and PDK-1 are both critical factors of TFG-β signalling and insulin/IGF-1 signalling respectively. We next investigated whether other components in these pathways influence *hlh-30* ARD survival. We constructed double mutants of *hlh-30* with *daf-7*, encoding the TGF-β ligand, and *daf-2*, encoding the IIS receptor. First, we measured ARD lifespan and observed that *daf-7* and *daf-2* loss of function mutations increased *hlh-30* ARD lifespan by 20% and 9% respectively, though not to the same extent *daf-1* and *pdk-1* mutations (Figure 14E). Second, we examined fat content by BODIPY staining and observed that *daf-7(e1372)* and *daf-2(e1368)* restored levels of fat in *hlh-30* mutant, similar to *daf-1(m40)* and *pdk-1(sa680)* (Figure 14F). Brood size assays to measure progeny production upon ARD recovery yielded results comparable to *daf-1(m40)* and

pdk-1(sa680), where *daf-7(e1372)* partially rescued the brood size of *hlh-30* mutants to WT, but *daf-2;hlh-30* double mutants were unable to produce progeny upon recovery from ARD (Figure 14H). Lastly, mutations in *daf-7* and *daf-2* prevented the shrinkage in body size of *hlh-30(tm1978)* in ARD (Figure 14G). These results further validate the involvement of the TGF-β and IIS signalling pathways in *hlh-30* ARD survival and recovery.

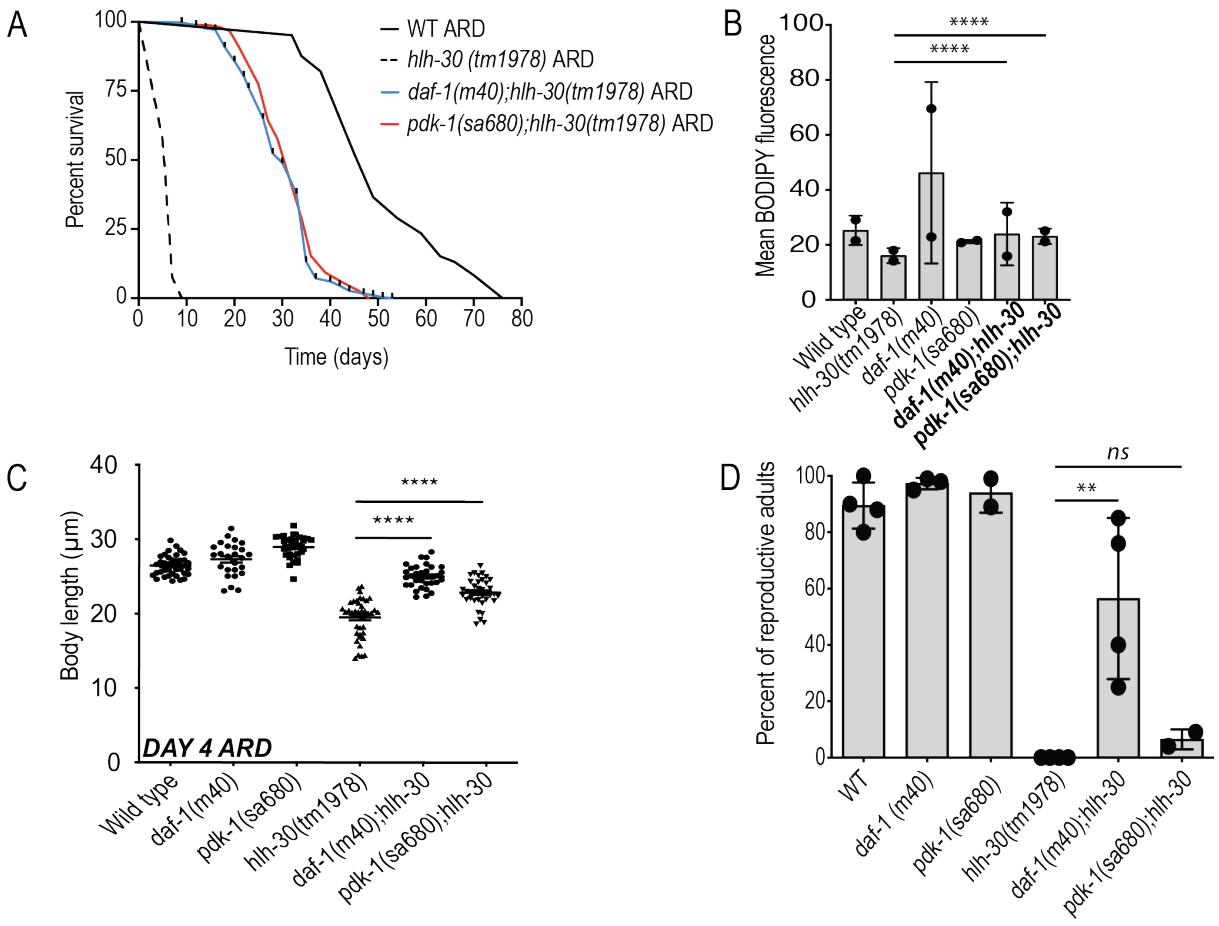

(Figure 14: refer to page 67 for legend)

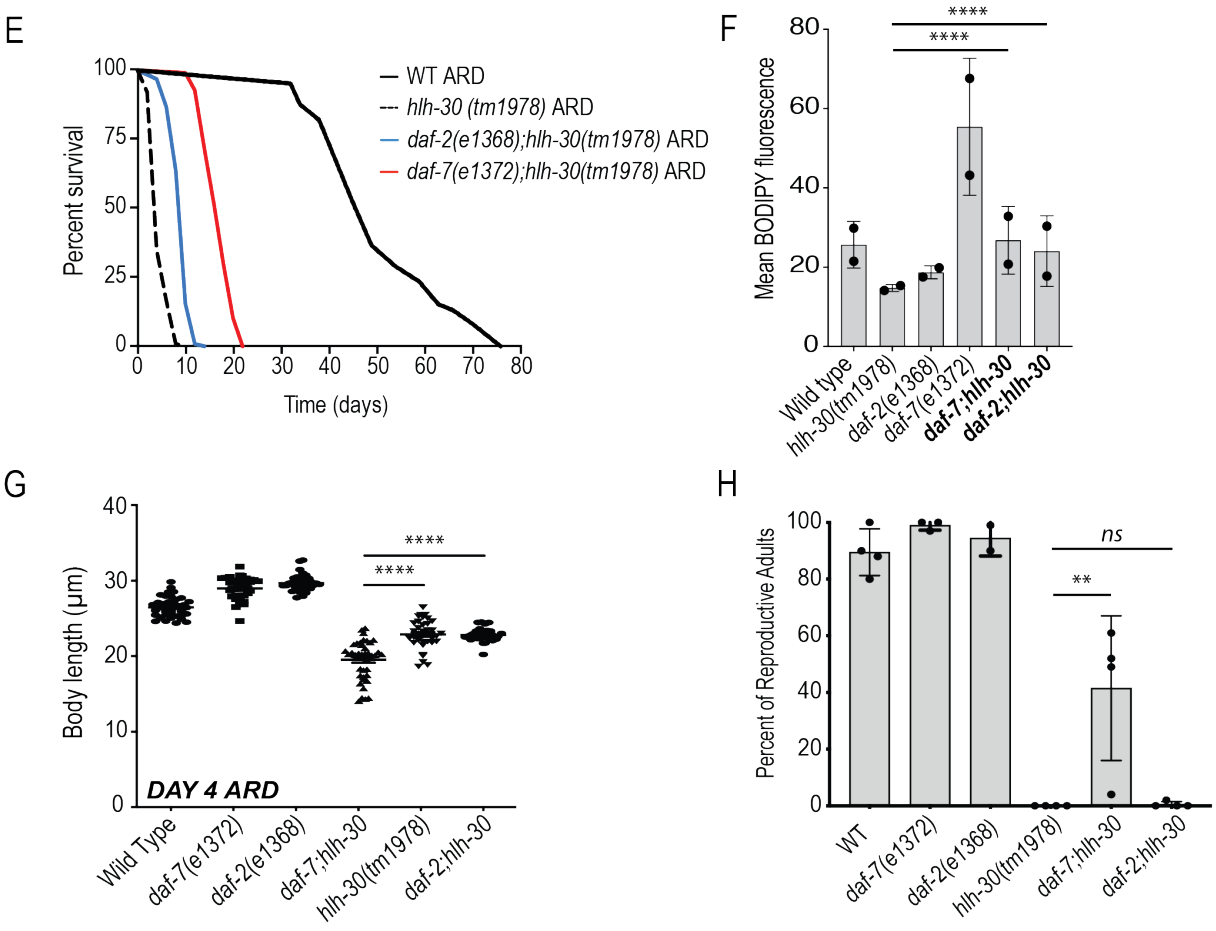

Figure 14. TGF-β and IIS signalling mutants restore *hlh-30* survival and recovery. A) *daf-1(m40)* and *pdk-1(sa680)* rescue the short lifespan of *hlh-30(tm1978)* in ARD (Mantel-Cox Log Rank test, n=3). **B)** *daf-1(m40)* and *pdk-1(sa680)* restore the loss of neutral lipids associated with *hlh-30* mutants in ARD measured by bodiPY staining and using the Biosorter after 48hr in ARD, (n=2). Each dot represents one experiment (600 worms per experiment), error bars indicate SEM, anova test, **** p<0.0001). **C)** *daf-1(m40)* and *pdk-1(sa680)* increase the body size of *hlh-30* mutant at day 4 ARD. Images of worms were taken using 40X DIC microscope and the length was determined using image J. (n=2, each dot represents one worm, >25 worms used per experiment, error bars indicate SEM, t-test, **** p<0.0001). **D)** Brood size assays reveal that *daf-1(m40)* but not *pdk-1(sa680)* promotes recovery of *hlh-30* mutants after 24hr of ARD. (n=2, each dot represents one experiment, 60 worms per experiment), error bars indicate SEM, t-test, **p<0.079). The same analysis was conducted for *daf-7(e1372)* and *daf-2(e1368)* and yielded similar results to *daf-1(m40)* and *pdk-1(sa680)* respectively for E) lifespan, F) bodiPY staining, G) body size and H) brood size. **E – H**) Experiments with *daf-7(e1372)* and *daf-2(e1368)* were conducted the same way as with *daf-1(m40)* and *pdk-1(sa680)* using the same statistical tests.

6.3.3 TGF-β signalling depends on downstream transcription factors to rescue *hlh-30* ARD phenotypes

From the previous results, we speculated TGF-β signalling had a greater impact on *hlh-30* ARD survival than IIS signalling since downregulation *of daf-1* and *daf-7* rescued *hlh-30(tm1978)* phenotypes not only during ARD but also upon ARD recovery. Therefore, we decided to focus on unravelling how TGF-β signalling is involved in *hlh-30* survival and recovery in ARD. As previously described, DAF-7 interacts with receptor subtypes, DAF-1 and DAF-4, to induce the phosphorylation of DAF-8 and DAF-14, resulting in their nuclear localisation and inhibiting the function of DAF-3 and DAF-5 (da Graca et al., 2004; Estevez et al., 1993; Georgi et al., 1990; Inoue & Thomas, 2000; Patterson et al., 1997; Ren et al., 1996). We conducted epistasis experiments to observe if the effect of *daf-1* on *hlh-30(tm1978)* operated through *daf-3* or *daf-5*. I constructed triple mutants of *daf-1;hlh-30;daf-3* and *daf-1;hlh-30;daf-5* and measured the ARD lifespan. I found that the loss of *daf-3* and *daf-5* completely abolished the increased ARD lifespan of *daf-1;hlh-30* to *hlh-30(tm1978)* ARD lifespan (Figure 15A). Previous reports have shown that the TGF-β pathway regulates also longevity via insulin signalling by inducing nuclear localisation of DAF-16 and transcription of DAF-16 target genes (Shaw et al., 2007). We speculated TGF-β also operates via a similar mechanism in *hlh-30* mutants in ARD. I conducted epistasis experiments using triple mutants of *daf-1;hlh-30;daf-16* and measured ARD lifespan. Interestingly, I found that the triple mutant lifespan was comparable to *hlh-30* lifespan in ARD (Figure 15A) suggesting ARD lifespan increase of *hlh-30* mutants by *daf-1* downregulation is dependent on *daf-16*. We also found that *daf-3(e1376)* and *daf-5(e1386)* showed a similar ARD lifespan compared to wild type, however *daf-1(m40)* showed a 1.7 fold increase in ARD lifespan suggesting a parallel pathway (Figure 15B). The *daf-3(e1376);daf-5(e1386)* also displayed a 0.7 fold increased in ARD lifespan. In summary, this data suggests a crucial role of the full canonical TGF-β pathway in influencing *hlh-30* ARD lifespan, which might ultimately act through *daf-16*.

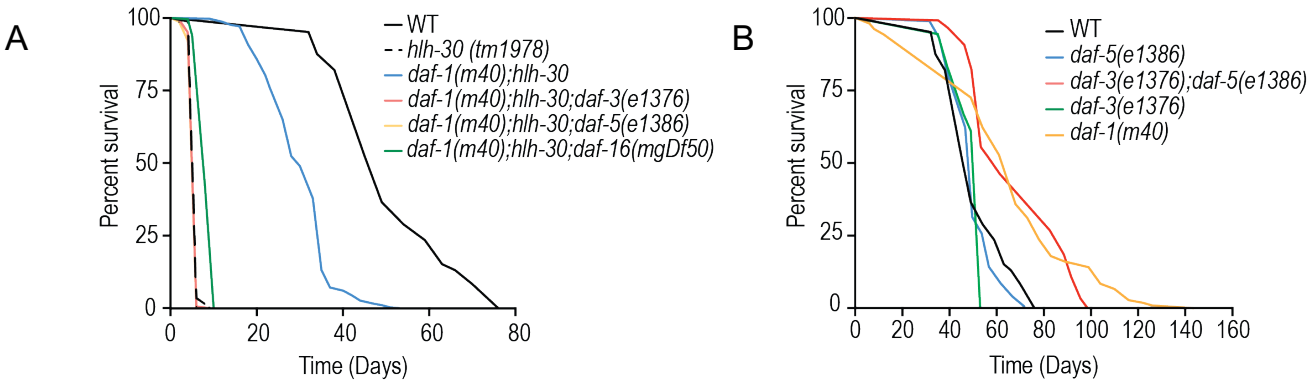

Figure 15. *daf-1* rescue of *hlh-30* ARD lifespan is dependent on downstream transcription factors. A) Triple mutant lifespan analysis of *daf-1;hlh-30;daf-3*, *daf;1;hlh-30;daf-5* and *daf;1;hlh-30;daf-16* abolished the lifespan extension by loss of *daf-1* in *hlh-30(tm1978)* (Mantel-Cox Log Rank test n=2, refer to appendix table 4 for statistics). **B)** ARD lifespan analysis of *daf-3(e1376)*, *daf-5(e1386)*, *daf-1(m40)* and *daf-3(e1376);daf-5(e1386)* (Mantel-Cox Log Rank test n=2, refer to appendix table 4 for statistics).

6.3.4 *hlh-30* regulates TGF-β signalling in ARD

From the results above, we speculated that *hlh-30* might regulate TGF-β signalling. To address this hypothesis we took advantage of a *daf-1p::gfp* transgenic line and crossed it to *hlh-30(tm1978)*, induced ARD and measured green fluorescence using the Copas Biosorter – an apparatus allowing fluorescent analysis of large worm populations, thereby strengthening statistical significance. After 0hr, 24hr and 48hr of ARD, we collected synchronised worms and measured GFP expression in WT and *hlh-30(tm1978)* backgrounds. We discovered at 0hr ARD *hlh-30(tm1978)* already expressed higher levels of green fluorescence compared to WT. After 48hr of ARD, *hlh-30(tm1978)* expressed even higher levels of fluorescence compared to WT (Figure 16A). To explore this hypothesis further, I examined the transcriptional levels of *daf-1* and *daf-7* in *hlh-30(tm1978)* compared to WT at 0hr, 24hr and 48hr of ARD by qPCR. I observed increased mRNA expression levels of *daf-1* (Figure 16B) in *hlh-30(tm1978)* compared to WT at 0hr ARD, which was further enhanced after 48hr in ARD. Together these results suggest *hlh-30* regulates components of the TGF-β signalling pathway in ARD. mRNA expression was normalised to F44B9.5 as this gene was unchanged in AL and ARD conditions.

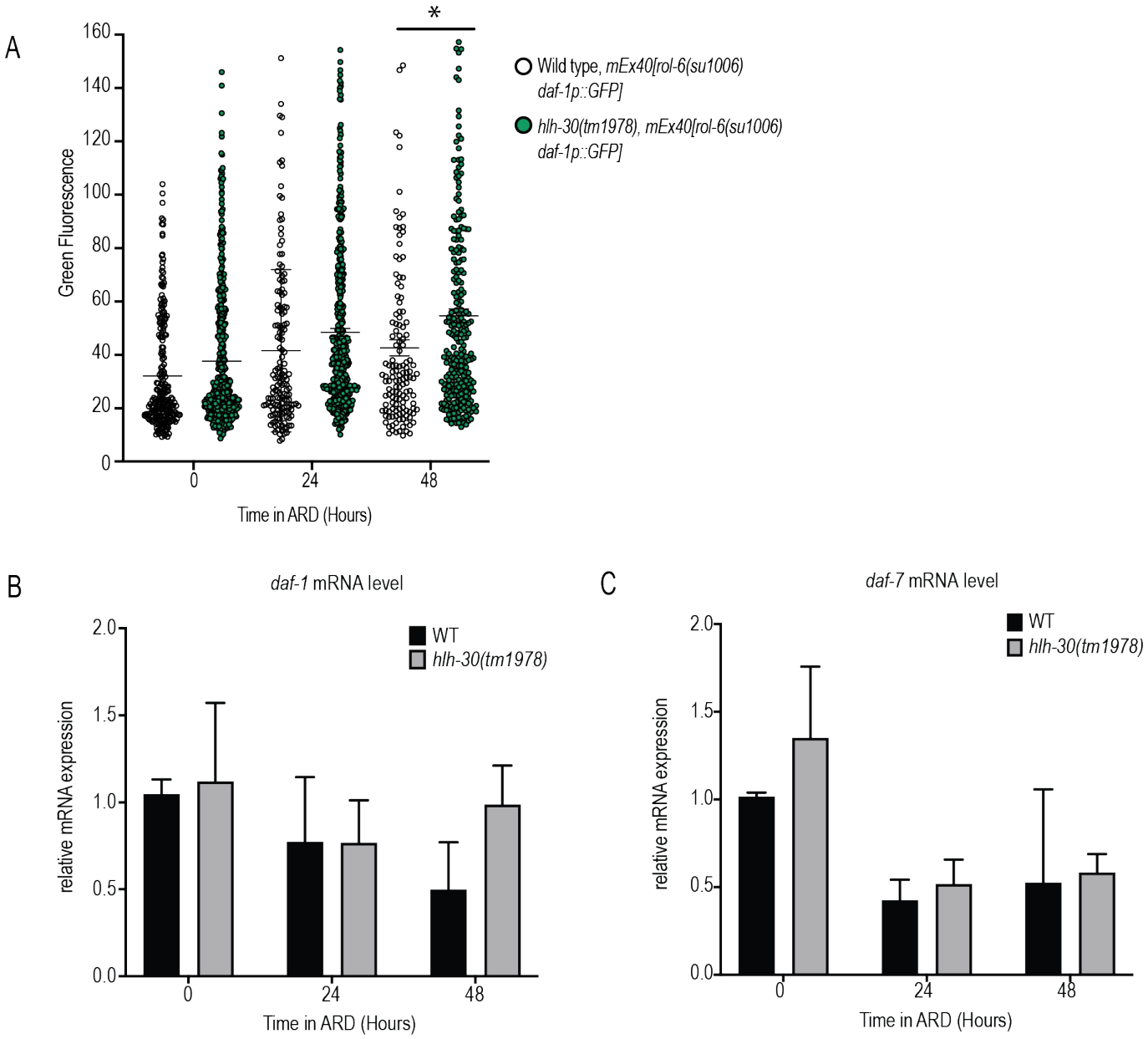

Figure16. *hlh-30* regulates expression of *daf-1* and *daf-7*. A) *hlh-30(tm1978)* regulates expression of *daf-1p::GFP* at 0hr, 24hr and 48hr of ARD measured by the Corpus Biosorter, Each dot represents one worm (n=3, error bar indicting SEM, t-test * p<0.01). Transcript levels of **B)** *daf-1* and **C)** *daf-7* in *hlh-30* mutants at 0hr, 24hr and 48hr of ARD measured by qPCR (n=4, error bar indicates SEM).

6.3.5 Transcriptomic analyses of *hlh-30* and *daf-1* interactions in ARD and upon ARD recovery

Given the effect of TGF-β signalling in *hlh-30* mutants in ARD, we reasoned that the identification of differentially regulated genes and processes upon downregulation of TGF-β in *hlh-30* mutants could shed light on the mechanism

of ARD survival in the absence of *hlh-30*. We took an unbiased global approach and performed transcriptomic analysis comparing N2/WT, *hlh-30(tm1978)*, *daf-1(m40)* and *daf-1;hlh-30* double mutant, after 48hr in ARD and upon 12hr of recovery to capture differences upon ARD and recovery. Principle component analysis revealed clear separation of all genotypes in ARD. However, upon recovery, *daf-1;hlh-30* clustered more closely with WT than *hlh-30* mutants (Figure 17A). Heat maps depicting differentially expressed transcripts of wild type, *hlh-30(tm1978)* mutants and *daf-1(m40);hlh-30(tm1978)* double mutants revealed the similar expression pattern of wild type and *daf-1;hlh-30* double mutant after 48hr in ARD and upon ARD recovery (Figure 17A & B).

A

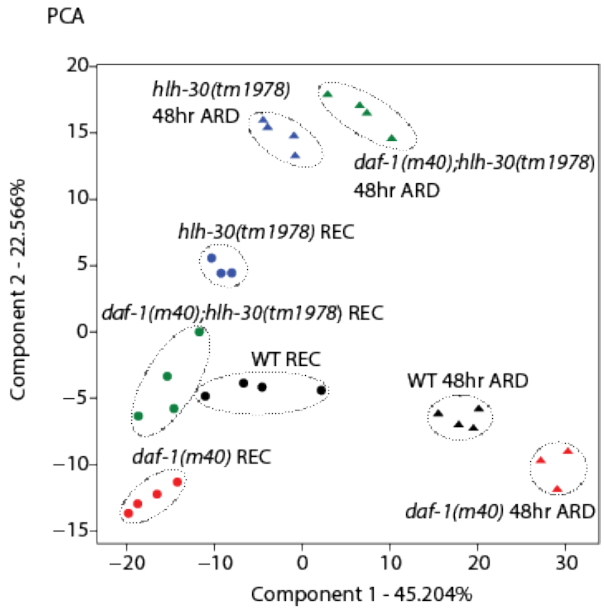

(Figure 17: refer to page 74 for figure legend)

B

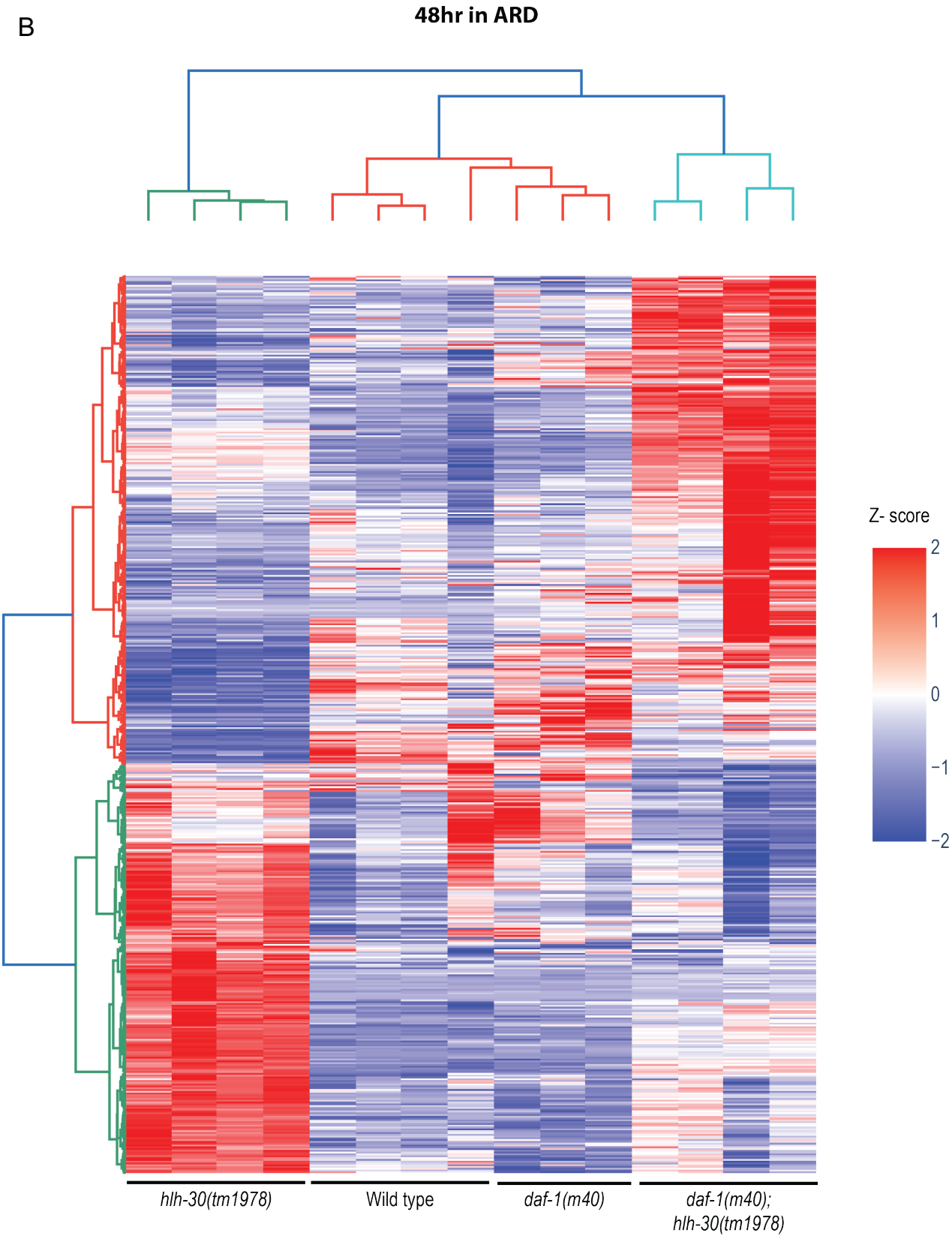

(Figure 17: refer to page 74 for figure legend)

C

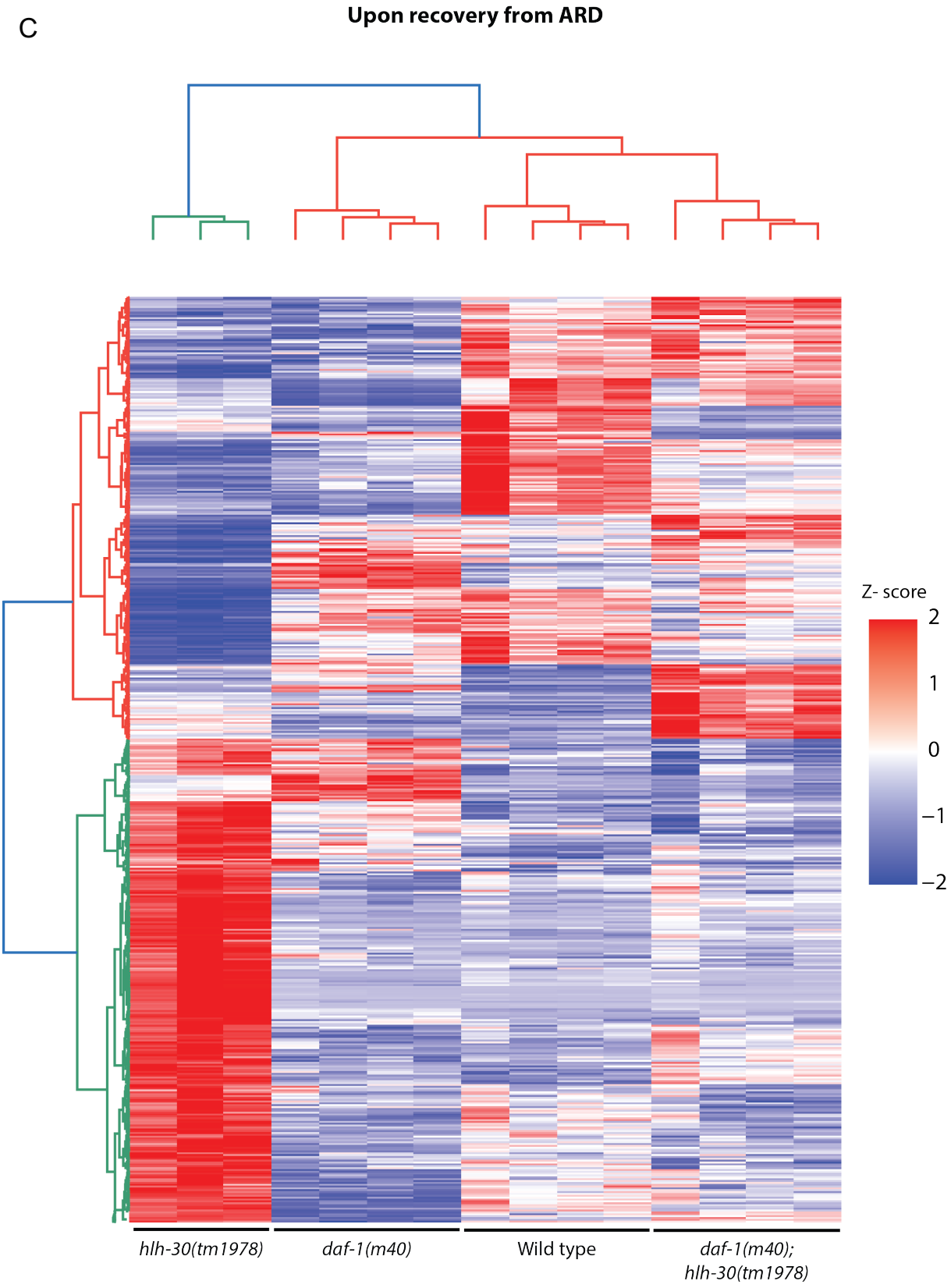

(Figure 17: refer to page 74 for figure legend)

Figure 17. Transcriptomic analysis comparing factors regulating TFG-β signalling in *hlh-30* mutants in ARD and upon recovery. A) Principal component (PC) analysis with replicates showing global transcriptome patterns of *hlh-30* mutants and *daf-1;hlh-30* in ARD and upon ARD recovery. **B)** Heat map of clustered expression profiles of 5365 transcripts in wild type, *hlh-30(tm1978)* and *daf-1(m40);hlh-30(tm1978)* after 48hr in ARD (blue = decrease; white = no change; red = increase). **C)** Heat map of clustered expression profiles of 4353 transcripts in wild type, *hlh-30(tm1978)* and *daf-1(m40);hlh-30(tm1978)* upon ARD recovery (blue = decrease; white = no change; red = increase).

To gain insight into the role of *daf-1(m40)* in *hlh-30* mutants after 48hr in ARD and upon ARD recovery, I analysed the differentially expressed genes (DEGs) between *hlh-30(tm1978)* vs N2 and *daf-1(m40);hlh-30(tm1978)* vs *hlh-30(tm1978)*. In particular I focused on reversal of gene expression reversal between these two datasets. For example I examined genes downregulated in *hlh-30(tm1978)* vs N2 which were then upregulated in *daf-1(m40);hlh-30(tm1978)* vs *hlh-30(tm1978)* and visa versa (Figure 18B & E). I performed this analysis for DEGs after 48hr in ARD and upon ARD recovery. Transcriptomic analysis identified 2648 and 1665 overlapping differentially regulated transcripts between *hlh-30* vs N2 and *daf-1;hlh-30* vs *hlh-30(tm1978)* (significance $p<0.05$) after 48hr in ARD and upon ARD recovery respectively (Figure 18A & D).

I further analysed the overlap for reversal of gene expression (Figure 18B & E) which diagrams the genes oppositely regulated in the different genotypes (quandrants 1, 4). 2648 of genes during ARD and 1665 gene upon recovery showed significant opposite expression, consistent with a profound reversal of phenotype. I then performed GO enrichment analysis to gain an overview of the enriched genes. During ARD, genes downregulated in *hlh-30* vs N2 and then upregulated in *daf-1;hlh-30* vs *hlh-30(tm1978)* were enriched for oxidation-reduction process, carboxylic acid metabolic process and metabolic processes for lipid and flavonoids. Genes upregulated in *hlh-30* vs N2 and then consequently downregulated in *daf-1;hlh-30* vs *hlh-30(tm1978)* were enriched for innate immune response, tRNA aminoacylation for protein translation and regeneration processes (Figure 18G).

Upon ARD recovery, GO enriched terms for immune response, membrane raft and response to bacterium were enriched for genes downregulated in *hlh-30* vs N2 and upregulated in *daf-1;hlh-30* vs *hlh-30(tm1978)*. There was enrichment for carboxylic acid metabolic process, glutamine family amino acid metabolic process and flavonoid metabolic and biosynthetic process for genes upregulated in *hlh-30* vs N2 and then downregulated in *daf-1;hlh-30* vs *hlh-30(tm1978)*. The transcriptomic data shows regulation of similar processes by *daf-1(m40)* in *hlh-30* mutants during ARD and upon ARD recovery (Figure 18H).

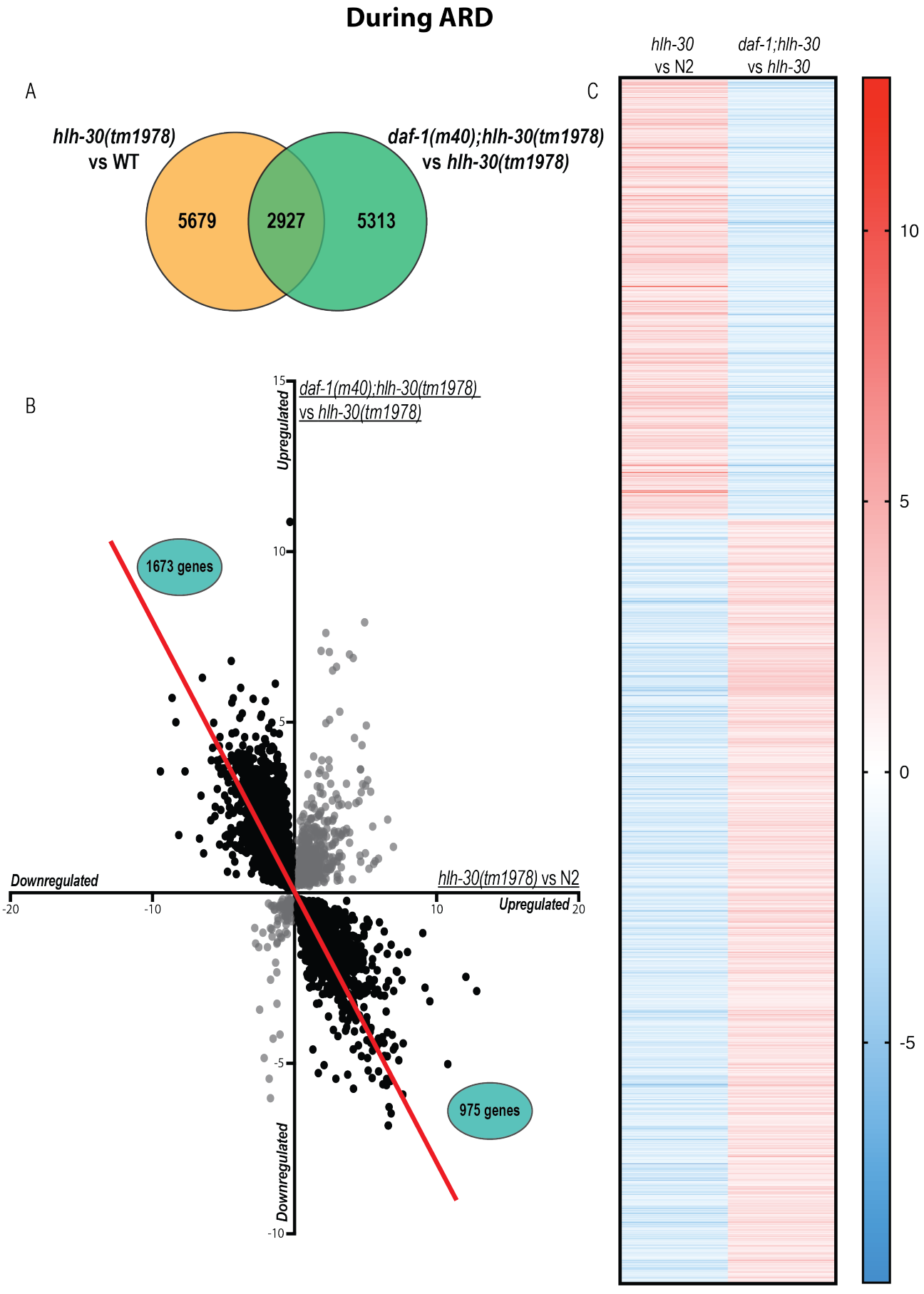

(Figure 18: refer to page 79 for figure legend)

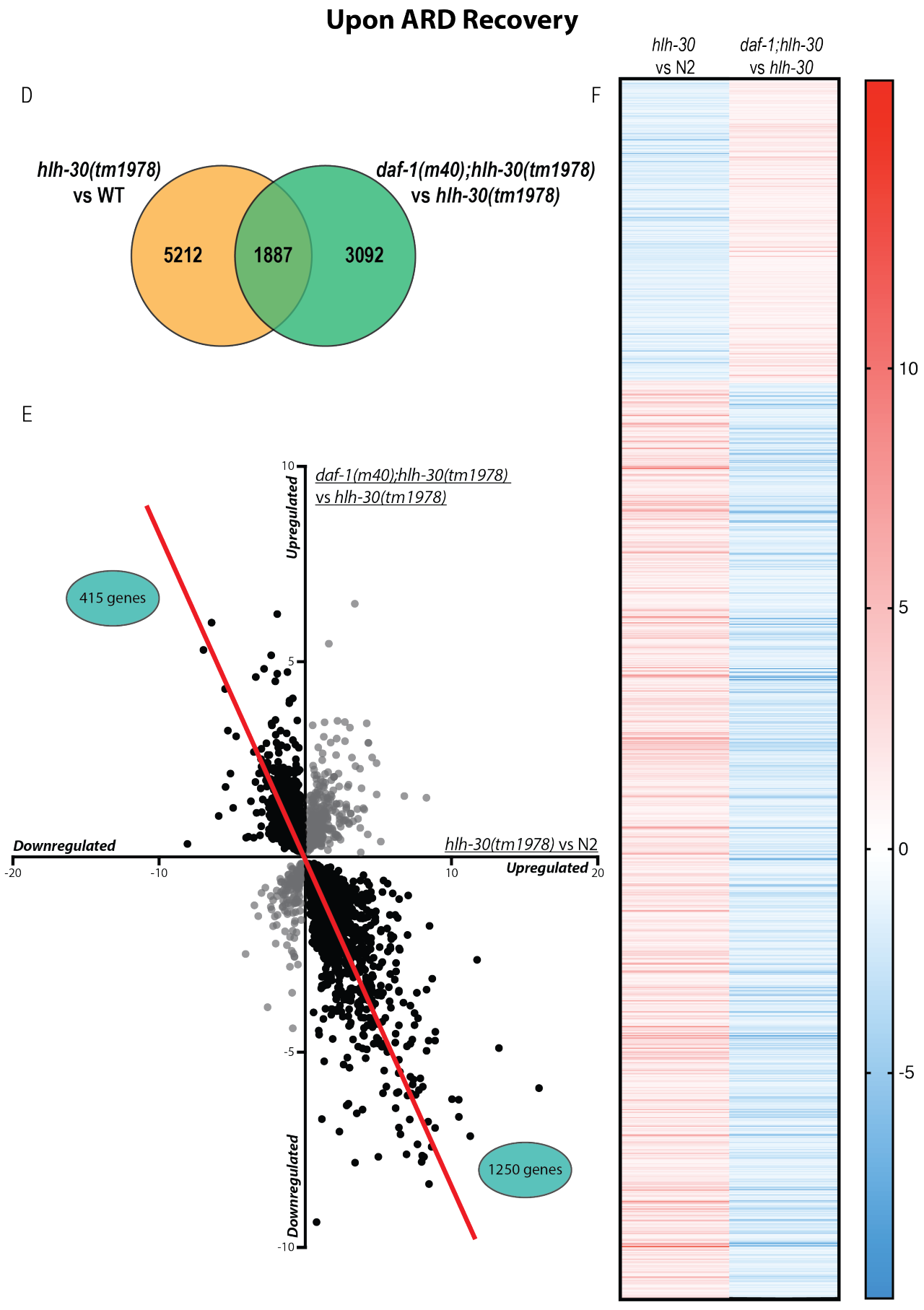

(Figure 18: refer to page 79 for figure legend)

G

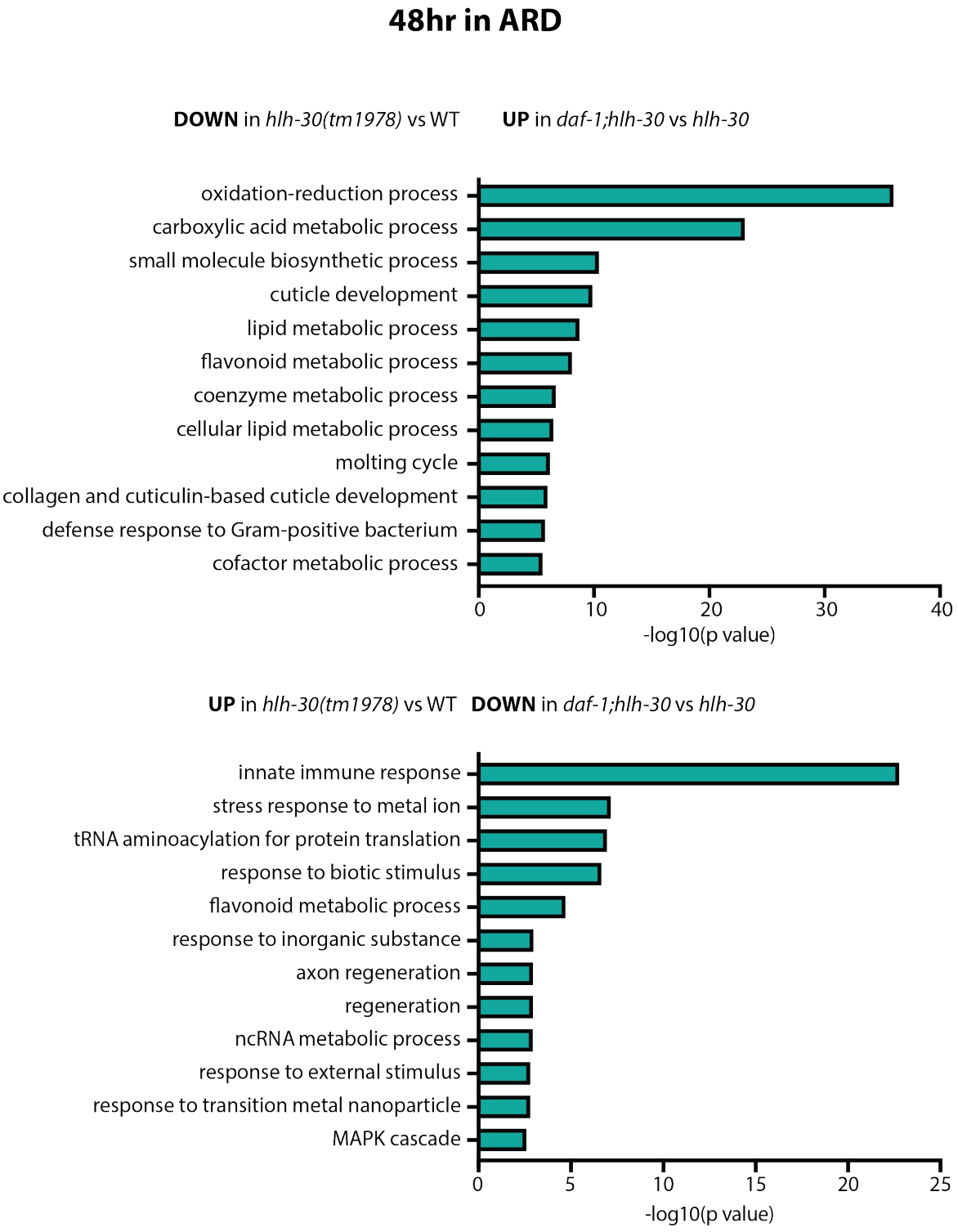

(Figure 18: refer to page 79 for figure legend)

H

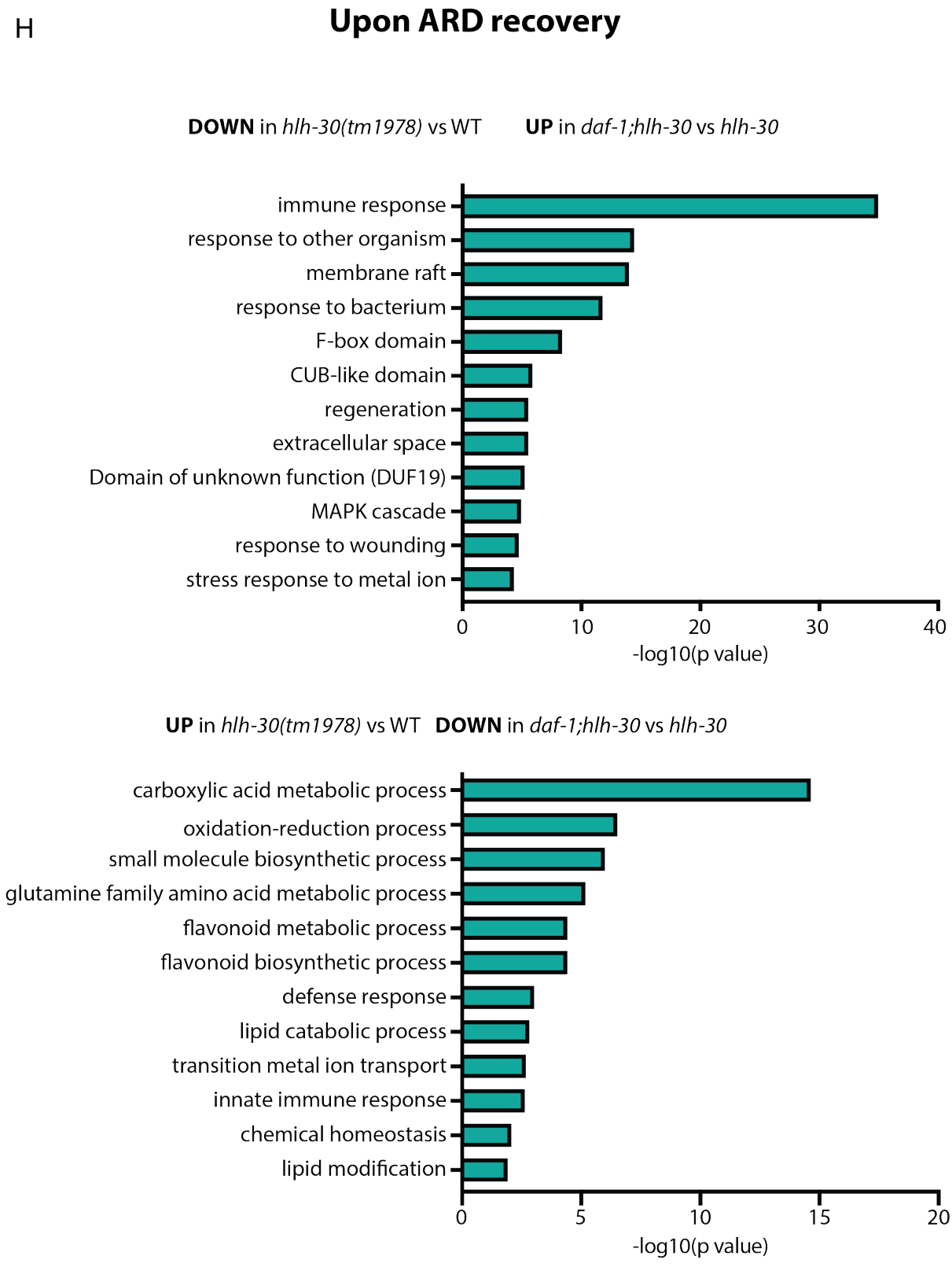

Figure 18. Comparison analysis of *hlh-30(tm1978)* vs WT and *daf-1;hlh-30 vs hlh-30* during ARD and upon recovery. A and D) Venn diagram representation of differentially expressed genes and common genes between *hlh-30(tm9178)* vs WT and *daf-1(m40);hlh-30(tm1978) vs hlh-30(tm1978)* during ARD (A) and upon recovery (D) (significance $p<0.05$). **B and E)** Scatter

plot of common differentially expressed genes in *hlh-30(tm9178)* vs WT and *daf-1(m40);hlh-30(tm1978) vs hlh-30(tm1978)*. X axis represents DEGs in *hlh-30(tm9178)* vs WT (left side = downregulation; right side = upregulation). Y axis represents DEGs in *daf-1(m40);hlh-30(tm1978) vs hlh-30(tm1978)* (top, upregulation; bottom, downregulation) during ARD (B) and upon recovery (E). Horizontal line represents genes of interest. **C and F)** Heat maps representing reversal of gene expression by *daf-1(m40)* in ARD (C) and upon recovery (F). **G and H)** GO enrichment term analysis for significantly changed genes during ARD (G) and upon recovery (H).

Work performed in our laboratory previously characterising ARD identified several genes involved in ARD survival (B. Gerisch et al., 2020). To gain insight if these genes were involved in the enhanced survival of *hlh-30* mutants by mutations on *daf-1*, I cross-referenced these genes with the overlapping DEGs between *hlh-30* vs N2 and *daf-1;hlh-30* vs *hlh-30(tm1978)* after 48hr in ARD and upon ARD recovery. Interestingly the extended HLH network factors, *mdl-1* and *mxl-3*, which are required for ARD survival, were downregulated in *hlh-30* mutants compared to wild type. This effect was reversed in *daf-1;hlh-30* compared to *hlh-30(tm1978)* which upregulated their expression 2 fold during ARD. This effect also occurs during ARD recovery but to a lesser extent suggesting a stronger role of these factors during ARD survival than in recovery. Similarly, *aak-2* also required for ARD survival, was downregulated in *hlh-30* but upregulated in *daf-1;hlh-30.* (Figure 19).

The expression of the lysosome lipase, *lipl-3*, exhibited similar patterns of regulation during ARD and upon recovery. *lipl-3* is downregulated in *hlh-30* mutants compared to WT but was upregulated 4 fold in *daf-1;hlh-30* compared to *hlh-30(tm1978)*. Another component of fat metabolism, *fat-5*, a fatty acid desaturase, also revealed a similar pattern of expression to *lipl-3* but to a lesser degree. Other fat metabolism genes *acs-2*, encoding an acyl-CoA synthetase, and *pod-2*, a, acetyl-CoA carboxylase, were only regulated during ARD and not upon recovery. (Figure 19)

Collectively, this data sheds lights on processes regulated during ARD and upon recovery and how mutations on *daf-1* induces the reversal of genes and processes to restore *hlh-30* ARD survival and recovery.

Gene	48hr in ARD		Upon ARD Recovery	
	hlh-30(tm2978) vs WT	*daf-1(m40);hlh-30* vs *hlh-30*	*hlh-30(tm2978)* vs WT	*daf-1(m40);hlh-30* vs *hlh-30*
aak-2	-1.09	0.77	0.00	0.00
acs-2	-3.61	3.59	0.00	0.00
daf-2	-0.70	0.00	0.00	0.00
daf-5	-1.19	0.00	-1.61	0.00
fat-5	-2.83	3.08	-1.26	1.72
ftn-1	-2.06	1.04	-1.32	1.23
ife-2	-0.71	0.00	0.00	0.00
lgg-2	-1.00	0.00	0.00	0.00
lipl-3	-4.40	4.67	-3.38	4.61
mdl-1	-4.63	2.28	-2.17	0.73
mml-1	-0.94	0.00	0.00	0.00
mxl-3	-3.08	2.33	-3.02	0.79
pod-2	-0.80	1.06	0.00	0.00
vha-2	0.00	0.75	0.00	0.00

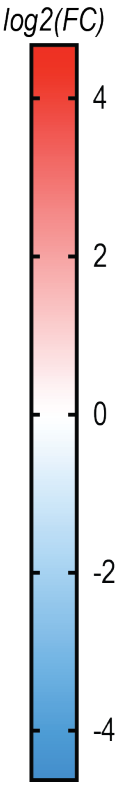

Figure 19. *daf-1(m40)* regulates genes involved in ARD survival and longevity in *hlh-30* mutants. Heat map representing expression of genes involved in ARD survival and recovery in *hlh-30(tm9178)* vs WT and *daf-1(m40);hlh-30(tm1978) vs hlh-30(tm1978)* during ARD and upon recovery (significance $p<0.05$).

7 DISCUSSION

The study of diapause states in model systems has led to some of the most profound discoveries in biology of ageing. Notably many of the first mutants affecting animal life span, such as *daf-2, age-1,* and *daf-16,* were first found for their role in regulating the *C. elegans* dauer diapause. Furthermore, several mammalian species use similar mechanisms to depress metabolic rate in response to unfavourable environmental conditions (Wu & Storey, 2016) which allow the organism to enter a quiescence to endure these stressful conditions. Thus, what is learned in simple models can inform physiology of somatic endurance and longevity in higher animals.

The adult reproductive diapause (ARD) represents a newly characterised state of long-lived quiescence in the nematode, *C. elegans*, whereby starvation in mid-L3 leads to the formation of long lived mini adults that can live up to 80 days, and upon refeeding, recover and produce progeny. However, the underlying mechanisms of entry, survivorship, and recovery are not fully understood. Previous work in our lab had shown that survivorship and recovery was highly dependent on HLH-30/TFEB transcription factor as a master regulator of ARD (B. Gerisch et al., 2020) but pathways downstream of HLH-30/TFEB remain unknown.

For this project, I employed a unique protocol utilising the quiescent state, ARD, to allow direct selection of longevity mutants following mutagenesis. This approach circumvents the high maintenance requirements of previous mutagenesis longevity screens and additionally yields insight into molecular determinants of ARD survival. From this approach, we discovered a role for pyrimidine metabolism in regulating ARD survival and longevity. We also discovered lesions in TGF-β and insulin signalling pathways as suppressors of HLH-30/TFEB. As well, we identified a handful of other potential candidate survival factors for further follow up and validation.

7.1 Using ARD as a tool to select for longevity mutants

From longevity screens in ARD, we obtained a large number of mutants that lived longer than wild type in ARD. However, upon *ad libitum* conditions, most of these mutants did not display longevity against wild type. This phenomenon could be due to a number of factors required to optimise the methodology. Firstly, ARD induction is performed on the whole population with bleaching of the F1 generation after mutagenesis. Successful ARD induction only occurs within a short period of the *C. elegans* life cycle and if induced too early or too late results in failure to enter the diapause state. As previously known, many longevity mutants exhibit a slow growth phenotype, such as insulin signalling mutants (*daf-2*), calories restriction (*eat-2*) and mitochondrial mutants (*isp-1*). Our current methodology did not fully consider potential slow growing mutants in the F2 generation and therefore unintentionally lost potential long-lived mutants. This can be overcome by inducing ARD after mutagenesis at different time points to incorporate slow growing mutants. Another factor to consider for the screen is the use of fluorodeoxyuridine (FUDR). FUDR inhibits thymidylate synthetase, blocking DNA synthesis, therefore preventing development of *C. elegans* progeny. Although, FUDR does not affect wild type lifespan, fluorodeoxyuridine treatment has been shown to affect the lifespan of several other phenotypes. Artifactual lifespan extension has been observed in animals with mutations in *tub-1*, a gene involved in fat storage (Aitlhadj & Stürzenbaum, 2010), *gas-1*, a mitochondrial mutant (van Raamsdonk & Hekimi, 2011), and *exo-3*, an apurinic/apyrimidinic endonuclease (Kato et al., 2016). FUDR is also implicated in extending lifespan, under conditions such as hypertonic stress (E. N. Anderson et al., 2016). Therefore, FUDR treatment is likely to cause false positives or negative outcomes for screening purposes for lifespan phenotypes where the opportunities to avoid using FUDR should be considered. Collectively, even with these limitations requiring optimisation, these results show a novel lower maintenance method for mutagenesis screens, allowing the direct selection for longevity.

7.2 Pyrimidine metabolism plays a role in ARD longevity and survival

Pyrimidine metabolism is an essential process, functioning in the synthesis of DNA, RNA, lipids and carbohydrates (Garavito et al., 2015). Disruption to pyrimidine metabolism has been associated with different disorders, such as Alzheimer's disease (Ansoleaga et al., 2015) and growth retardation (Simmonds et al., 1997). Previous studies have connected pyrimidine metabolism with ageing, where aged mice show differential expression of genes involved in pyrimidine metabolism (Brink et al., 2009) and studies using *C. elegans* reported intermediates of pyrimidine metabolism were downregulated in aged worms (Wan et al., 2017). In this work, we identified a causal role of pyrimidine metabolism in ARD longevity and survival. We found a mutation in *upp-1*, a gene encoding uridine phosphorylase which exhibits both uridine and thymidine phosphorylase activity in *C. elegans*, to extend ARD lifespan. We confirmed this effect with another independent allele of *upp-1* from our screen. It is still unknown if these non-synonymous point mutations are loss or gain of function alleles. However evidence may points towards a loss of function, previous studies using RNAi against *upp-1* show lifespan extension in *ad libitum* (AL) conditions (Wan et al., 2019). Our *upp-1* mutant also displays modest longevity against wild type in AL suggesting a loss of function mutation.

We also discovered the splicing factor, *prp-21*, to show mild lifespan extension in ARD and AL conditions. Upon refeeding, *upp-1* displayed increased resilience for recovery after long periods of starvation in ARD. A higher number of *upp-1* mutants became reproductive adults to produce progeny after 60 and 90 days of ARD compared to WT and *prp-21* mutants. This implies improved regeneration and rejuvenation in *upp-1* mutants and reveals a potential vital role of pyrimidine metabolism in ARD recovery.

In line with our work, a recent study demonstrated the lifespan-extending effects of supplementing intermediates of pyrimidine metabolism including, uridine and thymine, which function through the inhibition of reproductive signalling (Wan et al., 2019). Since UPP-1 exhibits uridine and thymidine phosphorylase activity in *C. elegans* we wondered if there was regulation of the different metabolites

involved in pyrimidine metabolism in our *upp-1* mutants. Targeted metabolomics revealed increased levels of uridine and thymine, and decreased levels of uracil and thymidine in our *upp-1* mutants. We hypothesised the *upp-1* ARD longevity was due to the increased levels of uridine and thymine and examined ARD lifespan whilst supplementing uridine and thymine to WT and *upp-1* mutants. Interestingly thymine supplementation increased ARD lifespans in WT but not in *upp-1* mutants, suggesting a parallel mechanism for thymine and *upp-1* mutants to increase ARD lifespan. Since we observed decreased levels of uracil and thymidine in *upp-1* mutants, we speculate supplementation with these metabolites would decreased ARD longevity in WT, to additionally validate this pathway in regulating ARD longevity.

Studies investigating nucleotide homeostasis and human health have established links between several diseases and increased levels of pyrimidine intermediate metabolites. Excessive pyrimidine biosynthesis causing overproduction of uracil results in urea cycle disorders (Matsumoto et al., 2019) while uncontrolled proliferation of cancer cells requires a high nucleotide supply (Chi & Han, 2016). However, deficiency of pyrimidine nucleotides are associated with behavioural abnormalities, seizures, developmental delay and immunodeficiency (Page et al., 1997). We discovered increasing pyrimidines metabolites, uridine and thymine, by mutations in *upp-1* or by exogenous supplementation increased ARD lifespan. *C. elegans* senses nucleotide levels through Notch signalling (Chi et al., 2016). During low levels of nucleotide availability, *C. elegans* shut down germline proliferation through the Notch pathway as a protective measure to avoid deleterious damage to mother and progeny, which exhausts the nucleotide pool (Chi et al., 2016). In ARD, germline proliferation is arrested thus preventing nucleotide pool exhaustion in the short term, but perhaps eventually leading to nucleotide pool exhaustion in the long term. With altered pyrimidine levels, such as the *upp-1* mutant, the nucleotide pool is maintained enhancing nucleic acid integrity, but germline proliferation remains arrested, extending ARD lifespan. In this scenario measuring Notch signalling in *upp-1* mutants may provide an insight into nucleotide pool

maintenance throughout ARD. Unbalanced nucleotide pools also leads to DNA damage by mis-incorporation during DNA synthesis in cells (Hastak et al., 2008). We speculate that the increased ARD longevity of *upp-1* mutants could also be due to reduced DNA damage compared to WT.

Several enzymes of the metabolic pathways responsible for the metabolism of ribo- and deoxyribo-nucleotides are located in the mitochondria (Desler et al., 2010). Inducing mitochondrial fragmentation, by mutation on *fzo-1*, reduces ARD longevity (B. Gerisch et al., 2020) potentially affecting these metabolic pathways and limiting the availability of these nucleotides leading to DNA damage. Pyrimidine metabolism in *upp-1* mutants may operate to maintain mitochondrial integrity to induce ARD longevity.

Taken together, these observations strongly imply a role for pyrimidine metabolism in ARD survival and longevity, where *upp-1* and thymine supplementation operate through a similar mechanism to extend ARD lifespan.

7.3 Downregulation of TGF-β signalling rescues *hlh-30* shortevity

ARD survival and longevity requires the transcription factor TFEB/HLH-30. Mutants of *hlh-30* exhibit drastic morphological and physiological changes in ARD, including shortened ARD lifespan, failure to recover from ARD and rapid decrease in body size upon ARD entry, suggesting TFEB/HLH-30 is a master regulator of ARD (B. Gerisch et al., 2020). To help understand factors involved in the critical role of HLH-30 for ARD survival we performed a *hlh-30* suppressor screen and discovered components of the TGF-β (*daf-1* – TGF-β receptor type I) and IIS (*pdk-1* – phosphoinositide-dependent kinase) signalling pathways to partially rescue *hlh-30* lifespan. Mutations on *daf-1* and *pdk-1*, not only increased *hlh-30* ARD lifespan, but also prevented the rapid body shrinkage and decreased fat content previously observed in *hlh-30* mutants in ARD. However, we observed that only *daf-1(m40)* rescued the inability of *hlh-30* mutants to recover from ARD and become reproductive adults. *C. elegans* have two highly conserved TFG-β signalling pathways, TFG-β/DAF-7 and TFG-β/DBL-1 pathways, where both pathways are associated with increasing reproductive

lifespan in *C. elegans*. Mutants of these pathways exhibit an extended reproductive period compared to wild type animals (Luo et al., 2009). In contrast, reduction of the insulin-signalling pathway results in decreased early progeny production of *C. elegans* (Hughes et al., 2007). This may explain the inability of *daf-2* mutants to recovery from ARD in *hlh-30* mutants. Our results suggest a similar mechanism affects the ability to produce progeny upon exit from ARD and reproductive lifespan, which requires insulin signalling.

Downstream of TFG-β signalling are the DAF-3/Co-smad and DAF-5/Sno/Ski transcription factors (da Graca et al., 2004; Patterson et al., 1997). TGF-β pathway also regulates longevity via insulin signalling by inducing nuclear localisation of DAF-16. We discovered *daf-1* rescue of *hlh-30* ARD shortevity is dependent on these transcription factors. Transcription expression of *daf-1p::GFP* and qPCR expression analysis of *daf-1* and *daf-7* indicated increased levels of these TGF-β components in *hlh-30(tm1978)* mutants suggesting an upstream regulatory mechanism of TGF-β signalling by *hlh-30*. On the one hand, these findings argue that HLH-30/TFEB and TGF-β signalling are part of a regulatory axis important for ARD survival and recovery. On the other hand, *daf-3* and *daf-5* single mutants were not essential for ARD survival and d*af-1* single mutation increased ARD longevity suggesting a parallel pathway. However *daf-3*;*daf-5* double mutants displayed ARD longevity, suggesting knockdown of both genes are required for ARD lifespan extension implying a compensatory mechanism operating between *daf-3* and *daf-5*. Nevertheless, *daf-16* mutants decreased ARD longevity by 40% (B. Gerisch et al., 2020) suggesting the importance of TGF-β signalling acting through *daf-16* for ARD survival. In accordance with this view, previous studies have discovered upon reduced nutrient availability, neuroendocrine signalling acts through DAF-7 allowing animals to sense low abundance of food resulting in activation of DAF-16 (Fletcher & Kim, 2017). Despite the rescue of *hlh-30* shortevity by *daf-1* being dependant on *daf-16, daf-3* and *daf-5*, our data suggests *daf-16* may player a larger role in influencing *hlh-30* ARD lifespan through TGF-β signalling, similar to what is previously known (Figure 20).

Nutrient deprivation during adulthood triggers several mechanisms to respond to starvation to enhance survival in *C. elegans* (Henderson et al., 2006; Mair & Dillin, 2008). As previously mentioned, secretion of DAF-7, TGF- β ligand, promotes lifespan extension in response to dietary restriction (DR) by suppressing activity of DAF-3 (Fletcher & Kim, 2017). When DAF-7 activity is reduced or absent, increasing DAF-3 activity also abolishes the lifespan extension of DR. DAF-7 is upregulated upon refeeding after fasting suggesting it also mediates food sensing (J. Wang & Kim, 2003) where *daf-7* mutants are also long lived depending on the availability of food (Entchev et al., 2015), further linking TGF-β signalling and nutrient deprivation. Earlier studies have also highlighted a central role of HLH-30/TFEB in starvation responses (Lapierre et al., 2013; O'Rourke & Ruvkun, 2013; Peña-Llopis et al., 2011), where *hlh-30* mutants prematurely die during starvation (Lapierre et al., 2013). Our work strengthens the links between components of TGF-β signalling and the response to starvation and provides a potential novel mechanism for surviving nutrient deprivation in the absence of HLH-30/TFEB, through TGF-β and IIS signalling.

DAF-7 is a key neuroendocrine signal in ASI neurons to induce lifespan extension under dietary restriction (Fletcher & Kim, 2017). Previous transcriptomic data also revealed *hlh-30* mutants in ARD exhibited elevated levels of *daf-7* compared to wild type. Tissue specific ARD longevity is unknown; however, this work may allude to neuronal specific ARD lifespan extension or uncover cell non-autonomous effects of *daf-7* in *hlh-30* mutant for ARD survival and longevity.

Transcriptomic analysis comparing *hlh-30(tm1978)* with *daf-1(m40);hlh-30(tm1978)* in ARD revealed interesting changes in gene expression upon downregulation of TGF-β signalling. As previously mentioned, *hlh-30* mutants are unable to recover after 48hr of ARD. Global transcriptions patterns of *hlh-30(tm1978)* and WT upon recovery from ARD differ greatly, however downregulation of TGF-β signalling in *hlh-30* mutants showed a similar pattern to WT suggesting the restoration of the gene expression of *hlh-30* mutants to a

similar pattern to WT. The expression profile during ARD between WT, *daf-1(m40)* and *daf-1(m40);hlh-30(tm1978)* also displays clustering of gene expression compared to *hlh-30(tm1978)* but to a lesser extent than upon recovery suggesting a greater role for *daf-1* during ARD.

In accord with a signalling pathway, we observed a reversal of *hlh-30* dependant transcriptional changes by *daf-1*. Specifically, we observed 4814 genes with reversal of expression showing transcriptional epistasis by *daf-1(m40)*. This comparison of the transcriptomic analysis suggests *daf-1* operates to reverse processes involved in the innate immune response and oxidation-reduction process to counteract the loss of *hlh-30* in ARD and upon recovery. It is interesting genes involved in the immune response become enriched upon *daf-1* mutations in *hlh-30* mutants. HLH-30/TFEB is also a known key transcription factor for host defence against infection. Activation of HLH-30 occurs upon early infection, where *hlh-30* mutants display a defect against pathogenic bacteria (Visvikis et al., 2014). We could speculate that from our data the absence of HLH-30/TFEB in ARD regulates immunity though downregulation of the TGF-β pathway preventing pathogenic mechanisms, leading to increased ARD survival.

As previously mentioned, work in our lab identified several genes vital for ARD survival (B. Gerisch et al., 2020). We wondered if there was regulation of these genes in *hlh-30* mutants reversed by mutations on *daf-1*. Interestingly, factors of the extended HLH network, *mdl-1* and *mxl-3*, previously shown to promote ARD survival, were upregulated by *daf-1(m40)* in *hlh-30* mutants, suggesting that reducing *daf-1* activity induces expression of these factors to aid ARD survival in *hlh-30* mutants, implying an inhibitory role of the TGF-β pathway for these factors. The energy sensing AMPK, is a conserved target of mammalian TFEB which plays a key role in cellular and organismal survival during stress via the ability to maintain metabolic homeostasis (Salminen et al., 2011). Previously we showed that AMP-kinase subunit *aak-2* is required for ARD survival. We found *aak-2*, was downregulated in *hlh-30* mutants but upregulated

by *daf-1(m40)* suggesting activation of *aak-2* through the *hlh-30/daf-1* axis is important for increased ARD longevity and survival (Figure 20).

Interestingly the transcriptomic data also revealed the reversal of *upp-1* expression by *daf-1* in *hlh-30* mutants in ARD and upon recovery. Expression of *upp-1* was upregulated in *hlh-30* mutants; but downregulated by *daf-1* consistent with the idea that downregulated *upp-1* extends survival. Existent data from the Modencode project (Celniker et al., 2009) also reveals that the *upp-1* promoter binds HLH-30 and DAF-16 and potentially connects pyrimidine metabolism and *hlh-30* for ARD survival. We speculated that *hlh-30* mutants in ARD have increased DNA damage causing the pathological decrease of ARD longevity. Our data revealed increased NAD levels in *upp-1* mutants (Figure 11E). Since NAD influences DNA repair mechanisms (Croteau et al., 2017), we hypothesised the downregulation of *upp-1* by *daf-1* aids in repairing the DNA damage of *hlh-30* mutants by the increased NAD levels (Figure 11E).

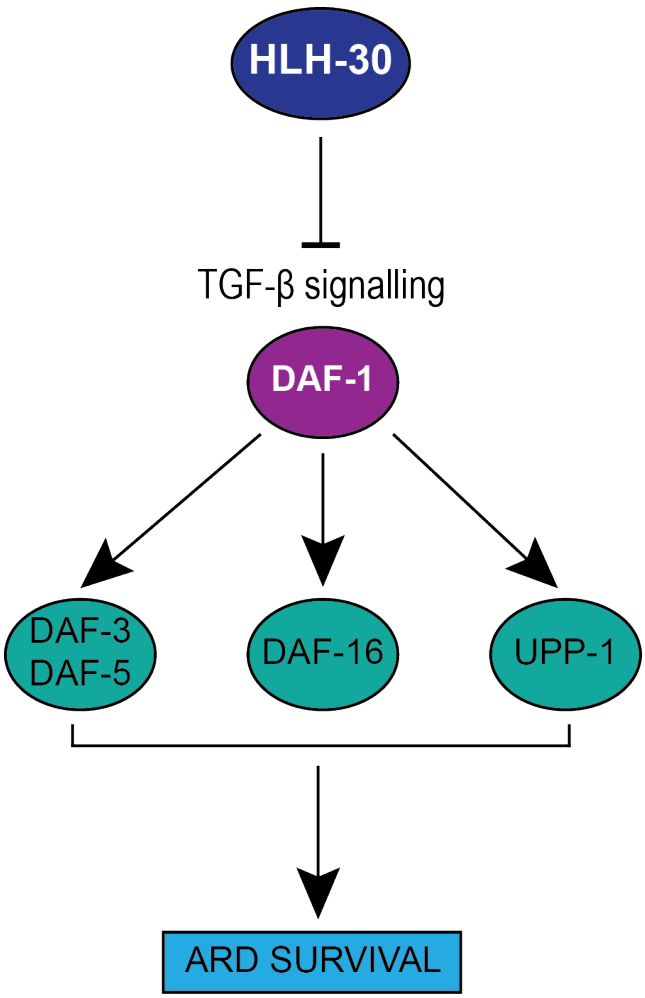

Figure 20. HLH-30 downregulated TGF-β signalling to regulate ARD longevity and survival. *hlh-30* regulates ARD longevity and survival through TGF-β signalling. This is dependent on downstream transcription factors, *daf-3, daf-5* and *daf-16,* and potentially through pyrimidine metabolism via *upp-1*.

Our second genetic screen revealed some interesting genes that potentially rescue *hlh-30* ARD shortevity. *mxl-2,* part of the Myc superfamily, which regulates gonadal longevity as well as other longevity pathways (Nakamura et al., 2016), forms a complex with *mml-1* which was shown to be downregulated by *hlh-30* in ARD. Repressors of the Myc superfamily comprises *mxl-1* and *mdl-1*, where our transcriptomic data also showed regulation of *mdl-1* by *daf-1* in *hlh-30* mutants potentially highlighting the Myc superfamily as a major player for *hlh-30* ARD survival. Interestingly, *daf-3,* also emerged as a candidate. DAF-1 activation in the TGF-β pathway inhibits the activity of DAF-3 (Hu, 2007), therefore *daf-1* mutants have increased DAF-3 activity. We know from our data

daf-1 mutation rescues *hlh-30* ARD shortevity, so we hypothesise the mutation we obtained from the second screen is potentially a *daf-3* gain of function mutation. Another interesting candidate is *ceh-60*. This homeodomain transcription factor normally co-ordinates a transcriptional networks to repress longevity and stress response genes while simultaneously activating genes involved in reproduction (Dowen, 2019). The *C. elegans* orthologue of mammalian mTOR, *let-363*, was also highlighted as a candidate. Reduced TOR signalling, activates autophagy and extends lifespan (Wullschleger et al., 2006). Both gain of function and reduction of mTOR led to shortened ARD lifespan, suggesting that the fine tuning of mTOR signalling is important (B. Gerisch et al., 2020). Starved *hlh-30* mutants have decreased levels of *let-363* compared to wild type (J. T. Murphy et al., 2019) suggesting *hlh-30* promotes transcription of *let-363* during starvation. This potentially implies our *let-363* mutation is gain of function. Another interesting candidate is *tax-4*. This gene encodes the subunits of the cGMP-gated ion channel part of the guanylyl cyclase pathway which functions upstream of TGF-β and IIS pathways in dauer regulation (Hu, 2007). Altogether, these candidates represent some exciting novel genes in the regulation of *hlh-30* during ARD to be validated in the future.

8 FUTURE PERSPECTIVES

8.1 Further characterisation of *upp-1* mutants

Our results clearly show there is a connection between pyrimidine metabolism and ARD survival. By increasing levels of uridine and thymine genetically through *upp-1* mutants or supplementation with these metabolites we observed enhanced longevity in ARD. We also found improved recovery of *upp-1* mutants after 60 days of ARD suggesting enhanced survival after long periods of starvation. However, the mechanism of how these intermediates contributes to ARD longevity remains unclear. Previous reports have shown supplementation of thymine or *upp-1* RNAi increased AL lifespan, however missense or nonsense *upp-1* mutants were short lived. They speculated these mutants enhances pyrimidine metabolite to detrimental levels affecting the physiological state (Wan et al., 2019). We would first address if our *upp-1* mutants are loss of gain of function alleles. Since our *upp-1* mutant displayed a mild lifespan extension in AL, this suggests a loss of function allele, however using qPCR to measure expression of *upp-1* will aid to address this question.

A study investigating the pyrimidine biosynthesis pathway screened for resistance to 5-fluorouracil (5-FU), a major pyrimidine antagonist currently used in cancer chemotherapies, identified mutations in *upp-1* renders worms resistant to 5-FU (S. Kim et al., 2009). Several *upp-1* mutants displayed resistance to 5-FU and exhibited very low levels of enzyme activity. Conferring resistance to 5-FU, may suggests low enzymatic activity of *upp-1(syb659)* and *upp-1(syb2043)* mutants imply potential loss of function alleles. We also plan to obtain a *upp-1::GFP* line to track expression of *upp-1* during ARD. This can potentially highlight any tissue specific effects of *upp-1* during ARD and upon recovery, which may uncover cell non-autonomous effects of *upp-1*.

We only measured the intermediates of pyrimidine metabolism after 10 days of ARD. It would be interesting to see how the levels of these metabolites changes throughout the ARD lifespan, if levels of the pyrimidine metabolites remains increased through the ARD lifespan or they decreased after a certain time since

high levels of uridine may have detrimental effects (Wan et al., 2019). We plan to induce ARD in WT and *upp-1* mutants and perform targeted metabolomics to observe any changes throughout the lifespan.

8.2 Investigating NAD longevity and pyrimidine metabolism for ARD longevity.

Interestingly, from our metabolomics data, we found increased levels of nicotinamide adenine dinucleotide (NAD) and nicotinamide mononucleotide (NMN) in *upp-1 (syb659)* mutants after 10 days of ARD. Studies have previously connected NAD and longevity, revealing reduced NAD levels in aged mice and decreasing levels of NAD in *C. elegans* further reduces their lifespan (Mouchiroud et al., 2013). Dietary supplementation of NAD precursors such as nicotinamide riboside (NR) induced mitochondrial unfolded protein response leading to rejuvenation processes, delaying senescence in muscle tissue and increasing lifespan in aged mice (Zhang et al., 2016). We will analyse ARD lifespan with NAD and NMN supplementation to examine potential longevity effects in WT and *upp-1* mutants. It would be interesting to observe if there is an additive lifespan extension with NAD or NMN supplementation in *upp-1* mutants to investigate if the mechanism of *upp-1* ARD longevity operates in a parallel or distinct pathway to NAD supplementation.

Poly (ADP-ribose) (PAR) is synthesised from NAD by PAR polymerases (PARP) to modulate cell survival and cell death programmes (Schreiber et al., 2006). PARPs are key players in DNA break repairs responses as well as inflammation and apoptosis induction. Increasing PARP activity can potentially delay ageing by maintaining DNA integrity. We speculate the higher NAD levels in *upp-1* results in increased PARP, enhancing processes maintaining DNA damage leading to improved cellular homeostasis and longevity. To examine this theory, we plan to measure levels of DNA damage by western blot of the product of the enzymatic activity of PARP1, polyADP-ribose (ADPr). Upon DNA damage the levels of ADPr increases dramatically (Q. Chen et al., 2018). We will collect samples from WT and *upp-1* mutants at different time points of ARD to measure

ADPr and hypothesise lower levels of ADPr will be present in *upp-1 (syb659)* mutants.

To solidify the potential connection between NAD and pyrimidine metabolism a study discovered the role of uridine monophosphate synthetase, *umps-1*, to enable NAD biosynthesis (McReynolds et al., 2017). Operating upstream of UPP-1 in the pyrimidine metabolism pathway, UMPS-1, exhibits orotate phosphoribosyltransferase and orotidine-5'-phosphate decarboxylase activity. We plan to analyse the ARD lifespan of *umps-1* mutant to examine potential longevity effects. ARD longevity observed in these mutants can strengthen the link between downregulation of pyrimidine metabolism and ARD longevity, through potential increased NAD levels to maintain DNA damage after long periods of starvation.

8.3 Finding novel regulators of *hlh-30* in ARD

As previously mentioned, we conducted a second *hlh-30* suppressor screen to uncover novel genes involved in bypassing the requirement of *hlh-30* for ARD longevity and survival. Through whole genome sequencing and SNP analysis, we are currently validating potential novel candidates through the construction of double mutants with *hlh-30(tm1918)* to examine potential rescue of *hlh-30* ARD shortevity. Positive genes will be further characterised for their role in *hlh-30* ARD.

8.4 Connection to mammals

Connecting our work to higher organism will allow translation of this work to humans. Investigating starvation mechanisms in *C. elegans* has revealed highly conserved pathways, which are informative towards potential dietary interventions, or therapeutic targets for improving health span of humans. Studying ARD in *C. elegans* further enhances our understanding of dietary restriction, nutrient sensing, rejuvenation and lifespan extension. Starvation induced quiescence in mammals initiates a reduced metabolic rate and reprogramming as a response to extreme environmental conditions to enter a state of torpor or hibernation (Wu & Storey, 2016). The mechanisms governing

this metabolic depression is likely to be conserved across species and similar adaptive stress responses such as dauer diapause, since studies have shown stress resistance signalling during hibernation through pathways such as FOXO signalling (Seim et al., 2013). It would be interesting to examine if the genes and pathways regulating ARD survival, also influence torpor or hibernation mechanisms in mammals.

9 MATERIALS AND METHODS

9.1 Methods

9.9.1 *C. elegans* stains and culture

Nematodes were cultured and maintained at 20^{o}C on nematode growth media (NGM) agar plates seeded with the E. coli OP50 bacteria strain. The following strains were used (Table 1) provided by the C. elegans Genomic Centre (CGC) with the exception of DR1767 (*mEx40[rol-6(su1006) daf-1p::GFP*]) from the Donald L Riddle laboratory, University of British Columbia; and PHX656 (*alg-1(syb656)*), PHX635 (*alg-4(syb635)*), PHX742 (*anoh-1(syb742)*), PHX658 (*piki-1(syb658)*), PHX755 (*prp-21(syb755)*), PHX633 (*ptr-10(syb633)*), PHX659 (*upp-1(syb659)*), PHX2043 (*upp-1(syb2043)*), PHX682 (*xpb-1(syb682)*), PHX662 (ZC581.7(*syb662*)), PHX2331 (C09H5.7(*syb2331*)), PHX2718 (*let-363(syb2692)*), PHX2905 (*pde-2(syb2905)*), PHX2984 (*cgt-2(syb2984)*), PHX3033 (*fgt-2(syb3033)*) which were created by Suny Biotech; and AA4975 (*ogdh-1(dh1202*)), AA4976 (*elpc-2(dh1203)*), AA4973 (*marc-6(dh1204)*) and AA4977 (*png-1(dh1205)*) which were created by our lab. These strains were then crossed into the respective genotypes. To decontaminate strains and to obtain an aged synchronised population, worms were treated with bleach solution (sodium hypochlorite, potassium hydroxide and water). Animals were washed off the plated with M9 buffer into a 15ml falcon tube. Once the worms had settled to the bottom and the supernatant was discarded, bleach solution was applied and incubated at room temperature for 5-10 minutes. Examination via microscopy for fully dissolved worms was performed before eggs were washed four times in M9 buffer and transferred to plates seeded with *E. coli* OP50 bacteria.

Table 1: List of strains used for the experiments described in this thesis

Strain Name	Genotype
AA60	*daf-16(mgDf50) I*
PHX656	*alg-1(syb656) X*
PHX635	*alg-4(syb635)*
PHX742	*anoh-1(syb742) III*
PHX658	*piki-1(syb658) X*
PHX755	*prp-21(syb755) II*
PHX633	*ptr-10(syb633) I.*
PHX659	*upp-1(syb659) III*
PHX2043	*upp-1(syb2043)*
PHX682	*xpb-1(syb682) III*
PHX657	Y55F3BR.1*(syb657) IV*
PHX662	ZC581.7*(syb662) I*
AA3658	*hlh-30(tm1978) IV*
DR40	*daf-1(m40) IV*
JT9609	*pdk-1(sa680) X*
DR1572	*daf-2(e1368) III*
CB1372	*daf-7(e1372ts) III*
AA5029	*daf-1(m40); hlh-30(tm1978)*
AA5031	*daf-2(e1368); hlh-30(tm1978)*
AA5033	*pdk-1(sa680); hlh-30(tm1978)*
AA5030	*daf-7(e1372); hlh-30(tm1978)*
AA5034	*daf-1(m40); hlh-30; daf-3(e1376)*
AA5036	*daf-1(m40); hlh-30; daf-16(mgDf50)*
AA5035	*daf-1(m40); hlh-30; daf-5(e1386)*
CB1376	*daf-3(e1376) X*
CB1386	*daf-5(e1386) II*
DR1767	*mEx40[rol-6(su1006) daf-1p::GFP]*
	hlh-30(tm1978);mEx40[rol-6(su1006) daf-1p::GFP]
PHX2331	*C09H5.7(syb2331)*
VC988	*ceh-60(ok1485) X.*
PHX2718	*daf-3(syb2718)*
PHX2692	*let-363(syb2692)*
PR678	*tax-4(p678) III*
PHX2905	*pde-2(syb2905)*
PHX2984	*cgt-2(syb2984)*
PHX3033	*fgt-2(syb3033)*
	lep-2(ok900)
AA4975	*odgh-1(dh1202)*
AA4976	*elpc-2(dh1203)*
AA4973	*marc-6(dh1204)*
AA4977	*png-1(dh1205)*
AA4974	*marc-6(dh1203); daf-16(mgDf50)*

9.1.2 Adult Reproductive Diapause (ARD) induction, recovery and lifespan

Nematodes were age synchronised by hypochlorite treatment 42-43 hours prior to ARD induction. Optimal adult diapause entry occurred if the population of animals are observed to be in the mid L3 larval stage, assessed by DIC microscopy for the migration of the gonad arms. Animals were collected from seeded NGM plates in M9 buffer and washed four times with M9 buffer in 5ml Eppendorf tubes. Animals were left to settle for 20 minutes after every wash to allow for expulsion of bacteria from the gut. The worms were then plated onto unseeded 3cm agarose plates containing 4ml Nematode Growth Medium containing UltraPureTM agarose (Thermo Fisher Scientific) and 50mg/ml ampicillin, at a density of approximately 500 worms per plate. One day after ARD induction, plates were wrapped in parafilm and maintained at 20^{o}C. The plates were monitored regularly for contamination in which case plates were discarded.

To recover from ARD, the animals were gently washed off the plates with M9 buffer and transferred to a 10 cm NGM plate seeded with E. coli OP50. Successful exit and recovery of animals from ARD was determined by visual improvements (body size, motility, intestine colouration, germline growth) and the ability to produce progeny, indicating regeneration of the germline. Adults were categorised as adults with progeny, sterile and unrecovered worms.

To examine the lifespan of animals in ARD, plates were scored every 2-3 days where dead worms were picked off the plate. Day 0 corresponds to the time of induction at the L3 stage. ARD lifespan was determined by scoring a population of around 500 worms per genotype. The first day of scoring was dependant on the genotype, for example, scoring was initiated on day 25-30 for wild type worms since they do not show sign of mortality before this day, compared to the *hlh-30(tm1978)* which starts to show signs of death after 48hr of ARD. Lifespan plates were monitored regularly for contamination and discarded if

contamination was present. Supplementation lifespans were performed on plates containing either 0.5mM uridine, 1mM uridine, 0.5mM thymine and 1mM thymine. Metabolites were added in aqueous solution into the NGM agar at the indicated concentrations.

9.1.3 ARD longevity and *hlh-30* suppressor screen

Wild type (Bristol N2) and *hlh-30(tm1978)* strains were used for the ARD longevity and *hlh-30* suppressor screen respectively. Synchronised L4 larvae were exposed to 0.15-0.5% ethyl methane sulfonate (EMS) in M9 buffer for 4 hours. After the EMS incubation period, worms were washed in M9 4 times before overnight recovery on seeded 10cm NGM plates. The following day, the P_0 generation were transferred to new plates, 10 worms per plate, and allowed to lay eggs overnight. P_0 were discarded the following day allowing the F1 to lay eggs. ARD was induced in the F2 generation to examine the longevity in a wild type or *hlh-30* background. Longevity mutants were picked or washed off and transferred to 10cm NGM plates seeded with E. coli OP50 to promote exit from ARD and recovery.

9.1.4 RNAi screen of ARD longevity candidates

E. coli HT115 (DE3) bacteria expressing dsRNA targeting the gene of interest were obtained from the Ahringer or Vidal libraries (Boutros & Ahringer, 2008; Rual et al., 2004). RNAi clones were grown overnight at 37^{o}C in Luri Broth with 50 µg/ml ampicillin. Cultures were spun down at 4000rpm, 4^{o}C for 10 mins, and diluted 1 in 4 fold, before being seeded onto agar plates containing 1M IPTG to induce dsRNA expression. *unc-22* RNAi was used a control for RNAi induction as this produces an uncoordinated and 'twitching' phenotype.

9.1.5 Lifespan Assays

For lifespan analysis, animals were transferred every day onto fresh NGM plates seeded with E. coli OP50 until reproduction had ceased. All assays were carried out and 20^{o}C and scored every second day for alive and dead worms. Worms

were logged as dead after failure to respond to mechanical stimulation by a platinum wire or pharyngeal pumping had ceased. Worms displaying internal hatch, explosion through vulva or had crawled off the plate were censored. Assays initially started with 150 worms across five 6cm seeded NGM plates. Three biological replicates were performed for each lifespan experiment and carried out blinded. For the ARD screen, lifespan analysis was carried out on plates containing 50 μM 5-Fluoro-2′- deoxyuridine (FUDR, Sigma). RNAi ARD longevity candidates were performed using N2 upon RNAi knockdown from egg on and *luci* as a control. To determine significance between the lifespan curved (Mantel-Cox) analysis was used.

9.1.6 Whole genome sequencing and Galaxy Mimodd analysis

Mutant strains were grown on 10cm seeded NGM plates, collected in M9 buffer and washed with M9 buffer four times preceding genomic DNA preparation (QIAGEN Gentra PureGene tissue kit). Sequence libraries were created using the TruSeq DNA sample prep (Illumina, San Diego, CA). Libraries were sequenced on a HiSeq 2500 (Illumina, San Diego, CA) to generate single-end 50bp reads. The reference genome used for alignment was obtained from WormBase version WS220 (www.wormbase.org). Sequencing data was analysed by Galaxy software (www.usegalaxy.org).

9.1.7 CRISPR alleles and microinjections

CRISPR guideRNA were designed using http:://crispr.mit.edu/guides and developed into oligos to order with NeBio sgRNA designer. Two guides were designed per targeted gene. Engen sgRNA synthesis kit was used to synthesise the guides and analysed by gel electrophoresis and NanoDrop. Guides were stored immediately at -80^{o}C. Repair templates containing the SNP change were designed using SeqBuilder (DNASTAR) targeting the desired gene and area of interested. Synonomous mutations were included to change the PAM sequence to prevent further cutting by Cas9. An injection mix comprising of Cas9 EnGen (NEB), *dpy-10* sgRNA, *dpy-10* repair template, KCl, Hepes pH 7.4 and water

with either sgRNA targeting *marc-6, elpc-2, ogdh-1* and *png-1* and their respective repair templates were prepared. L4 N2 larvae were used for the microinjections. Worms were placed in a drop of halocarbon oil (Sigma) on a 2% agarose pad. Injections were performed using a Carl Zeiss imager Z1 microscope, which was installed with a manual micromanipulator connected to a microinjector (Femtojet4). The F1 generation was monitored for a dpy phenotype and singled out for genotyping for the either *marc-6, elpc-2, ogdh-1* and *png-1* SNP change.

9.1.8 BODIPY Staining in ARD animals

C1-BODIPY-C12 solution (5mM/L) was dissolved in DMSO and stored at -20^{o}C. Solutions were freshly prepared and diluted in M9 to 1uM/L concentration, 100uL of BODIPY solution was applied to the surface of the ARD plate and left for 2.5 hours to allow the BODIPY solution to absorb into the ARD worms. After 2.5 hours, ARD worms were collected and fluorescence was measured on the Biosorter.

9.1.9 Dauer Assay

To determine dauer formation worms were age synchronised by allowing 20 worms to lay eggs for 4 hours. 100 eggs were picked to another plate and incubated at 25^{o}C or 27^{o}C for 48 hours. Dauer characteristics such as constricted pharynx, long and thin body shape, small gonads and dauer alae (using a Zeiss Axio Imager Z1 microscope (DIC contrast, 63x and 100x)) determined dauer larvae.

9.1.10 Brood Size Assay

Single worms were maintained on single 3cm NGM plates containing OP50 and transferred every day until reproduction has ceased. The number of progeny produced each day was scored. Minimum of 10 worms were used for each genotype and was repeated 3 times.

9.1.11 Body size determination

Images of worms were taken with Zeiss Axio Imager Z1 microscope using the Axiovisiob program. Body length was determined using Image J to measure the length of the worm. At least 25 worms were used per genotype.

9.1.12 Quantitative RT-PCR and RNA sequencing analysis

For quantification of transcript levels of *daf-1* and *daf-7* in N2 and *hlh-30(tm1978)* worms, samples were collected after 0hr, 24hr and 48hr in ARD in TRIzol (Invitrogen), snap frozen in liquid nitrogen and stored at -80^{o}C. For RNA isolation, samples were thawed at 37^{o}C in a water bath and snap frozen in liquid nitrogen for five cycles. Samples were lysed using the water bath sonicator, Bioraptor, for 30mins in 30sec on and off cycles at 4^{o}C. 120µl Chloroform was added to the samples and spun down at 12000 x g at 4^{o}C. The aqueous phase was isolated for RNA extraction using the RNeasy Mini kit (Qiagen) according to the instructions. RNA concentration and quality were determined using the NanoDrop 2000c (peqLab) for each sample.

cDNA was prepared in respect to the quantity of each sample with reverse transcriptase using iScript cDNA Synthesis Kit (BioRad). Pipetting of 384 well mRNA plates was performed using the JANUS automated workstation (PerkinElmer). To RNA quantification, Power SYBR Green Master Mix (Applied Biosystems) was used. Four technical replicates of the reaction were measured with ViiA 7 RealTime PCR system (Applied Biosystems). The standard program for comparative CT values including the melting curve was used. Primer validation was confirmed with the standard curve program. F44B9.5 was used as an internal control for RNA (See table 2 for primer sequence).

For RNA sequencing analysis a minimum of 3000 worms were collected for each genotype and condition in TRIzol. Sample were prepared as described above. Libraries were quantified, followed be sequencing-by-synthesis on a HiSeq2500 at the Max Planck Genome Center (Cologne, Germany)

(https://mpgc.mpipz.mpg.de/home/). Reads were quality trimmed with Flexbar version 2.5, then mapped to the reference genome (WBcel235.80) using hisat2 version 2.0.4. Respective assemblies were merged with cuffmerge, version 2.2.1, differential gene expression analysis was performed with Cuffquant version 2.2.1 and Cuffdiff version 2.2.1. GO annotation and enrichment was performed using DAVID bioinformatics resource database analysis via the Flaski (version 6b4e5ee) developed by the Bioinformatics Core Facility of the Max Planck Institute for Biology of Ageing, Cologne, Germany.

9.1.13 *daf-1p::GFP* Fluorescence expression with Copus Biosorter

The strain DR1767 (mEx40[rol-6(su1006) daf-1p::GFP]) was used and crossed with *hlh-30(tm1978).* Samples were collected after 0hr, 24h and 48hr ARD in 50ml Falcon tube and measured on the Copus Biosorter. GFP expression was captured using Union Biometric Copus Biosorter and measured using FlowJo.

9.1.14 Imaging

For imaging ARD worms, each genotype was mounted on 5% agarose pads in M9 and imaged using the Zeiss Axio Imager Z1 microscope using Zeiss Axiocam 506 mono camera using AxioVision software. Images were taken using 63X DIC. A minimum of 15-20 worms were quantified.

9.1.15 Untargeted metabolomics

After 10 days in ARD, N2 and *upp-1(syb659)* samples were collected in five biological replicates in single tubes and washed 3 times in buffer M9 solution, before being snap frozen in liquid nitrogen and stored at -80^{o}C. Worm pellets were homogenised using Qigen tissue lyser for 30mins at 4^{o}C. Protein concentration was determined using a BCA kit and the lysate volume corresponding to 150 µg of proteins was subjected to Bligh and Dyer extraction (chloroform: methanol, 2:1) for 1 hour at 4°C. Samples were centrifuged at maximum speed for 5 min at 4°C and supernatant was transferred into a new tube for drying. Before LC injections samples were reconstituted in 10%

aqueous acetonitrile. Samples were analysed using an untargeted method for total metabolomics.

Analytes were separated using an UHPLC system (Vanquish, Thermo Fisher Scientific, Bremen, Germany) coupled to an HRAM mass spectrometer (Q-Exactive Plus, Thermo Fischer Scientific GmbH, Bremen, Germany) using a modified RP-MS method from Wang L *et al* (L. Wang et al., 2019). Briefly, two microliters of the sample extract were injected into a X Select HSS T3 XP column, 100 Å, 2.5 µm, 2.1 mm x 100 mm (Waters), using a binary system A water with 0.1% formic acid, B: acetonitrile with 0.1 formic acid with a flowrate of 0.1 mL/min, with the column temperature kept at 30 °C. Gradient elution was conducted as follows: isocratic step at 0.1 % eluent B for 0.3 min, gradient increase up to 2% eluent B in 2 min, then increase up to 30% eluent B in 6 min and to 95% eluent B in 7 min, isocratic step at 95% eluent B for 2 min. Gradient decreases to 0.1 % eluent B in 3 min and held at 0.1% eluent B for 5 min. Mass spectra were recorded from 100-800 *m/z* at a mass resolution of 70,000 at *m/z* 400 in both positive and negative ion modes using data dependent acquisition (Top 3, dynamic exclusion list 10 seconds). Tandem mass spectra were acquired by performing CID (isolation 1,5 a.u., stepped collision energy 20 and 80 NCE). The *m/z* of Leucine enkephaline was used as lock mass. Sample injection order was randomized to minimize the effect of instrumental signal drift. MS data analysis was performed using Xcalibur software 4.0.

For compound identification and quantification, a metabolite search was performed using Compound discover2.0 and *m/z C*loud as online databases, considering precursor ions with a deviation > 5 ppm, 0.3 min maximum retention time shift, minimum peak intensity 100000, intensity tolerance 10, FT fragment mass tolerance 0.0025 Da, group covariance [%] less than 30, *p*-value less than 0.05 and area Max greater or equal to 10000. When at least 2 specific fragments were found in the MS^2 spectra, this was considered as correctly identified metabolites. Because of the high mass accuracy >3 ppm, predicted elemental

compositions of the unknown features were submitted to other online databases such as Chemspider (http://www.chemspider.com/), HMDB (http://www.hmdb.org/), KEGG (http://www.genome.jp/kegg/), METLIN (http://metlin.scripps.edu/). Unassigned features were additionally submitted to PIUMet algorithm for pathway prediction (http://fraenkel-nsf.csbi.mit.edu/piumet2/). The output was processed using R packages 'gplot' in order to visualize the cluster of metabolites and to highlight the connection between the predicted proteins and enzymes.

Quantification was performed using Trace finder 4.1, using genesis detection algorithm, nearest RT, S/N threshold 8, min peak height (S/N) equal to 3, peak S/N cutoff 2.00, valley rise 2%, valley S/N 1.10. Relative quantification was obtained by dividing the area of individual metabolites to spiked internal standards (Leucine enkephaline, myrystic acid and cysteamine sodium salt).

Materials

Solution	Composition
NMG plates	25 g Agarose 25 ml 1M KPO_4 3 g NaCl 2.25 g Peptone Make up to 1L with water AUTOCLAVE Add: 1 ml $CaCl_2$ 1M, 5mg/ml $MgSO_4$ 1M cholesterol 50mg/ml Ampicillin
ARD plates	12.5g Agarose (Ultrapure) 1.5g NaCl 1.26g Peptone 12.5ml 1M KPO_4 Make up to 500ml with water AUTOCLAVE Add: 500 l 1M $CaCl_2$

	500µl 1M$MgSO_4$ 500µl 5mg/ml Cholesterol 250 µl 50mg/ml Ampicillin
M9 Buffer	3 g KH_2PO_4 1 ml 1M $MgSO_4$ 5 g NaCl 6 g Na_2HPO_4 Make up to 1L AUTOCLAVE Add: $MgSO_4$
RNAi Plates	17 g Agarose 25 ml 1M KPO_4 3 g NaCl 2.5 g Peptone Make up to 1L AUTOCLAVE Add: 1 ml 1M $CaCl_2$ 5mg/ml $MgSO_4$ 1M cholesterol 50mg/ml Ampicillin 1M IPTG
LB medium	10 g NaCl 10 g tryptone 5 g yeast Make up to 1L Adjust the pH to 7.0 using 1N NaOH
Single worm lysis buffer	50 mM KCl 2.5 mM $MgCl_2$ 0.45 % NP-40 (or Triton-X100) 10 mM Tris pH 8.3 0.45 % Tween

10 REFERENCES

Ailion, M., Inoue, T., Weaver, C. I., Holdcraft, R. W., & Thomas, J. H. (1999). Neurosecretory control of aging in Caenorhabditis elegans. *Proceedings of the National Academy of Sciences of the United States of America*. https://doi.org/10.1073/pnas.96.13.7394

Aitlhadj, L., & Stürzenbaum, S. R. (2010). The use of FUdR can cause prolonged longevity in mutant nematodes. *Mechanisms of Ageing and Development*. https://doi.org/10.1016/j.mad.2010.03.002

Altun, Z. F., & Hall, D. H. (2009). Introduction. *WormAtlas*. https://doi.org/10.3908/wormatlas.1.1

Anderson, E. N., Corkins, M. E., Li, J. C., Singh, K., Parsons, S., Tucey, T. M., Sorkaç, A., Huang, H., Dimitriadi, M., Sinclair, D. A., & Hart, A. C. (2016). C. elegans lifespan extension by osmotic stress requires FUdR, base excision repair, FOXO, and sirtuins. *Mechanisms of Ageing and Development*. https://doi.org/10.1016/j.mad.2016.01.004

Anderson, R. M., Shanmuganayagam, D., & Weindruch, R. (2009). Caloric restriction and aging: Studies in mice and monkeys. In *Toxicologic Pathology*. https://doi.org/10.1177/0192623308329476

Angelo, G., & Van Gilst, M. R. (2009). Starvation protects germline stem cells and extends reproductive longevity in C. elegans. *Science*. https://doi.org/10.1126/science.1178343

Ansoleaga, B., Jové, M., Schlüter, A., Garcia-Esparcia, P., Moreno, J., Pujol, A., Pamplona, R., Portero-Otín, M., & Ferrer, I. (2015). Deregulation of purine metabolism in Alzheimer's disease. *Neurobiology of Aging*. https://doi.org/10.1016/j.neurobiolaging.2014.08.004

Antebi, A. (2006). Nuclear hormone receptors in C. elegans. In *WormBook : the online review of C. elegans biology*. https://doi.org/10.1895/wormbook.1.64.1

Antebi, A., Yeh, W. H., Tait, D., Hedgecock, E. M., & Riddle, D. L. (2000). daf-12 encodes a nuclear receptor that regulates the dauer diapause and developmental age in C. elegans. *Genes and Development*. https://doi.org/10.1101/gad.14.12.1512

Aoyama, Y., Urushiyama, S., Yamada, M., Kato, C., Ide, H., Higuchi, S., Akiyama, T., & Shibuya, H. (2004). MFB-1, an F-box-type ubiquitin ligase, regulates TGF-β signalling. *Genes to Cells*. https://doi.org/10.1111/j.1365-2443.2004.00792.x

Apfeld, J., & Kenyon, C. (1998). Cell nonautonomy of C. elegans daf-2 function in the regulation of diapause and life span. *Cell*. https://doi.org/10.1016/S0092-8674(00)81751-1

Apfeld, J., O'Connor, G., McDonagh, T., DiStefano, P. S., & Curtis, R. (2004). The AMP-activated protein kinase AAK-2 links energy levels and insulin-like signals to lifespan in C. elegans. *Genes and Development*. https://doi.org/10.1101/gad.1255404

Arantes-Oliveira, N., Apfeld, J., Dillin, A., & Kenyon, C. (2002). Regulation of life-span by germ-line stem cells in Caenorhabditis elegans. *Science*. https://doi.org/10.1126/science.1065768

Baugh, L. R. (2013). To grow or not to grow: Nutritional control of development

during Caenorhabditis elegans L1 Arrest. In *Genetics*. https://doi.org/10.1534/genetics.113.150847
Baugh, L. R., & Sternberg, P. W. (2006). DAF-16/FOXO Regulates Transcription of cki-1/Cip/Kip and Repression of lin-4 during C. elegans L1 Arrest. *Current Biology*. https://doi.org/10.1016/j.cub.2006.03.021
Berman, J. R., & Kenyon, C. (2006). Germ-cell loss extends C. elegans life span through regulation of DAF-16 by kri-1 and lipophilic-hormone signaling. *Cell*. https://doi.org/10.1016/j.cell.2006.01.039
Bernardi, R., Guernah, I., Jin, D., Grisendi, S., Alimonti, A., Teruya-Feldstein, J., Cordon-Cardo, C., Celeste Simon, M., Rafii, S., & Pandolfi, P. P. (2006). PML inhibits HIF-1α translation and neoangiogenesis through repression of mTOR. *Nature*. https://doi.org/10.1038/nature05029
Birnby, D. A., Link, E. M., Vowels, J. J., Tian, H., Colacurcio, P. L., & Thomas, J. H. (2000). A transmembrane guanylyl cyclase (DAF-11) and Hsp90 (DAF-21) regulate a common set of chemosensory behaviors in Caenorhabditis elegans. *Genetics*.
Bjedov, I., Toivonen, J. M., Kerr, F., Slack, C., Jacobson, J., Foley, A., & Partridge, L. (2010). Mechanisms of Life Span Extension by Rapamycin in the Fruit Fly Drosophila melanogaster. *Cell Metabolism*. https://doi.org/10.1016/j.cmet.2009.11.010
Boutros, M., & Ahringer, J. (2008). The art and design of genetic screens: RNA interference. In *Nature Reviews Genetics*. https://doi.org/10.1038/nrg2364
Brenner, S. (1974). The genetics of Caenorhabditis elegans. *Genetics*, 71–94.
Brink, T. C., Demetrius, L., Lehrach, H., & Adjaye, J. (2009). Age-related transcriptional changes in gene expression in different organs of mice support the metabolic stability theory of aging. *Biogerontology*. https://doi.org/10.1007/s10522-008-9197-8
Burnaevskiy, N., Chen, S., Mailig, M., Reynolds, A., Karanth, S., Mendenhall, A., van Gilst, M., & Kaeberlein, M. (2018). Reactivation of RNA metabolism underlies somatic restoration after adult reproductive diapause in C. Elegans. *ELife*. https://doi.org/10.7554/eLife.36194
Butcher, R. A. (2017). Small-molecule pheromones and hormones controlling nematode development. In *Nature Chemical Biology*. https://doi.org/10.1038/nchembio.2356
Cassada, R. C., & Russell, R. L. (1975). The dauerlarva, a post-embryonic developmental variant of the nematode Caenorhabditis elegans. *Developmental Biology*. https://doi.org/10.1016/0012-1606(75)90109-8
Celniker, S. E., Dillon, L. A. L., Gerstein, M. B., Gunsalus, K. C., Henikoff, S., Karpen, G. H., Kellis, M., Lai, E. C., Lieb, J. D., MacAlpine, D. M., Micklem, G., Piano, F., Snyder, M., Stein, L., White, K. P., & Waterston, R. H. (2009). Unlocking the secrets of the genome. In *Nature*. https://doi.org/10.1038/459927a
Chang, T. Y., Reid, P. C., Sugii, S., Ohgami, N., Cruz, J. C., & Chang, C. C. Y. (2005). Niemann-Pick type C disease and intracellular cholesterol trafficking. In *Journal of Biological Chemistry*. https://doi.org/10.1074/jbc.R400040200
Chen, D., Thomas, E. L., & Kapahi, P. (2009). HIF-1 modulates dietary

restriction-mediated lifespan extension via IRE-1 in Caenorhabditis elegans. *PLoS Genetics*. https://doi.org/10.1371/journal.pgen.1000486
Chen, Q., Kassab, M. A., Dantzer, F., & Yu, X. (2018). PARP2 mediates branched poly ADP-ribosylation in response to DNA damage. *Nature Communications*. https://doi.org/10.1038/s41467-018-05588-5
Chi, C., & Han, M. (2016). Notch signaling protects animals from nucleotide deficiency. In *Cell Cycle*. https://doi.org/10.1080/15384101.2016.1181878
Chi, C., Ronai, D., Than, M. T., Walker, C. J., Sewell, A. K., & Han, M. (2016). Nucleotide levels regulate germline proliferation through modulating GLP-1/Notch signaling in C. elegans. *Genes and Development*. https://doi.org/10.1101/gad.275107.115
Coburn, C. M., & Bargmann, C. I. (1996). A putative cyclic nucleotide-gated channel is required for sensory development and function in C. elegans. *Neuron*. https://doi.org/10.1016/S0896-6273(00)80201-9
Coburn, C. M., Mori, I., Ohshima, Y., & Bargmann, C. I. (1998). A cyclic nucleotide-gated channel inhibits sensory axon outgrowth in larval and adult Caenorhabditis elegans: A distinct pathway for maintenance of sensory axon structure. *Development*.
Croteau, D. L., Fang, E. F., Nilsen, H., & Bohr, V. A. (2017). NAD+ in DNA repair and mitochondrial maintenance. In *Cell Cycle*. https://doi.org/10.1080/15384101.2017.1285631
Curran, S. P., & Ruvkun, G. (2007). Lifespan regulation by evolutionarily conserved genes essential for viability. *PLoS Genetics*. https://doi.org/10.1371/journal.pgen.0030056
da Graca, L. S., Zimmerman, K. K., Mitchell, M. C., Kozhan-Gorodetska, M., Sekiewicz, K., Morales, Y., & Patterson, G. I. (2004). DAF-5 is a SKi oncoprotein homolog that functions in a neuronal TGFβ pathway to regulate C. elegans dauer development. *Development*. https://doi.org/10.1242/dev.00922
Daniels, S. A., Ailion, M., Thomas, J. H., & Sengupta, P. (2000). egl-4 Acts through a transforming growth factor-β/SMAD pathway in Caenorhabditis elegans to regulate multiple neuronal circuits in response to sensory cues. *Genetics*.
De Magalhães, J. P., & Toussaint, O. (2004). GenAge: A genomic and proteomic network map of human ageing. *FEBS Letters*. https://doi.org/10.1016/j.febslet.2004.07.006
Dekanty, A., Lavista-Llanos, S., Irisarri, M., Oldham, S., & Wappner, P. (2005). The insulin-PI3K/TOR pathway induces a HIF-dependent transcriptional response in Drosophila by promoting nuclear localization of HIF-α /Sima. *Journal of Cell Science*. https://doi.org/10.1242/jcs.02648
Denzel, M. S., Storm, N. J., Gutschmidt, A., Baddi, R., Hinze, Y., Jarosch, E., Sommer, T., Hoppe, T., & Antebi, A. (2014). Hexosamine pathway metabolites enhance protein quality control and prolong life. *Cell*. https://doi.org/10.1016/j.cell.2014.01.061
Desler, C., Lykke, A., & Rasmussen, L. J. (2010). The effect of mitochondrial dysfunction on cytosolic nucleotide metabolism. In *Journal of Nucleic Acids*. https://doi.org/10.4061/2010/701518

Dillin, A., Crawford, D. K., & Kenyon, C. (2002). Timing requirements for insulin/IGF-1 signaling in C. elegans. *Science*. https://doi.org/10.1126/science.1074240

Dillin, A., Hsu, A. L., Arantes-Oliveira, N., Lehrer-Graiwer, J., Hsin, H., Fraser, A. G., Kamath, R. S., Ahringer, J., & Kenyon, C. (2002). Rates of behavior and aging specified by mitochondrial function during development. *Science*. https://doi.org/10.1126/science.1077780

Dowen, R. H. (2019). CEH-60/PBX and UNC-62/MEIS Coordinate a Metabolic Switch that Supports Reproduction in C. elegans. *Developmental Cell*. https://doi.org/10.1016/j.devcel.2019.03.002

E. Yanos, M., F. Bennett, C., & Kaeberlein, M. (2012). Genome-Wide RNAi Longevity Screens in Caenorhabditis elegans. *Current Genomics*. https://doi.org/10.2174/138920212803251391

Entchev, E. V., Patel, D. S., Zhan, M., Steele, A. J., Lu, H., & Chng, Q. L. (2015). A gene-expression-based neural code for food abundance that modulates lifespan. *ELife*. https://doi.org/10.7554/eLife.06259

Estevez, M., Attisano, L., Wrana, J. L., Albert, P. S., Massagué, J., & Riddle, D. L. (1993). The daf-4 gene encodes a bone morphogenetic protein receptor controlling C. elegans dauer larva development. *Nature*. https://doi.org/10.1038/365644a0

Evason, K., Huang, C., Yamben, I., Covey, D. F., & Kornfeld, K. (2005). Anticonvulsant medications extend worm life-span. *Science*. https://doi.org/10.1126/science.1105299

Feinbaum, R., & Ambros, V. (1999). The timing of lin-4 RNA accumulation controls the timing of postembryonic developmental events in Caenorhabditis elegans. *Developmental Biology*. https://doi.org/10.1006/dbio.1999.9272

Fernandes de Abreu, D. A., Caballero, A., Fardel, P., Stroustrup, N., Chen, Z., Lee, K. H., Keyes, W. D., Nash, Z. M., López-Moyado, I. F., Vaggi, F., Cornils, A., Regenass, M., Neagu, A., Ostojic, I., Liu, C., Cho, Y., Sifoglu, D., Shen, Y., Fontana, W., … Ch'ng, Q. L. (2014). An Insulin-to-Insulin Regulatory Network Orchestrates Phenotypic Specificity in Development and Physiology. *PLoS Genetics*. https://doi.org/10.1371/journal.pgen.1004225

Fielenbach, N., & Antebi, A. (2008). C. elegans dauer formation and the molecular basis of plasticity. In *Genes and Development*. https://doi.org/10.1101/gad.1701508

Fire, A., Xu, S., Montgomery, M. K., Kostas, S. A., Driver, S. E., & Mello, C. C. (1998). Potent and specific genetic interference by double-stranded RNA in caenorhabditis elegans. *Nature*. https://doi.org/10.1038/35888

Flachsbart, F., Caliebe, A., Kleindorp, R., Blanché, H., Von Eller-Eberstein, H., Nikolaus, S., Schreiber, S., & Nebel, A. (2009). Association of FOX03A variation with human longevity confirmed in German centenarians. *Proceedings of the National Academy of Sciences of the United States of America*. https://doi.org/10.1073/pnas.0809594106

Fletcher, M., & Kim, D. H. (2017). Age-Dependent Neuroendocrine Signaling from Sensory Neurons Modulates the Effect of Dietary Restriction on

Longevity of Caenorhabditis elegans. *PLoS Genetics*. https://doi.org/10.1371/journal.pgen.1006544
Fontana, L., Partridge, L., & Longo, V. D. (2010). Extending healthy life span-from yeast to humans. In *Science*. https://doi.org/10.1126/science.1172539
Frank, D. J., & Roth, M. B. (1998). ncl-1 is required for the regulation of cell size and ribosomal RNA synthesis in Caenorhabditis elegans. *Journal of Cell Biology*. https://doi.org/10.1083/jcb.140.6.1321
Friedman, D. B., & Thomas, E. (1987). A Mutation in the age-1 Gene in Caenorhabditis elegans Lengthens Life and Reduces Hermaphrodite Fertility. *Genetics*, *Martin 1978*.
Fukuyama, M., Rougvie, A. E., & Rothman, J. H. (2006). C. elegans DAF-18/PTEN Mediates Nutrient-Dependent Arrest of Cell Cycle and Growth in the Germline. *Current Biology*. https://doi.org/10.1016/j.cub.2006.02.073
Fukuyama, M., Sakuma, K., Park, R., Kasuga, H., Nagaya, R., Atsumi, Y., Shimomura, Y., Takahashi, S., Kajiho, H., Rougvie, A., Kontani, K., & Katada, T. (2012). C. Elegans AMPKs promote survival and arrest germline development during nutrient stress. *Biology Open*. https://doi.org/10.1242/bio.2012836
Furuyama, T., Nakazawa, T., Nakano, I., & Mori, N. (2000). Identification of the differential distribution patterns of mRNAs and consensus binding sequences for mouse DAF-16 homologues. *Biochemical Journal*. https://doi.org/10.1042/0264-6021:3490629
Garavito, M. F., Narváez-Ortiz, H. Y., & Zimmermann, B. H. (2015). Pyrimidine Metabolism: Dynamic and Versatile Pathways in Pathogens and Cellular Development. In *Journal of Genetics and Genomics*. https://doi.org/10.1016/j.jgg.2015.04.004
Gems, D., Sutton, A. J., Sundermeyer, M. L., Albert, P. S., King, K. V., Edgley, M. L., Larsen, P. L., & Riddle, D. L. (1998). Two pleiotropic classes of daf-2 mutation affect larval arrest, adult behavior, reproduction and longevity in Caenorhabditis elegans. *Genetics*.
Georgi, L. L., Albert, P. S., & Riddle, D. L. (1990). daf-1, a C. elegans gene controlling dauer larva development, encodes a novel receptor protein kinase. *Cell*. https://doi.org/10.1016/0092-8674(90)90475-T
Gerisch, B., Tharyan, R. G., Mak, J., Denzel, S. I., Popkes-van Oepen, T., Henn, N., & Antebi, A. (2020). HLH-30/TFEB Is a Master Regulator of Reproductive Quiescence. *Developmental Cell*, *53*(3). https://doi.org/10.1016/j.devcel.2020.03.014
Gerisch, Birgit, & Antebi, A. (2004). Hormonal signals produced by DAF-9/cytochrome P450 regulate C. elegans dauer diapause in response to environmental cues. *Development*. https://doi.org/10.1242/dev.01068
Gerisch, Birgit, Rottiers, V., Li, D., Motola, D. L., Cummins, C. L., Lehrach, H., Mangelsdorf, D. J., & Antebi, A. (2007). A bile acid-like steroid modulates Caenorhabditis elegans lifespan through nuclear receptor signaling. *Proceedings of the National Academy of Sciences of the United States of America*. https://doi.org/10.1073/pnas.0700847104
Gerisch, Birgit, Weitzel, C., Kober-Eisermann, C., Rottiers, V., & Antebi, A.

(2001). A Hormonal Signaling Pathway Influencing C. elegans Metabolism, Reproductive Development, and Life Span. *Developmental Cell*. https://doi.org/10.1016/S1534-5807(01)00085-5

Gil, E. B., Link, E. M., Liu, L. X., Johnson, C. D., & Lees, J. A. (1999). Regulation of the insulin-like developmental pathway of Caenorhabditis elegans by a homolog of the PTEN tumor suppressor gene. *Proceedings of the National Academy of Sciences of the United States of America*. https://doi.org/10.1073/pnas.96.6.2925

Gill, M. S., Olsen, A., Sampayo, J. N., & Lithgow, G. J. (2003). An automated high-throughput assay for survival of the nematode Caenorhabditis elegans. *Free Radical Biology and Medicine*. https://doi.org/10.1016/S0891-5849(03)00328-9

Golden, J. W., & Riddle, D. L. (1982). A pheromone influences larval development in the nematode Caenorhabditis elegans. *Science*. https://doi.org/10.1126/science.6896933

Gomes, L. C., & Scorrano, L. (2011). Mitochondrial elongation during autophagy: A stereotypical response to survive in difficult times. *Autophagy*. https://doi.org/10.4161/auto.7.10.16771

Goudeau, J., Bellemin, S., Toselli-Mollereau, E., Shamalnasab, M., Chen, Y., & Aguilaniu, H. (2011). Fatty acid desaturation links germ cell loss to longevity through NHR-80/HNF4 in C. elegans. *PLoS Biology*. https://doi.org/10.1371/journal.pbio.1000599

Gunther, C. V., Georgi, L. L., & Riddle, D. L. (2000). A Caenorhabditis elegans type I TGFβ receptor can function in the absence of type II kinase to promote larval development. *Development*.

Hahm, J. H., Kim, S., & Paik, Y. K. (2009). Endogenous cGMP regulates adult longevity via the insulin signaling pathway in Caenorhabditis elegans. *Aging Cell*. https://doi.org/10.1111/j.1474-9726.2009.00495.x

Halaschek-Wiener, J., Khattra, J. S., McKay, S., Pouzyrev, A., Stott, J. M., Yang, G. S., Holt, R. A., Jones, S. J. M., Marra, M. A., Brooks-Wilson, A. R., & Riddle, D. L. (2005). Analysis of long-lived C. elegans daf-2 mutants using serial analysis of gene expression. *Genome Research*. https://doi.org/10.1101/gr.3274805

Hamilton, B., Dong, Y., Shindo, M., Liu, W., Odell, I., Ruvkun, G., & Lee, S. S. (2005). A systematic RNAi screen for longevity genes in C. elegans. In *Genes and Development*. https://doi.org/10.1101/gad.1308205

Hansen, M., Hsu, A. L., Dillin, A., & Kenyon, C. (2005). New genes tied to endocrine, metabolic, and dietary regulation of lifespan from a Caenorhabditis elegans genomic RNAi screen. *PLoS Genetics*. https://doi.org/10.1371/journal.pgen.0010017

Hansen, M., Taubert, S., Crawford, D., Libina, N., Lee, S. J., & Kenyon, C. (2007). Lifespan extension by conditions that inhibit translation in Caenorhabditis elegans. *Aging Cell*. https://doi.org/10.1111/j.1474-9726.2006.00267.x

Harrison, D. E., Strong, R., Sharp, Z. D., Nelson, J. F., Astle, C. M., Flurkey, K., Nadon, N. L., Wilkinson, J. E., Frenkel, K., Carter, C. S., Pahor, M., Javors, M. A., Fernandez, E., & Miller, R. A. (2009). Rapamycin fed late in

life extends lifespan in genetically heterogeneous mice. *Nature*. https://doi.org/10.1038/nature08221

Hastak, K., Paul, R. K., Agarwal, M. K., Thakur, V. S., Amin, A. R. M. R., Agrawal, S., Sramkoski, R. M., Jacobberger, J. W., Jackson, M. W., Stark, G. R., & Agarwal, M. L. (2008). DNA synthesis from unbalanced nucleotide pools causes limited DNA damage that triggers ATR-CHK1-dependent p53 activation. *Proceedings of the National Academy of Sciences of the United States of America*. https://doi.org/10.1073/pnas.0802080105

Heimbucher, T., Liu, Z., Bossard, C., McCloskey, R., Carrano, A. C., Riedel, C. G., Tanasa, B., Klammt, C., Fonslow, B. R., Riera, C. E., Lillemeier, B. F., Kemphues, K., Yates, J. R., O'Shea, C., Hunter, T., & Dillin, A. (2015). The Deubiquitylase MATH-33 Controls DAF-16 Stability and Function in Metabolism and Longevity. *Cell Metabolism*. https://doi.org/10.1016/j.cmet.2015.06.002

Henderson, S. T., Bonafè, M., & Johnson, T. E. (2006). daf-16 protects the nematode Caenorhabditis elegans during food deprivation. *Journals of Gerontology - Series A Biological Sciences and Medical Sciences*. https://doi.org/10.1093/gerona/61.5.444

Henderson, S. T., & Johnson, T. E. (2001). daf-16 integrates developmental and environmental inputs to mediate aging in the nematode Caenorhabditis elegans. *Current Biology*. https://doi.org/10.1016/S0960-9822(01)00594-2

Hibshman, J. D., Leuthner, T. C., Shoben, C., Mello, D. F., Sherwood, D. R., Meyer, J. N., & Baugh, L. R. (2018). Nonselective autophagy reduces mitochondrial content during starvation in caenorhabditis elegans. *American Journal of Physiology - Cell Physiology*. https://doi.org/10.1152/ajpcell.00109.2018

Hong, Y., Roy, R., & Ambros, V. (1998). Developmental regulation of a cyclin-dependent kinase inhibitor controls postembryonic cell cycle progression in Caenorhabditis elegans. *Development*.

Hsin, H., & Kenyon, C. (1999). Signals from the reproductive system regulate the lifespan of C. elegans. *Nature*. https://doi.org/10.1038/20694

Hsu, A. L., Murphy, C. T., & Kenyon, C. (2003). Regulation of aging and age-related disease by DAF-16 and heat-shock factor. *Science*. https://doi.org/10.1126/science.1083701

Hu, P. J. (2007). Dauer. In *WormBook : the online review of C. elegans biology*. https://doi.org/10.1895/wormbook.1.144.1

Hu, P. J., Xu, J., & Ruvkun, G. (2006). Two membrane-associated tyrosine phosphatase homologs potentiate C. elegans AKT-1/PKB signaling. *PLoS Genetics*. https://doi.org/10.1371/journal.pgen.0020099

Hughes, S. E., Evason, K., Xiong, C., & Kornfeld, K. (2007). Genetic and pharmacological factors that influence reproductive aging in nematodes. *PLoS Genetics*. https://doi.org/10.1371/journal.pgen.0030025

Hui, A. S., Bauer, A. L., Striet, J. B., Schnell, P. O., & Czyzyk-Krzeska, M. F. (2006). Calcium signaling stimulates translation of HIF-α during hypoxia. *The FASEB Journal*. https://doi.org/10.1096/fj.05-5086com

Hung, W. L., Wang, Y., Chitturi, J., & Zhen, M. (2014). A Caenorhabditis elegans developmental decision requires insulin signaling-mediated neuron-intestine communication. *Development (Cambridge)*. https://doi.org/10.1242/dev.103846

Inoue, T., & Thomas, J. H. (2000). Targets of TGF-β signaling in caenorhabditis elegans dauer formation. *Developmental Biology*. https://doi.org/10.1006/dbio.1999.9545

Jia, K., Albert, P. S., & Riddle, D. L. (2002). DAF-9, a cytochrome P450 regulating C. elegans larval development and adult longevity. *Development*.

Jia, K., Chen, D., & Riddle, D. L. (2004). The TOR pathway interacts with the insulin signaling pathway to regulate C. elegans larval development, metabolism and life span. *Development*. https://doi.org/10.1242/dev.01255

Johnson, T. E., Henderson, S., Murakami, S., De Castro, E., De Castro, S. H., Cypser, J., Rikke, B., Tedesco, P., & Link, C. (2002). Longevity genes in the nematode Caenorhabditis elegans also mediate increased resistance to stress and prevent disease. *Journal of Inherited Metabolic Disease*. https://doi.org/10.1023/A:1015677828407

Johnson, Thomas E., De Castro, E., Hegi de Castro, S., Cypser, J., Henderson, S., & Tedesco, P. (2001). Relationship between increased longevity and stress resistance as assessed through gerontogene mutations in Caenorhabditis elegans. In *Experimental Gerontology*. https://doi.org/10.1016/S0531-5565(01)00144-9

Kaeberlein, M. (2007). Longevity Genomics Across Species. *Current Genomics*. https://doi.org/10.2174/138920207780368196

Kaeberlein, M., & Kapahi, P. (2009). Aging is rsky business. In *Science*. https://doi.org/10.1126/science.1181034

Kaeberlein, M., Westman, E., Dang, N., Kerr, E., Powers III, R., Steffen, K., Hu, D., Kennedy, B., Kirkland, K., & Fields, S. (2005). Regulation of Yeast Replicative Life Span by TOR and Sch9 in Response to Nutrients. *Science*.

Kao, G., Nordenson, C., Still, M., Rönnlund, A., Tuck, S., & Naredi, P. (2007). ASNA-1 Positively Regulates Insulin Secretion in C. elegans and Mammalian Cells. *Cell*. https://doi.org/10.1016/j.cell.2006.12.031

Kapahi, P., Zid, B. M., Harper, T., Koslover, D., Sapin, V., & Benzer, S. (2004). Regulation of lifespan in Drosophila by modulation of genes in the TOR signaling pathway. *Current Biology*. https://doi.org/10.1016/j.cub.2004.03.059

Kaplan, R. E. W., & Baugh, L. R. (2016). L1 arrest, daf-16 /FoxO and nonautonomous control of post-embryonic development . *Worm*. https://doi.org/10.1080/21624054.2016.1175196

Kaplan, R. E. W., Chen, Y., Moore, B. T., Jordan, J. M., Maxwell, C. S., Schindler, A. J., & Baugh, L. R. (2015). dbl-1/TGF-β and daf-12/NHR Signaling Mediate Cell-Nonautonomous Effects of daf-16/FOXO on Starvation-Induced Developmental Arrest. *PLoS Genetics*. https://doi.org/10.1371/journal.pgen.1005731

Kaplan, R. E. W., Maxwell, C. S., Codd, N. K., & Baugh, L. R. (2019).

Pervasive positive and negative feedback regulation of insulin-like signaling in Caenorhabditis elegans. *Genetics*. https://doi.org/10.1534/genetics.118.301702

Kaplan, R. E. W., Webster, A. K., Chitrakar, R., Dent, J. A., & Baugh, L. R. (2018). Food perception without ingestion leads to metabolic changes and irreversible developmental arrest in C. elegans. *BMC Biology*. https://doi.org/10.1186/s12915-018-0579-3

Kasuga, H., Fukuyama, M., Kitazawa, A., Kontani, K., & Katada, T. (2013). The microRNA miR-235 couples blast-cell quiescence to the nutritional state. *Nature*. https://doi.org/10.1038/nature12117

Kato, Y., Miyaji, M., & Zhang-Akiyama, Q. M. (2016). Fudr extends the lifespan of the short-lived AP endonuclease mutant in Caenorhabditis elegans in a fertility-dependent manner. *Genes and Genetic Systems*. https://doi.org/10.1266/ggs.15-00064

Kenyon, C. (2011). The first long-lived mutants : discovery of the insulin / IGF-1 pathway for ageing. *Philos. Trans. R. Soc. Lond. B. Biol. Sci.*, 9–16. https://doi.org/10.1098/rstb.2010.0276

Kenyon, C., Chang, J., Gensch, E., Rudner, A., & Tabtiang, R. (1993). A C. elegans mutant that lives twice as long as wild type. *Nature*. https://doi.org/10.1038/366461a0

Kenyon, C. J. (2010). The genetics of ageing. In *Nature*. https://doi.org/10.1038/nature08980

Kim, K., Sato, K., Shibuya, M., Zeiger, D. M., Butcher, R. A., Ragains, J. R., Clardy, J., Touhara, K., & Sengupta, P. (2009). Two chemoreceptors mediate developmental effects of dauer pheromone in C. elegans. *Science*, *326*(5955), 994–998. https://doi.org/10.1126/science.1176331

Kim, S. K., Lund, J., Kiraly, M., Duke, K., Jiang, M., Stuart, J. M., Eizinger, A., Wylie, B. N., & Davidson, G. S. (2001). A gene expression map for Caenorhabditis elegans. *Science*. https://doi.org/10.1126/science.1061603

Kim, S., Park, D. H., Kim, T. H., Hwang, M., & Shim, J. (2009). Functional analysis of pyrimidine biosynthesis enzymes using the anticancer drug 5-fluorouracil in Caenorhabditis elegans. *FEBS Journal*. https://doi.org/10.1111/j.1742-4658.2009.07168.x

Kim, Y., & Sun, H. (2007). Functional genomic approach to identify novel genes involved in the regulation of oxidative stress resistance and animal lifespan. *Aging Cell*. https://doi.org/10.1111/j.1474-9726.2007.00302.x

Klass, M. R. (1983). A method for the isolation of longevity mutants in the nematode Caenorhabditis elegans and initial results. *Mechanisms of Ageing and Development*. https://doi.org/10.1016/0047-6374(83)90082-9

Komatsu, H., Mori, I., Rhee, J. S., Akaike, N., & Ohshima, Y. (1996). Mutations in a cyclic nucleotide-gated channel lead to abnormal thermosensation and chemosensation in C. elegans. *Neuron*. https://doi.org/10.1016/S0896-6273(00)80202-0

Lakowski, B., & Hekimi, S. (1998). The genetics of caloric restriction in Caenorhabditis elegans. *Proceedings of the National Academy of Sciences of the United States of America*. https://doi.org/10.1073/pnas.95.22.13091

Lapierre, L. R., De Magalhaes Filho, C. D., McQuary, P. R., Chu, C. C., Visvikis, O., Chang, J. T., Gelino, S., Ong, B., Davis, A. E., Irazoqui, J. E., Dillin, A., & Hansen, M. (2013). The TFEB orthologue HLH-30 regulates autophagy and modulates longevity in Caenorhabditis elegans. *Nature Communications*. https://doi.org/10.1038/ncomms3267

Lapierre, L. R., Gelino, S., Meléndez, A., & Hansen, M. (2011). Autophagy and lipid metabolism coordinately modulate life span in germline-less C. elegans. *Current Biology*. https://doi.org/10.1016/j.cub.2011.07.042

Lapierre, L. R., & Hansen, M. (2012). Lessons from C. elegans: Signaling pathways for longevity. In *Trends in Endocrinology and Metabolism*. https://doi.org/10.1016/j.tem.2012.07.007

Larsen, P. L., Albert, P. S., & Riddle, D. L. (1995). Genes that regulate both development and longevity in Caenorhabditis elegans. *Genetics*.

Lee, I., Hendrix, A., Kim, J., Yoshimoto, J., & You, Y. J. (2012). Metabolic Rate Regulates L1 Longevity in C. elegans. *PLoS ONE*. https://doi.org/10.1371/journal.pone.0044720

Lee, R. Y. N., Hench, J., & Ruvkun, G. (2001). Regulation of C. elegans DAF-16 and its human ortholog FKHRL1 by the daf-2 insulin-like signaling pathway. *Current Biology*. https://doi.org/10.1016/S0960-9822(01)00595-4

Lee, S. S., Lee, R. Y. N., Fraser, A. G., Kamath, R. S., Ahringer, J., & Ruvkun, G. (2003). A systematic RNAi screen identifies a critical role for mitochondria in C. elegans longevity. *Nature Genetics*. https://doi.org/10.1038/ng1056

Lehtinen, M. K., Yuan, Z., Boag, P. R., Yang, Y., Villén, J., Becker, E. B. E., DiBacco, S., de la Iglesia, N., Gygi, S., Blackwell, T. K., & Bonni, A. (2006). A Conserved MST-FOXO Signaling Pathway Mediates Oxidative-Stress Responses and Extends Life Span. *Cell*. https://doi.org/10.1016/j.cell.2006.03.046

Li, J., Brown, G., Ailion, M., Lee, S., & Thomas, J. H. (2004). NCR-1 and NCR-2, the C. elegans homologs of the human Niemann-Pick type C1 disease protein, function upstream of DAF-9 in the dauer formation pathways. *Development*. https://doi.org/10.1242/dev.01408

Li, Weiqing, Kennedy, S. G., & Ruvkun, G. (2003). daf-28 encodes a C. elegans insulin superfamily member that is regulated by environmental cues and acts in the DAF-2 signaling pathway. *Genes and Development*. https://doi.org/10.1101/gad.1066503

Li, Wensheng, Gao, B., Lee, S. M., Bennett, K., & Fang, D. (2007). RLE-1, an E3 Ubiquitin Ligase, Regulates C. elegans Aging by Catalyzing DAF-16 Polyubiquitination. *Developmental Cell*. https://doi.org/10.1016/j.devcel.2006.12.002

Libina, N., Berman, J. R., & Kenyon, C. (2003). Tissue-Specific Activities of C. elegans DAF-16 in the Regulation of Lifespan. *Cell*. https://doi.org/10.1016/S0092-8674(03)00889-4

Lin, K., Hsin, H., Libina, N., & Kenyon, C. (2001). Regulation of the Caenorhabditis elegans longevity protein DAF-16 by insulin/IGF-1 and germline signaling. *Nature Genetics*. https://doi.org/10.1038/88850

Lin, X. X., Sen, I., Janssens, G. E., Zhou, X., Fonslow, B. R., Edgar, D.,

Stroustrup, N., Swoboda, P., Yates, J. R., Ruvkun, G., & Riedel, C. G. (2018). DAF-16/FOXO and HLH-30/TFEB function as combinatorial transcription factors to promote stress resistance and longevity. *Nature Communications*. https://doi.org/10.1038/s41467-018-06624-0

Liu, T., Zimmerman, K. K., & Patterson, G. I. (2004). Regulation of signaling genes by TGFβ during entry into dauer diapause in C. elegans. *BMC Developmental Biology*. https://doi.org/10.1186/1471-213X-4-11

López-Lluch, G., Hernández-Camacho, J. D., Fernández-Ayala, D. J. M., & Navas, P. (2018). Mitochondrial dysfunction in metabolism and ageing: shared mechanisms and outcomes? *Biogerontology*. https://doi.org/10.1007/s10522-018-9768-2

López-Otín, C., Blasco, M. A., Partridge, L., Serrano, M., & Kroemer, G. (2013). The hallmarks of aging. *Cell*, *153*(6). https://doi.org/10.1016/j.cell.2013.05.039

Lucanic, M., Garrett, T., Yu, I., Calahorro, F., Asadi Shahmirzadi, A., Miller, A., Gill, M. S., Hughes, R. E., Holden-Dye, L., & Lithgow, G. J. (2016). Chemical activation of a food deprivation signal extends lifespan. *Aging Cell*. https://doi.org/10.1111/acel.12492

Lucanic, M., Lithgow, G. J., & Alavez, S. (2013). Pharmacological lifespan extension of invertebrates. In *Ageing Research Reviews*. https://doi.org/10.1016/j.arr.2012.06.006

Ludewig, A. H., Kober-Eisermann, C., Weitzel, C., Bethke, A., Neubert, K., Gerisch, B., Hutter, H., & Antebi, A. (2004). A novel nuclear receptor/coregulator complex controls C. elegans lipid metabolism, larval development, and aging. *Genes and Development*. https://doi.org/10.1101/gad.312604

Ludewig, A., & Schroeder, F. (2013). *Ascaroside signalling in C.elegans*. WormBook, Ed. The C. Elegans Research Community. https://doi.org/10.1895/wormbook.1.1

Luo, S., Shaw, W. M., Ashraf, J., & Murphy, C. T. (2009). TGF-ß Sma/Mab signaling mutations uncouple reproductive aging from somatic aging. *PLoS Genetics*. https://doi.org/10.1371/journal.pgen.1000789

Mair, W., & Dillin, A. (2008). Aging and survival: The genetics of life span extension by dietary restriction. In *Annual Review of Biochemistry*. https://doi.org/10.1146/annurev.biochem.77.061206.171059

Mair, W., Morantte, I., Rodrigues, A. P. C., Manning, G., Montminy, M., Shaw, R. J., & Dillin, A. (2011). Lifespan extension induced by AMPK and calcineurin is mediated by CRTC-1 and CREB. *Nature*. https://doi.org/10.1038/nature09706

Mak, H. Y., & Ruvkun, G. (2004). Intercellular signaling of reproductive development by the C. elegans DAF-9 cytochrome P450. *Development*. https://doi.org/10.1242/dev.01069

Matsumoto, S., Häberle, J., Kido, J., Mitsubuchi, H., Endo, F., & Nakamura, K. (2019). Urea cycle disorders—update. In *Journal of Human Genetics*. https://doi.org/10.1038/s10038-019-0614-4

Matsunaga, Y., Gengyo-Ando, K., Mitani, S., Iwasaki, T., & Kawano, T. (2012). Physiological function, expression pattern, and transcriptional regulation of

a Caenorhabditis elegans insulin-like peptide, INS-18. *Biochemical and Biophysical Research Communications*. https://doi.org/10.1016/j.bbrc.2012.05.145
McElwee, J., Bubb, K., & Thomas, J. H. (2003). Transcriptional outputs of the Caenorhabditis elegans forkhead protein DAF-16. *Aging Cell*. https://doi.org/10.1046/j.1474-9728.2003.00043.x
McGrath, P. T., Xu, Y., Ailion, M., Garrison, J. L., Butcher, R. A., & Bargmann, C. I. (2011). Parallel evolution of domesticated Caenorhabditis species targets pheromone receptor genes. *Nature*. https://doi.org/10.1038/nature10378
McReynolds, M. R., Wang, W., Holleran, L. M., & Hanna-Rose, W. (2017). Uridine monophosphate synthetase enables eukaryotic de novo NAD+ biosynthesis from quinolinic acid. *Journal of Biological Chemistry*. https://doi.org/10.1074/jbc.C117.795344
Mehta, R., Steinkraus, K. A., Sutphin, G. L., Ramos, F. J., Shamieh, L. S., Huh, A., Davis, C., Chandler-Brown, D., & Kaeberlein, M. (2009). Proteasomal regulation of the hypoxic response modulates aging in C. elegans. *Science*. https://doi.org/10.1126/science.1173507
Meijer, A. J., & Codogno, P. (2008). Nutrient sensing: TOR's ragtime. *Nature Cell Biology*. https://doi.org/10.1038/ncb0808-881
Mihaylova, V. T., Borland, C. Z., Manjarrez, L., Stern, M. J., & Sun, H. (1999). The PTEN tumor suppressor homolog in Caenorhabditis elegans regulates longevity and dauer formation in an insulin receptor-like signaling pathway. *Proceedings of the National Academy of Sciences of the United States of America*. https://doi.org/10.1073/pnas.96.13.7427
Morita, K., Shimizu, M., Shibuya, H., & Ueno, N. (2001). A DAF-1-binding protein BRA-1 is a negative regulator of DAF-7 TGF-β signaling. *Proceedings of the National Academy of Sciences of the United States of America*. https://doi.org/10.1073/pnas.111409798
Motola, D. L., Cummins, C. L., Rottiers, V., Sharma, K. K., Li, T., Li, Y., Suino-Powell, K., Xu, H. E., Auchus, R. J., Antebi, A., & Mangelsdorf, D. J. (2006). Identification of Ligands for DAF-12 that Govern Dauer Formation and Reproduction in C. elegans. *Cell*. https://doi.org/10.1016/j.cell.2006.01.037
Mouchiroud, L., Houtkooper, R. H., Moullan, N., Katsyuba, E., Ryu, D., Cantó, C., Mottis, A., Jo, Y. S., Viswanathan, M., Schoonjans, K., Guarente, L., & Auwerx, J. (2013). XThe NAD+/sirtuin pathway modulates longevity through activation of mitochondrial UPR and FOXO signaling. *Cell*. https://doi.org/10.1016/j.cell.2013.06.016
Muñoz, M. J., & Riddle, D. L. (2003). Positive selection of Caenorhabditis elegans mutants with increased stress resistance and longevity. *Genetics*.
Murakami, M., Koga, M., & Ohshima, Y. (2001). DAF-7/TGF-β expression required for the normal larval development in C. elegans is controlled by a presumed guanylyl cyclase DAF-11. *Mechanisms of Development*. https://doi.org/10.1016/S0925-4773(01)00507-X
Murphy, C. T., Lee, S. J., & Kenyon, C. (2007). Tissue entrainment by feedback regulation of insulin gene expression in the endoderm of

Caenorhabditis elegans. *Proceedings of the National Academy of Sciences of the United States of America*. https://doi.org/10.1073/pnas.0709613104

Murphy, C. T., McCarroll, S. A., Bargmann, C. I., Fraser, A., Kamath, R. S., Ahringer, J., Li, H., & Kenyon, C. (2003). Genes that act downstream of DAF-16 to influence the lifespan of Caenorhabditis elegans. *Nature*. https://doi.org/10.1038/nature01789

Murphy, J. T., Liu, H., Ma, X., Shaver, A., Egan, B. M., Oh, C., Boyko, A., Mazer, T., Ang, S., Khopkar, R., Javaheri, A., Kumar, S., Jiang, X., Ory, D., Mani, K., Matkovich, S. J., Kornfeld, K., & Diwan, A. (2019). Simple nutrients bypass the requirement for HLH-30 in coupling lysosomal nutrient sensing to survival. *PLoS Biology*. https://doi.org/10.1371/journal.pbio.3000245

Nakamura, S., Karalay, Ö., Jäger, P. S., Horikawa, M., Klein, C., Nakamura, K., Latza, C., Templer, S. E., Dieterich, C., & Antebi, A. (2016). Mondo complexes regulate TFEB via TOR inhibition to promote longevity in response to gonadal signals. *Nature Communications*. https://doi.org/10.1038/ncomms10944

Napolitano, G., & Ballabio, A. (2016). TFEB at a glance. *Journal of Cell Science*. https://doi.org/10.1242/jcs.146365

Neal, S. J., Takeishi, A., O'Donnell, M. P., Park, J. S., Hong, M., Butcher, R. A., Kim, K., & Sengupta, P. (2015). Feeding state-dependent regulation of developmental plasticity via CaMKI and neuroendocrine signaling. *ELife*. https://doi.org/10.7554/eLife.10110

O'Rourke, E. J., & Ruvkun, G. (2013). MXL-3 and HLH-30 transcriptionally link lipolysis and autophagy to nutrient availability. *Nature Cell Biology*. https://doi.org/10.1038/ncb2741

Ogg, S., & Ruvkun, G. (1998). The C. elegans PTEN homolog, DAF-18, acts in the insulin receptor-like metabolic signaling pathway. *Molecular Cell*. https://doi.org/10.1016/S1097-2765(00)80303-2

Oh, S. W., Mukhopadhyay, A., Svrzikapa, N., Jiang, F., Davis, R. J., & Tissenbaum, H. A. (2005). JNK regulates lifespan in Caenorhabiditis elegans by modulating nuclear translocation of forkhead transcription factor/DAF-16. *Proceedings of the National Academy of Sciences of the United States of America*. https://doi.org/10.1073/pnas.0500749102

Ohkura, K., Suzuki, N., Ishihara, T., & Katsura, I. (2003). SDF-9, a protein tyrosine phosphatase-like molecule, regulates the L3/dauer developmental decision through hormonal signaling in C. elegans. *Development*. https://doi.org/10.1242/dev.00540

Oldham, S., & Hafen, E. (2003). Insulin/IGF and target of rapamycin signaling: A TOR de force in growth control. In *Trends in Cell Biology*. https://doi.org/10.1016/S0962-8924(02)00042-9

Onken, B., & Driscoll, M. (2010). Metformin induces a dietary restriction-like state and the oxidative stress response to extend C. elegans healthspan via AMPK, LKB1, and SKN-1. *PLoS ONE*. https://doi.org/10.1371/journal.pone.0008758

Page, T., Yu, A., Fontanesi, J., & Nyhan, W. L. (1997). Developmental

disorder associated with increased cellular nucleotidase activity. *Proceedings of the National Academy of Sciences of the United States of America*. https://doi.org/10.1073/pnas.94.21.11601

Panowski, S. H., Wolff, S., Aguilaniu, H., Durieux, J., & Dillin, A. (2007). PHA-4/Foxa mediates diet-restriction-induced longevity of C. elegans. *Nature*. https://doi.org/10.1038/nature05837

Paradis, S., Ailion, M., Toker, A., Thomas, J. H., & Ruvkun, G. (1999). A PDK1 homolog is necessary and sufficient to transduce AGE-1 PI3 kinase signals that regulate diapause in Caenorhabditis elegans. *Genes and Development*. https://doi.org/10.1101/gad.13.11.1438

Paradis, S., & Ruvkun, G. (1998). Caenorhabditis elegans Akt/PKB transduces insulin receptor-like signals from age-1 PI3 kinase to the DAF-16 transcription factor. *Genes and Development*. https://doi.org/10.1101/gad.12.16.2488

Park, D., O'Doherty, I., Somvanshi, R. K., Bethke, A., Schroeder, F. C., Kumar, U., & Riddle, D. L. (2012). Interaction of structure-specific and promiscuous G-protein-coupled receptors mediates small-molecule signaling in Caenorhabditis elegans. *Proceedings of the National Academy of Sciences of the United States of America*. https://doi.org/10.1073/pnas.1202216109

Patterson, G. I., Koweek, A., Wong, A., Liu, Y., & Ruvkun, G. (1997). The DAF-3 Smad protein antagonizes TGF-β-related receptor signaling in the Caenorhabditis elegans dauer pathway. *Genes and Development*. https://doi.org/10.1101/gad.11.20.2679

Peña-Llopis, S., Vega-Rubin-De-Celis, S., Schwartz, J. C., Wolff, N. C., Tran, T. A. T., Zou, L., Xie, X. J., Corey, D. R., & Brugarolas, J. (2011). Regulation of TFEB and V-ATPases by mTORC1. *EMBO Journal*. https://doi.org/10.1038/emboj.2011.257

Petrascheck, M., Ye, X., & Buck, L. B. (2007). An antidepressant that extends lifespan in adult Caenorhabditis elegans. *Nature*. https://doi.org/10.1038/nature05991

Petrascheck, M., Ye, X., & Buck, L. B. (2009). A high-throughput screen for chemicals that increase the lifespan of caenorhabditis elegans. *Annals of the New York Academy of Sciences*. https://doi.org/10.1111/j.1749-6632.2009.04377.x

Pickett, C. L., & Kornfeld, K. (2013). Age-related degeneration of the egg-laying system promotes matricidal hatching in Caenorhabditis elegans. *Aging Cell*. https://doi.org/10.1111/acel.12079

Pierce, S. B., Costa, M., Wisotzkey, R., Devadhar, S., Homburger, S. A., Buchman, A. R., Ferguson, K. C., Heller, J., Platt, D. M., Pasquinelli, A. A., Liu, L. X., Doberstein, S. K., & Ruvkun, G. (2001). Regulation of DAF-2 receptor signaling by human insulin and ins-1, a member of the unusually large and diverse C. elegans insulin gene family. *Genes and Development*. https://doi.org/10.1101/gad.867301

Pletcher, S. D., Macdonald, S. J., Marguerie, R., Certa, U., Stearns, S. C., Goldstein, D. B., & Partridge, L. (2002). Genome-wide transcript profiles in aging and calorically restricted Drosophila melanogaster. *Current Biology*.

https://doi.org/10.1016/S0960-9822(02)00808-4
Ren, P., Lim, C. S., Johnsen, R., Albert, P. S., Pilgrim, D., & Riddle, D. L. (1996). Control of C. elegans larval development by neuronal expression of a TGF-β homolog. *Science*. https://doi.org/10.1126/science.274.5291.1389
Riddle, D. L., & Albert, P. S. (1997). Genetic and Environmental Regulation of Dauer Larva Development. In *C. elegans II*.
Riddle, D. L., Swanson, M. M., & Albert, P. S. (1981). Interacting genes in nematode dauer larva formation. *Nature*. https://doi.org/10.1038/290668a0
Rohl, C., Price, Y., Fischer, T. B., Paczkowski, M., Zettel, M. F., & Tsai, J. (2006). Cataloging the relationships between proteins: A review of interaction databases. In *Molecular Biotechnology*. https://doi.org/10.1385/MB:34:1:69
Rottiers, V., Motola, D. L., Gerisch, B., Cummins, C. L., Nishiwaki, K., Mangelsdorf, D. J., & Antebi, A. (2006). Hormonal control of C. elegans dauer formation and life span by a Rieske-like oxygenase. *Developmental Cell*. https://doi.org/10.1016/j.devcel.2006.02.008
Rouault, J. P., Kuwabara, P. E., Sinilnikova, O. M., Duret, L., Thierry-Mieg, D., & Billaud, M. (1999). Regulation of dauer larva development in Caenorhabditis elegans by daf-18, a homologue of the tumour suppressor PTEN. *Current Biology*. https://doi.org/10.1016/S0960-9822(99)80143-2
Rual, J. F., Ceron, J., Koreth, J., Hao, T., Nicot, A. S., Hirozane-Kishikawa, T., Vandenhaute, J., Orkin, S. H., Hill, D. E., van den Heuvel, S., & Vidal, M. (2004). Toward improving Caenorhabditis elegans phenome mapping with an ORFeome-based RNAi library. *Genome Research*. https://doi.org/10.1101/gr.2505604
Salminen, A., Hyttinen, J. M. T., & Kaarniranta, K. (2011). AMP-activated protein kinase inhibits NF-κB signaling and inflammation: Impact on healthspan and lifespan. In *Journal of Molecular Medicine*. https://doi.org/10.1007/s00109-011-0748-0
Savage-Dunn, C. (2005). TGF-β signaling. *WormBook*. https://doi.org/10.1895/wormbook.1.22.1
Schackwitz, W. S., Inoue, T., & Thomas, J. H. (1996). Chemosensory neurons function in parallel to mediate a pheromone response in C. elegans. *Neuron*. https://doi.org/10.1016/S0896-6273(00)80203-2
Schaedel, O. N., Gerisch, B., Antebi, A., & Sternberg, P. W. (2012). Hormonal signal amplification mediates environmental conditions during development and controls an irreversible commitment to adulthood. *PLoS Biology*. https://doi.org/10.1371/journal.pbio.1001306
Schindler, A. J., Baugh, L. R., & Sherwood, D. R. (2014). Identification of Late Larval Stage Developmental Checkpoints in Caenorhabditis elegans Regulated by Insulin/IGF and Steroid Hormone Signaling Pathways. *PLoS Genetics*. https://doi.org/10.1371/journal.pgen.1004426
Schreiber, V., Dantzer, F., Amé, J. C., & De Murcia, G. (2006). Poly(ADP-ribose): Novel functions for an old molecule. In *Nature Reviews Molecular Cell Biology*. https://doi.org/10.1038/nrm1963
Schulenburg, H., & Félix, M. A. (2017). The natural biotic environment of

Caenorhabditis elegans. *Genetics*. https://doi.org/10.1534/genetics.116.195511
Seim, I., Fang, X., Xiong, Z., Lobanov, A. V., Huang, Z., Ma, S., Feng, Y., Turanov, A. A., Zhu, Y., Lenz, T. L., Gerashchenko, M. V., Fan, D., Hee Yim, S., Yao, X., Jordan, D., Xiong, Y., Ma, Y., Lyapunov, A. N., Chen, G., … Gladyshev, V. N. (2013). Genome analysis reveals insights into physiology and longevity of the Brandt's bat Myotis brandtii. *Nature Communications*. https://doi.org/10.1038/ncomms3212
Selman, C., Tullet, J. M. A., Wieser, D., Irvine, E., Lingard, S. J., Choudhury, A. I., Claret, M., Al-Qassab, H., Carmignac, D., Ramadani, F., Woods, A., Robinson, L. C. A., Schuster, E., Batterham, R. L., Kozma, S. C., Thomas, G., Carling, D., Okkenhaug, K., Thornton, J. M., … Withers, D. J. (2009). Ribosomal protein S6 kinase 1 signaling regulates mammalian life span. *Science*. https://doi.org/10.1126/science.1177221
Settembre, C., Di Malta, C., Polito, V. A., Arencibia, M. G., Vetrini, F., Erdin, S., Erdin, S. U., Huynh, T., Medina, D., Colella, P., Sardiello, M., Rubinsztein, D. C., & Ballabio, A. (2011). TFEB links autophagy to lysosomal biogenesis. *Science*. https://doi.org/10.1126/science.1204592
Shaw, W. M., Luo, S., Landis, J., Ashraf, J., & Murphy, C. T. (2007). The C. elegans TGF-β Dauer Pathway Regulates Longevity via Insulin Signaling. *Current Biology*. https://doi.org/10.1016/j.cub.2007.08.058
Sheaffer, K. L., Updike, D. L., & Mango, S. E. (2008). The Target of Rapamycin Pathway Antagonizes pha-4/FoxA to Control Development and Aging. *Current Biology*. https://doi.org/10.1016/j.cub.2008.07.097
Shen, Y., Wollam, J., Magner, D., Karalay, O., & Antebi, A. (2012). A steroid receptor-microRNA switch regulates life span in response to signals from the gonad. *Science*. https://doi.org/10.1126/science.1228967
Simmonds, H. A., Duley, J. A., Fairbanks, L. D., & McBride, M. B. (1997). When to investigate for purine and pyrimidine disorders. Introduction and review of clinical and laboratory indications. *Journal of Inherited Metabolic Disease*. https://doi.org/10.1023/A:1005308923168
Stoltzfus, J. D., Bart, S. M., & Lok, J. B. (2014). cGMP and NHR Signaling Co-regulate Expression of Insulin-Like Peptides and Developmental Activation of Infective Larvae in Strongyloides stercoralis. *PLoS Pathogens*. https://doi.org/10.1371/journal.ppat.1004235
Sulston, J. E., & Brenner, S. (1974). The DNA of Caenorhabditis elegans. *Genetics*.
Sun, X., Chen, W. D., & Wang, Y. D. (2017). DAF-16/FOXO transcription factor in aging and longevity. In *Frontiers in Pharmacology*. https://doi.org/10.3389/fphar.2017.00548
Sym, M., Basson, M., & Johnson, C. (2000). A model for Niemann-Pick type C disease in the nematode Caenorhabditis elegans. *Current Biology*. https://doi.org/10.1016/S0960-9822(00)00468-1
Tabara, H., Grishok, A., & Mello, C. C. (1998). RNAi in C. elegans: Soaking in the Genome sequence. In *Science*. https://doi.org/10.1126/science.282.5388.430
Tacutu, R., Budovsky, A., & Fraifeld, V. E. (2010). The NetAge database: A

compendium of networks for longevity, age-related diseases and associated processes. In *Biogerontology*. https://doi.org/10.1007/s10522-010-9265-8

Tacutu, R., Budovsky, A., Wolfson, M., & Fraifeld, V. E. (2010). MicroRNA-regulated protein-protein interaction networks: How could they help in searching for pro-longevity targets? *Rejuvenation Research*. https://doi.org/10.1089/rej.2009.0980

Tacutu, R., Shore, D. E., Budovsky, A., de Magalhães, J. P., Ruvkun, G., Fraifeld, V. E., & Curran, S. P. (2012). Prediction of C. elegans Longevity Genes by Human and Worm Longevity Networks. *PLoS ONE*. https://doi.org/10.1371/journal.pone.0048282

Tewari, M., Hu, P. J., Ahn, J. S., Ayivi-Guedehoussou, N., Vidalain, P. O., Li, S., Milstein, S., Armstrong, C. M., Boxem, M., Butler, M. D., Busiguina, S., Rual, J. F., Ibarrola, N., Chaklos, S. T., Bertin, N., Vaglio, P., Edgley, M. L., King, K. V., Albert, P. S., … Vidal, M. (2004). Systematic interactome mapping and genetic perturbation analysis of a C. elegans TGF-β signaling network. *Molecular Cell*. https://doi.org/10.1016/S1097-2765(04)00033-4

Thomas, J. H., Birnby, D. A., & Vowels, J. J. (1993). Evidence for parallel processing of sensory information controlling dauer formation in Caenorhabditis elegans. In *Genetics*.

Tiku, V., Jain, C., Raz, Y., Nakamura, S., Heestand, B., Liu, W., Späth, M., Suchiman, H. E. D., Müller, R. U., Slagboom, P. E., Partridge, L., & Antebi, A. (2016). Small nucleoli are a cellular hallmark of longevity. *Nature Communications*. https://doi.org/10.1038/ncomms16083

Timmons, L., & Fire, A. (1998). Specific interference by ingested dsRNA [10]. In *Nature*. https://doi.org/10.1038/27579

Treins, C., Giorgetti-Peraldi, S., Murdaca, J., Semenza, G. L., & Van Obberghen, E. (2002). Insulin stimulates hypoxia-inducible factor 1 through a phosphatidylinositol 3-kinase/target of rapamycin-dependent signaling pathway. *Journal of Biological Chemistry*. https://doi.org/10.1074/jbc.M204152200

Tullet, J. M. A., Hertweck, M., An, J. H., Baker, J., Hwang, J. Y., Liu, S., Oliveira, R. P., Baumeister, R., & Blackwell, T. K. (2008). Direct Inhibition of the Longevity-Promoting Factor SKN-1 by Insulin-like Signaling in C. elegans. *Cell*. https://doi.org/10.1016/j.cell.2008.01.030

Uno, M., & Nishida, E. (2016). Lifespan-regulating genes in c. Elegans. *Npj Aging and Mechanisms of Disease*. https://doi.org/10.1038/npjamd.2016.10

van Raamsdonk, J. M., & Hekimi, S. (2011). FUdR causes a twofold increase in the lifespan of the mitochondrial mutant gas-1. *Mechanisms of Ageing and Development*. https://doi.org/10.1016/j.mad.2011.08.006

Vellai, T. (2009). Autophagy genes and ageing. In *Cell Death and Differentiation*. https://doi.org/10.1038/cdd.2008.126

Vellai, Tibor, Takacs-Vellai, K., Zhang, Y., Kovacs, A. L., Orosz, L., & Müller, F. (2003). Influence of TOR kinase on lifespan in C. elegans. *Nature*. https://doi.org/10.1038/426620a

Visvikis, O., Ihuegbu, N., Labed, S. A., Luhachack, L. G., Alves, A. M. F., Wollenberg, A. C., Stuart, L. M., Stormo, G. D., & Irazoqui, J. E. (2014). Innate host defense requires TFEB-mediated transcription of cytoprotective and antimicrobial genes. *Immunity*. https://doi.org/10.1016/j.immuni.2014.05.002

Vowels, J. J., & Thomas, J. H. (1992). Genetic analysis of chemosensory control of dauer formation in Caenorhabditis elegans. *Genetics*.

Vowels, J. J., & Thomas, J. H. (1994). Multiple chemosensory defects in daf-11 and daf-21 mutants of Caenorhabditis elegans. *Genetics*.

Wan, Q. L., Meng, X., Fu, X., Chen, B., Yang, J., Yang, H., & Zhou, Q. (2019). Intermediate metabolites of the pyrimidine metabolism pathway extend the lifespan of C. elegans through regulating reproductive signals. *Aging*. https://doi.org/10.18632/aging.102033

Wan, Q. L., Shi, X., Liu, J., Ding, A. J., Pu, Y. Z., Li, Z., Wu, G. S., & Luo, H. R. (2017). Metabolomic signature associated with reproduction-regulated aging in Caenorhabditis elegans. *Aging*. https://doi.org/10.18632/aging.101170

Wang, J., & Kim, S. K. (2003). Global analysis of dauer gene expression in Caenorhabditis elegans. In *Development*. https://doi.org/10.1242/dev.00363

Wang, L., Naser, F. J., Spalding, J. L., & Patti, G. J. (2019). A protocol to compare methods for untargeted metabolomics. In *Methods in Molecular Biology*. https://doi.org/10.1007/978-1-4939-8769-6_1

Wang, Y., & Levy, D. E. (2006). C. elegans STAT cooperates with DAF-7/TGF-β signaling to repress dauer formation. *Current Biology*. https://doi.org/10.1016/j.cub.2005.11.061

Weinkove, D., Halstead, J. R., Gems, D., & Divecha, N. (2006). Long-term starvation and ageing induce AGE-1/PI 3-kinase-dependent translocation of DAF-16/FOXO to the cytoplasm. *BMC Biology*. https://doi.org/10.1186/1741-7007-4-1

Willcox, B. J., Donlon, T. A., He, Q., Chen, R., Grove, J. S., Yano, K., Masaki, K. H., Willcox, D. C., Rodriguez, B., & Curb, J. D. (2008). FOXO3A genotype is strongly associated with human longevity. *Proceedings of the National Academy of Sciences of the United States of America*. https://doi.org/10.1073/pnas.0801030105

Wolkow, C. A., Kimura, K. D., Lee, M. S., & Ruvkun, G. (2000). Regulation of C. elegans life-span by insulinlike signaling in the nervous system. *Science*. https://doi.org/10.1126/science.290.5489.147

Wollam, J., Magomedova, L., Magner, D. B., Shen, Y., Rottiers, V., Motola, D. L., Mangelsdorf, D. J., Cummins, C. L., & Antebi, A. (2011). The Rieske oxygenase DAF-36 functions as a cholesterol 7-desaturase in steroidogenic pathways governing longevity. *Aging Cell*. https://doi.org/10.1111/j.1474-9726.2011.00733.x

Wu, C. W., & Storey, K. B. (2016). Life in the cold: Links between mammalian hibernation and longevity. In *Biomolecular Concepts*. https://doi.org/10.1515/bmc-2015-0032

Wullschleger, S., Loewith, R., & Hall, M. N. (2006). TOR signaling in growth

and metabolism. In *Cell*. https://doi.org/10.1016/j.cell.2006.01.016
Xian, B., Shen, J., Chen, W., Sun, N., Qiao, N., Jiang, D., Yu, T., Men, Y., Han, Z., Pang, Y., Kaeberlein, M., Huang, Y., & Han, J. D. J. (2013). WormFarm: A quantitative control and measurement device toward automated Caenorhabditis elegans aging analysis. *Aging Cell*. https://doi.org/10.1111/acel.12063
Yamawaki, T. M., Berman, J. R., Suchanek-Kavipurapu, M., McCormick, M., Gaglia, M. M., Lee, S. J., & Kenyon, C. (2010). The somatic reproductive tissues of C. elegans promote longevity through steroid hormone signaling. *PLoS Biology*. https://doi.org/10.1371/journal.pbio.1000468
Yan, R., Wan, L., Pizzorno, G., & Cao, D. (2006). Uridine phosphorylase in breast cancer: A new prognostic factor? In *Frontiers in Bioscience*. https://doi.org/10.2741/2005
Yang, H., Lee, B. Y., Yim, H., & Lee, J. (2020). Neurogenetics of nictation, a dispersal strategy in nematodes. In *Journal of Neurogenetics*. https://doi.org/10.1080/01677063.2020.1788552
Ye, X., Linton, J. M., Schork, N. J., Buck, L. B., & Petrascheck, M. (2014). A pharmacological network for lifespan extension in Caenorhabditis elegans. *Aging Cell*. https://doi.org/10.1111/acel.12163
Zhang, H., Ryu, D., Wu, Y., Gariani, K., Wang, X., Luan, P., D'Amico, D., Ropelle, E. R., Lutolf, M. P., Aebersold, R., Schoonjans, K., Menzies, K. J., & Auwerx, J. (2016). NAD+ repletion improves mitochondrial and stem cell function and enhances life span in mice. *Science*. https://doi.org/10.1126/science.aaf2693
Zwaal, R. R., Mendel, J. E., Sternberg, P. W., & Plasterk, R. H. A. (1997). Two neuronal G proteins are involved in chemosensation of the Caenorhabditis elegans dauer-inducing pheromone. *Genetics*.

11 APPENDIX

Table 2: Primers used for genotyping, qPCR designed using SeqBuilder (DNASTAR) and CRISPR oligos.

Gene	Sequence
Genotyping primers	
marc-6 F	TCTAAATGATCCCGACTTTAATCCAATC
marc-6 R	TAGAAGTGATGGAATAAGTGATGAGATTATGTTG
png-1 F	CTTGCCGCTCTTAATCTGGAATCTCGCT
png-1 R	TTCTCGTTTTCTCGGCTCCGTTTGACCTT
elpc-2 F	TTAATGACAATCCCGATCATCTTCTCGTCC
elpc-2 R	GTTGATTGAGAAGAGATTAGCTGATGATGTCA
ogdh-1 F	CGCTCGTCTCCATATTGTACAGATGTTGGc
ogdh-1 R	AGCTCATTGTGTCCGTGACGC
daf-16(mfDf50) F	ACAACGAAAAAATTCCCCGC
daf-16(mfDf50) R	GAAGTGGATTCTGAGCACAC
daf-16(mfDf50) F mid	AGAATGGTATTGTTGGGGCC
alg-4(syb635) F	TCGTGGAATGAAGATTCGTGCGG
alg-4(syb635) R	ATTGGTGGTGGCTGGATGACACA
xpb-1(syb682) F	AAGCTCTTGCTCGCCGTGATG
xpb-1(syb682) R	GTTGAACTGATCTGTGGAATGCTTTTT
alg-1(syb656) F	ATGCTCAACGTGTCAAGTTCACCA
alg-1(syb656) R	AGCCTTAATCATTGTCGATGTCTGC
upp-1(syb659) F	CCAGGACGTTTCAAGTTGTATGCT
upp-1(syb659) R	CACCGACTCCTCCAGATGTTC
ZC581.7(syb662) F	AGCTGGTTGACTCAATGCAAAAAGAAA
ZC581.7(syb662) R	GCACGGCACATTCCAAAGTCA
Y55F3BR.1(syb657) F	GGCGGCACTGGCAAAAAGTCATTC
Y55F3BR.1(syb657) R	CAGAAGCAAACGTTTGAATATTCTGGAAAGTTTG
piki-1(syb658) F	AGTTCTTGTCAAGTGATAGCCTGC
piki-1(syb658) R	GTCCATTTTCGACAACACTTCCACTT
prp-21(syb755) F	CAGTGAAAGAGCACGTGAAAAAGG
prp-21(syb755) R	AAAAGTTATAAAGCTCACTTTTCCGCCAT
anoh-1(syb742) F	GATATTCATACATCCCTACTGAAAATCCTT
anoh-1(syb742) R	GTTCCCAATTCAAGCTCAAACTTCGT
vps-18(syb773) F	GAAAAAAAAAACAAAAAATTGTCTGCCTCCTC
vps-18(syb773) R	ATCACATTTTTTCGCATAAAATATCGCTGAA
ptr-10(syb633) F	GTGCCTACATCGCATCTGCCT
ptr-10(syb633) R	TCATCTTGCACATTCAAAAAGGTAGAGTTCTT
upp-1(syb2043) F	CTTGGAGATACCTATGTGCAAATCATC
upp-1(syb2043) R	AGCAGACTGGAATCCAGCGC
daf-7(e1372) F	CCAAGTTATGGAGAGAACCCGTC
daf-7(e1372) R	ATCCCTTTGTAGCGAAAATTCCAGAAG
daf-2(e1368) F	TGTGATAGCATATAGATTTCTGAGCAGT
daf-2(e1368) R	GGAAATCTGACGATCGAGATTCG
daf-3(e1376) F	GTCTTGAAATTGGTGGATCATTCGG
daf-3(e1376) R	ATATTAGCCATCCAAATCACTATTCCTAC
daf-5(e1386) F	TCATCGCTCTCCAACCATTCGCT
daf-5(e1386) R	CTTCCTACGCATCTCTCACTCTAA
pdk-1(sa680) F	GGAGATGCTAGCTGACGGAGA
pdk-1(sa680) R	ACGTATTCAGTTTTTAAAGTTTCATGTCAACCT
daf-1(m40) F	CGAAAGACCCGCACGCTACC
daf-1(m40) R	GAGGAAAATTGCAATGCCCAGGAG
hlh-30(tm1978) F	CTCGCGATCTTTTTGGAGCACTC
hlh-30(tm1978) R	GAAGGAACGAAACAAAAAAAAACCGGTT
hlh-30 (tm1978) R mid	AATTTGGAAAATTTAAGACTTACGGTGTAAAC

Gene	Sequence
qPCR primers	
daf-7 F qPCR 1	AAGATCGGATGGGACTGGATCG
daf-7 R qPCR 1	TCCGGTTTCCGCCAAGTTGAAG
daf-1 F qPCR 1	AAGTGGACTTGCGTTCCTGCAC
daf-1 R qPCR 1	TCGCTGGCTTGTTGGACTCTTTG
F44B9.5 F qPCR 1	AAGGTTACATTGGACGCTGGTACG
F44B9.5 R qPCR 1	TGGCGATTAACTTCGATCATCTGC
CRISPR injected oligos	
marc-6 guide 1	TTCTAATACGACTCACTATAGCCTTCATTGGATGGTTGGAAGTTTTA
marc-6 guide 2	TTCTAATACGACTCACTATAGATATTCCTTCATTGGATGGTGTTTTAG
marc-6 RT	TTCATGTCAATATTCCTTCACTGGATGGTGGGAATGATTTATGTATTT TATTCAGCGTCATTTGTAATACTTCTACGAGA
png-1 guide 1	TTCTAATACGACTCACTATAGTGGATACGGTAGTGATCATGGTTTTA
png-1 guide 2	TTCTAATACGACTCACTATAGATCATGTGGTTGACGTCACTGTTTTA
*png-*1 RT	GACACTGGGTTACTGTATTGGATACGGTAGTGACCATATGGTTGAC GTCACTTGGAGATATATTTGGGATTCCAAAAAATTGGT
ogdh-1 guide 1	TTCTAATACGACTCACTATAGACAGATGTTGGTCGTGTCGTGTTTTA
ogdh-1 guide 2	TTCTAATACGACTCACTATAGTCTCCATATTGTACAGATGTGTTTTAG
*ogdh-*1 RT	CGATCCAAGATCTTCTCGCTCGTCTCCATATTGTACAGATGCTGGTT GTGTCGTCGAATGCCCGATCTTCCACGTGAACG
elpc-2 guide 1	TTCTAATACGACTCACTATAGCATCTTCTCGTCGCCTCAGCGTTTTA
elpc-2 guide 2	TTCTAATACGACTCACTATAGATAAGTGTCTTGTCCAGCTGGTTTTA
elpc-2 RT	TCGATTGCTTTTAATGACAATCCCGATCATCTTCTCGTCGTCTCGGC TGGACAAGACACTTATGTCAGACTATGGGCAAT

Table 3: Complete metabolomics analysis of the differentially regulated metabolites between *upp-1(syb659)* and N2.

	N2						*upp-1(syb659)*						N2 vs *upp-1*	
Compounds	**R1**	**R2**	**R3**	**R4**	**R5**	**Average**	**R1**	**R2**	**R3**	**R4**	**R5**	**Average**	**P. VALUE**	**% Change**
a ketoglutarate	0.0013	0.0012	0.0015	0.0013	0.0010	0.0012	0.0022	0.0029	0.0022	0.0022	0.0034	0.0026	0.0009	51.9914
Acetyl Arginine	0.2565	0.2485	0.2271	0.2961	0.3173	0.2691	0.2478	0.2936	0.2105	0.1986	0.2871	0.2475	0.4197	-8.7129
Acetyl Carnitine	1.1369	0.8145	1.0498	1.0171	1.1479	1.0332	0.5186	0.6279	0.5210	0.3625	0.5363	0.5133	0.0001	-101.3048
Acetyl Glucosamine	0.0280	0.0163	0.0125	0.0217	0.0134	0.0184	0.0135	0.0178	0.0172	0.0101	0.0108	0.0139	0.2091	-32.4245
Acetyl ornithine	0.0630	0.0443	0.0548	0.0602	0.0679	0.0580	0.0300	0.0243	0.0242	0.0155	0.0439	0.0276	0.0012	-110.4196
Acetyl Serine	1.8566	1.4687	1.3852	2.7641	2.6383	2.0226	2.5101	2.1620	1.2461	2.1073	1.9850	2.0021	0.9556	-1.0227
Acetyl Spermidine	0.1273	0.2219	0.1222	0.1601	0.2605	0.1784	0.0605	0.0697	0.0828	0.0421	0.0542	0.0619	0.0110	-188.3217
Adenine	3.7878	2.9790	5.8402	2.3708	3.0157	3.5987	1.8350	2.0173	1.1033	1.6300	2.5183	1.8208	0.0251	-97.6445
Adenosine	0.1882	0.3067	0.1874	0.3467	0.3772	0.2813	0.3318	0.5724	0.2184	0.2848	0.3699	0.3555	0.3318	20.8767
Adernyl Succinic acid	0.1457	0.1147	0.0774	0.1061	0.1652	0.1218	0.1387	0.0781	0.1090	0.1342	0.1783	0.1277	0.8022	4.5939
ADP	0.0418	0.0878	0.1006	0.1050	0.1115	0.0893	0.0779	0.1143	0.0361	0.0779	0.1044	0.0821	0.7055	-8.7994
Amino_deoxy_phosph ono_gluconpyranose	0.0012	0.0025	0.0019	0.0024	0.0020	0.0020	0.0086	0.0054	0.0051	0.0124	0.0047	0.0072	0.0226	72.3692
Aminoadipic acid	0.1527	0.1277	0.1776	0.1974	0.1851	0.1681	0.1106	0.1477	0.1183	0.0970	0.1346	0.1216	0.0163	-38.1828
AMP	14.2629	9.3765	7.1189	12.9105	11.8066	11.0951	4.6226	4.9648	4.4779	3.2194	3.0128	4.0595	0.0038	-173.3113
Arginine	6.9981	8.6565	8.5809	10.7716	10.8569	9.1728	9.0837	12.9122	12.2839	11.6171	11.0927	11.3979	0.0534	19.5222
Aspartic acid	0.0134	0.0162	0.0150	0.0263	0.0245	0.0191	0.0437	0.0427	0.0412	0.0709	0.0284	0.0454	0.0076	57.9834
Betaine	11.2199	14.4283	14.6568	15.2134	16.1712	14.3379	12.6053	18.1227	11.8015	15.0231	13.5351	14.2175	0.9332	-0.8466
Biotin	0.0258	0.0292	0.0120	0.0221	0.0304	0.0239	0.0210	0.0179	0.0105	0.0175	0.0258	0.0185	0.2303	-29.0379
cAMP	0.0029	0.0053	0.0032	0.0013	0.0011	0.0028	0.0077	0.0076	0.0072	0.0092	0.0116	0.0087	0.0007	68.0988
Carnitine	2.5100	3.3285	3.4028	4.7800	4.3197	3.6682	3.3410	4.6300	2.8449	3.2806	4.0356	3.6264	0.9365	-1.1528
Carnosine	0.0010	0.0009	0.0005	0.0009	0.0005	0.0008	0.0014	0.0018	0.0015	0.0014	0.0011	0.0014	0.0017	46.2828
CDP ethanolamine	0.0206	0.0147	0.0159	0.0158	0.0097	0.0153	0.0133	0.0133	0.0122	0.0111	0.0173	0.0135	0.3792	-14.0339
cGMP	0.0010	0.0010	0.0015	0.0017	0.0023	0.0015	0.0017	0.0017	0.0019	0.0019	0.0016	0.0018	0.3697	14.4847
Choline	36.6963	35.5859	33.3350	47.2365	41.3538	38.8415	31.2133	43.5697	25.9697	35.8669	43.0594	35.9358	0.5087	-8.0858
Citric Acid	3.5916	3.3015	4.6343	3.6184	4.8872	4.0066	3.1057	3.4803	1.8119	1.8191	2.5989	2.5632	0.0139	-56.3141
Citrulline	0.0215	0.0307	0.0324	0.0392	0.0438	0.0335	0.0347	0.0421	0.0310	0.0515	0.0480	0.0415	0.1828	19.1146
CMP	0.0625	0.0514	0.0367	0.0604	0.0593	0.0541	0.0771	0.0754	0.0396	0.0665	0.0611	0.0639	0.2641	15.4737
Coenzyme A	0.0347	0.0522	0.0301	0.0311	0.0538	0.0404	0.0537	0.0438	0.0411	0.0293	0.0490	0.0434	0.6628	6.9468
Cythidine_diphosphocholine	0.0662	0.0380	0.0462	0.0790	0.0513	0.0561	0.0601	0.0824	0.0686	0.0972	0.0744	0.0765	0.0683	26.6519
Cytidine	0.0054	0.0086	0.0088	0.0057	0.0086	0.0074	0.0085	0.0127	0.0068	0.0071	0.0087	0.0088	0.3383	15.1705
Cytosine	0.0063	0.0059	0.0049	0.0076	0.0061	0.0062	0.0085	0.0081	0.0040	0.0061	0.0059	0.0065	0.7030	5.5727
D-Erythrose_4-phosphate	0.0014	0.0009	0.0011	0.0018	0.0010	0.0012	0.0048	0.0044	0.0020	0.0011	0.0017	0.0028	0.1049	56.1911
Deoxy-D-xylulose_5-phosphate	0.0447	0.0408	0.0399	0.0612	0.0438	0.0461	0.0609	0.0569	0.0464	0.0450	0.0485	0.0515	0.3037	10.6492
Deoxyadenosine	0.0001	0.0002	0.0001	0.0002	0.0002	0.0002	0.0001	0.0002	0.0001	0.0001	0.0001	0.0001	0.5574	-8.6362
Deoxyguanosine	0.1882	0.3138	0.2450	0.3450	0.3802	0.2945	0.3208	0.2022	0.2133	0.2791	0.3637	0.2758	0.6983	-6.7633
Diaminopimelic_acid	0.0221	0.0439	0.0204	0.0182	0.0230	0.0255	0.0507	0.0207	0.0299	0.0238	0.0498	0.0350	0.2662	27.0799
Dihydroxyacetone_phosphate	0.0126	0.0182	0.0101	0.0188	0.0097	0.0139	0.0141	0.0061	0.0074	0.0125	0.0154	0.0111	0.3271	-25.4332
Dimethylarginine	0.4692	0.5127	0.5142	0.5800	0.6782	0.5509	0.4128	0.3868	0.2714	0.3592	0.5792	0.4019	0.0433	-37.0757
Erythrulose	0.0060	0.0054	0.0115	0.0122	0.0134	0.0097	0.0059	0.0130	0.0067	0.0084	0.0058	0.0080	0.4369	-21.8821
FAD	0.0083	0.0092	0.0063	0.0121	0.0093	0.0090	0.0062	0.0078	0.0080	0.0086	0.0091	0.0079	0.3356	-13.6870
FMN	0.1602	0.2005	0.1335	0.1946	0.2116	0.1801	0.1919	0.1551	0.1424	0.1235	0.2141	0.1654	0.5218	-8.8985
Gamma_glutamyl_cysteine	0.0118	0.0549	0.0367	0.0635	0.0556	0.0445	0.0402	0.0526	0.0106	0.0246	0.0584	0.0373	0.5905	-19.2711
Gamma-Aminobutyric_acid	0.1270	0.0590	0.0680	0.1169	0.0668	0.0875	0.0388	0.1014	0.1096	0.1195	0.0665	0.0871	0.9851	-0.4574
Gamma-glutamyl-L-putrescine	0.0193	0.0465	0.0316	0.0326	0.0528	0.0366	0.0404	0.0302	0.0148	0.0265	0.0437	0.0311	0.5074	-17.4993
GDP	0.0054	0.0070	0.0035	0.0090	0.0052	0.0060	0.0079	0.0099	0.0104	0.0099	0.0084	0.0093	0.0149	35.1403
Glucosamine 6 P	0.0050	0.0025	0.0037	0.0054	0.0043	0.0042	0.0027	0.0054	0.0051	0.0047	0.0029	0.0041	0.9356	-1.5500
Glucose Bi P	0.0344	0.0341	0.0323	0.0521	0.0370	0.0380	0.0414	0.0520	0.0428	0.0345	0.0336	0.0409	0.5733	7.0646
Glutamic acid	2.1513	2.6654	3.3942	2.2031	3.8379	2.8504	3.8575	5.3137	4.0146	3.4059	3.7974	4.0778	0.0297	30.0994
Glutamic_gamma-semialdehyde	0.0018	0.0022	0.0034	0.0019	0.0019	0.0022	0.0012	0.0013	0.0012	0.0009	0.0020	0.0013	0.0292	-68.6090
Glutamine	2.7240	2.1792	2.2637	3.1003	3.0059	2.6546	3.1185	3.4319	2.8564	4.0299	3.0638	3.3001	0.0485	19.5592
GMP	1.5304	1.2585	1.1445	1.7505	1.6299	1.4628	1.0319	1.4137	1.4572	1.4148	1.5633	1.3762	0.5673	-6.2915
GSH ox	1.1582	1.7941	2.0937	2.1159	2.7560	1.9836	1.6178	1.5964	1.0978	1.0056	2.5127	1.5661	0.2950	-26.6574
GSH red	4.2376	4.0689	2.9755	4.9919	4.7706	4.2089	3.5921	4.4721	3.9874	5.0341	4.2415	4.2654	0.8978	1.3254
Guanine	0.1353	0.4009	0.4793	0.4577	0.2385	0.3424	0.1563	0.4077	0.1689	0.2418	0.2067	0.2363	0.2254	-44.8893
Guanosine	0.1027	0.1180	0.0995	0.1042	0.1637	0.1176	0.1070	0.1165	0.0944	0.0793	0.1257	0.1046	0.3948	-12.4561
Hexenoylcarnitine	0.0016	0.0017	0.0017	0.0016	0.0012	0.0016	0.0009	0.0019	0.0010	0.0021	0.0013	0.0014	0.6298	-9.0084
Hexose	0.0151	0.0159	0.0143	0.0109	0.0183	0.0149	0.0120	0.0215	0.0150	0.0109	0.0265	0.0172	0.5013	13.1288
Hexose Phosphate	0.1256	0.1245	0.1683	0.1813	0.1576	0.1515	0.2241	0.2736	0.1797	0.2857	0.1737	0.2274	0.0187	33.3853
Histidine	0.2383	0.3015	0.2519	0.2847	0.2648	0.2683	0.2836	0.2073	0.2427	0.1642	0.1572	0.2110	0.0618	-27.1357

	N2						*upp-1(syb659)*						N2 vs *upp-1*	
Compounds	**R1**	**R2**	**R3**	**R4**	**R5**	**Average**	**R1**	**R2**	**R3**	**R4**	**R5**	**Average**	**P. VALUE**	**% Change**
Homocitrulline	0.0011	0.0011	0.0012	0.0011	0.0012	0.0011	0.0013	0.0007	0.0011	0.0012	0.0012	0.0011	0.6691	-4.4967
Homocysteine	0.0024	0.0023	0.0025	0.0045	0.0039	0.0031	0.0027	0.0050	0.0044	0.0056	0.0039	0.0043	0.1117	27.8709
Hydroxy deoxy Guanosine	0.1027	0.1189	0.0952	0.1043	0.0983	0.1039	0.1070	0.1166	0.1195	0.1178	0.1530	0.1228	0.0652	15.4012
Hydroxy Pyruvic Acid	0.0050	0.0081	0.0064	0.0073	0.0082	0.0070	0.0054	0.0083	0.0039	0.0035	0.0043	0.0051	0.1070	-37.5225
Hypoxanthine	1.0654	3.2021	1.2404	1.8628	2.3362	1.9414	2.7888	2.8670	1.2852	2.0470	3.2208	2.4417	0.3643	20.4920
IMP	0.1447	0.1764	0.1599	0.1440	0.1795	0.1609	0.0984	0.2250	0.1454	0.0916	0.1458	0.1412	0.4688	-13.9130
Inosine	0.1170	0.1138	0.1973	0.2109	0.1147	0.1508	0.1076	0.1174	0.0928	0.1376	0.0956	0.1102	0.1208	-36.8002
Inosinic Acid	0.1539	0.1018	0.1904	0.1353	0.1418	0.1446	0.0889	0.1396	0.1235	0.1135	0.1809	0.1293	0.4848	-11.8827
Isoleucine	10.5133	9.9934	9.3702	13.2647	9.9518	10.6187	15.3877	12.9822	11.9441	14.0767	15.1068	13.8995	0.0083	23.6039
Kynurenine	0.0450	0.0560	0.0485	0.0563	0.0533	0.0518	0.0480	0.0528	0.0450	0.0367	0.0678	0.0500	0.7601	-3.5344
Leucine	5.1872	7.1738	7.4997	10.7378	7.8198	7.6837	4.6760	10.7628	5.5809	8.0348	6.6686	7.1446	0.7078	-7.5450
Lysine	0.1850	0.2600	0.2944	0.5416	0.3615	0.3285	0.3321	0.2996	0.4940	0.4258	0.3985	0.3900	0.4021	15.7702
Mannose Phosphate	1.3906	1.4001	1.1938	1.1259	1.2243	1.2669	1.0642	1.2595	1.1979	0.8134	1.2312	1.1132	0.1581	-13.8054
Methionine	4.4558	3.5734	2.8658	4.6348	3.7029	3.8465	1.8352	2.2678	2.0713	2.6550	2.6522	2.2963	0.0025	-67.5113
Methionine Sulfoxide	0.0132	0.0117	0.0164	0.0122	0.0174	0.0142	0.0065	0.0104	0.0053	0.0095	0.0098	0.0083	0.0050	-70.5597
Methyl Adenosine	0.0177	0.0248	0.0178	0.0138	0.0173	0.0183	0.0086	0.0278	0.0201	0.0199	0.0129	0.0179	0.9167	-2.2653
Methyl Guanosine	0.3882	0.4188	0.3071	0.3696	0.4894	0.3946	0.0931	0.2743	0.2144	0.3297	0.3577	0.2538	0.0356	-55.4693
N_Acetyl_putresceine	1.1095	1.4985	1.0782	1.7825	1.3494	1.3636	1.0973	1.1579	1.0678	1.4640	2.0512	1.3677	0.9861	0.2977
N-Acetyl-D-glucosamine	0.0348	0.0329	0.0235	0.0412	0.0365	0.0338	0.0133	0.0336	0.0228	0.0229	0.0339	0.0253	0.1176	-33.5756
NAD	0.0149	0.0100	0.0159	0.0124	0.0105	0.0127	0.0189	0.0216	0.0158	0.0187	0.0177	0.0185	0.0047	31.3118
Nicotinamide	0.0112	0.0163	0.0088	0.0085	0.0087	0.0107	0.0151	0.0172	0.0156	0.0149	0.0205	0.0167	0.0111	35.7954
Nicotinic Acid	12.5977	12.0826	10.2820	14.6677	13.8855	12.7031	10.3864	12.1340	11.1337	10.3641	14.8407	11.7718	0.4323	-7.9114
NMN	0.0193	0.0120	0.0117	0.0244	0.0428	0.0220	0.0810	0.0816	0.0759	0.0822	0.0955	0.0832	0.0000	73.5227
Octenoylcarnitine	0.0361	0.0246	0.0318	0.0318	0.0293	0.0307	0.0240	0.0340	0.0275	0.0326	0.0264	0.0289	0.5167	-6.2694
Ornithine	0.0343	0.0136	0.0211	0.0419	0.0182	0.0258	0.0163	0.0263	0.0191	0.0111	0.0206	0.0187	0.2581	-38.1385
Orotic acid	0.0017	0.0012	0.0018	0.0017	0.0016	0.0016	0.0041	0.0039	0.0038	0.0024	0.0028	0.0034	0.0045	52.6936
Panthotenic acid	0.7599	0.7523	0.5207	0.8612	0.8506	0.7489	0.5963	0.7379	0.4691	0.6444	0.7596	0.6414	0.2194	-16.7583
Phenylalanine	24.8582	20.4343	17.3976	29.4185	20.9074	22.6032	13.8080	23.7812	9.3686	26.7642	21.1637	18.9771	0.3718	-19.1077
Phosphoenolpyruvic_acid	0.0536	0.0602	0.0957	0.0871	0.0851	0.0764	0.0630	0.0580	0.0848	0.0301	0.0394	0.0551	0.1291	-38.6776
Phosphopanthenine	0.0109	0.0214	0.0342	0.0302	0.0238	0.0241	0.0174	0.0200	0.0117	0.0306	0.0272	0.0214	0.6201	-12.6535
Phosphoserine	0.0103	0.0364	0.0236	0.0241	0.0206	0.0230	0.0120	0.0255	0.0088	0.0277	0.0236	0.0195	0.5564	-17.7505
Phosphotreonine	0.0020	0.0014	0.0019	0.0037	0.0020	0.0022	0.0010	0.0026	0.0020	0.0017	0.0016	0.0018	0.3978	-23.3386
Proline	5.4164	5.1496	6.0206	7.9506	6.5700	6.2214	5.0694	7.8102	4.8793	6.9734	6.5421	6.2549	0.9656	0.5345
Propionyl Carnitine	0.5534	0.6204	0.4591	0.3327	0.4035	0.4738	0.4318	0.5138	0.4499	0.2392	0.3841	0.4038	0.3401	-17.3496
Pyridoxal 5 Phosphate	0.0051	0.0053	0.0045	0.0082	0.0055	0.0057	0.0038	0.0060	0.0049	0.0056	0.0051	0.0051	0.4396	-11.8581
Pyroglutamic acid	0.6100	0.3792	0.5770	0.3594	0.7141	0.5279	0.6624	0.8084	0.5372	0.4317	0.6919	0.6263	0.3287	15.7079
Ribose/xylulose_phosphate	0.1574	0.1435	0.1010	0.1159	0.1535	0.1343	0.0781	0.1047	0.0962	0.0970	0.1560	0.1064	0.1432	-26.1942
S adenosyl methionine	0.1262	0.1006	0.0818	0.1185	0.1001	0.1055	0.0750	0.0862	0.0812	0.0570	0.0982	0.0795	0.0366	-32.5813
Spermidine	3.1438	2.8543	2.1398	2.1491	2.3999	2.5374	1.9863	2.3357	3.0696	1.9380	1.8743	2.2408	0.3495	-13.2379
Spermine	0.0010	0.0011	0.0011	0.0012	0.0011	0.0011	0.0010	0.0013	0.0011	0.0011	0.0012	0.0011	0.4643	4.4439
Sucrose/Maltose	3.8222	3.8239	4.1329	3.9605	5.1721	4.1823	3.9052	4.8013	2.9554	2.6006	4.6557	3.7836	0.4562	-10.5368
Threonine	0.1908	0.1197	0.2168	0.2348	0.1999	0.1924	0.2560	0.3073	0.3168	0.1931	0.1951	0.2537	0.1001	24.1468
Thymidine	0.0088	0.0095	0.0092	0.0157	0.0116	0.0110	0.0016	0.0019	0.0075	0.0044	0.0012	0.0033	0.0024	-230.8507
Thymine	0.0010	0.0006	0.0002	0.0007	0.0002	0.0005	0.0085	0.0090	0.0074	0.0137	0.0105	0.0098	0.0009	94.4168
Tryptophan	12.6484	9.9477	8.2174	9.8999	10.8189	10.3065	8.9065	12.6470	11.2808	9.0944	9.2140	10.2285	0.9418	-0.7621
Tyrosine	3.7840	4.5094	4.0872	6.4532	4.9301	4.7528	3.1786	6.2845	4.7693	6.5538	4.2684	5.0109	0.7508	5.1513
UDP	0.0014	0.0016	0.0013	0.0014	0.0012	0.0014	0.0031	0.0027	0.0032	0.0022	0.0034	0.0029	0.0001	52.4701
Uracil	0.0084	0.0093	0.0167	0.0104	0.0085	0.0107	0.0039	0.0047	0.0056	0.0051	0.0016	0.0042	0.0053	-154.2542
Uric Acid	1.3923	1.2231	1.3318	1.5332	1.6503	1.4261	1.0028	1.1466	1.2060	1.1850	1.2552	1.1591	0.0150	-23.0380
Uridine	0.0047	0.0042	0.0103	0.0062	0.0064	0.0064	0.0530	0.0852	0.0500	0.0934	0.0888	0.0741	0.0018	91.3971
Valine	2.9473	4.0522	3.0171	4.7696	3.5073	3.6587	4.2899	4.1512	2.6917	1.7230	4.6821	3.5076	0.8234	-4.3086
Xanthine	2.5528	2.1338	2.0789	2.3338	2.9197	2.4038	1.7658	2.0408	2.0385	1.3002	2.3415	1.8974	0.0612	-26.6928
Xanthosine	0.0144	0.0148	0.0175	0.0181	0.0198	0.0169	0.0181	0.0101	0.0097	0.0135	0.0190	0.0141	0.2325	-20.1782
Xanthosine 5 phosphate	0.0015	0.0033	0.0029	0.0028	0.0025	0.0026	0.0038	0.0036	0.0029	0.0042	0.0037	0.0036	0.0253	28.4061

Table 4: Lifespan analysis, p-values for statistical analysis were calculated using Mantel-Cox Log Rank test. Worms displaying internal hatching or burst vulva and escaped from the plate were censored.

Strain/Treatment	Mean lifespan	Mean % change	Max lifespan	Median	25th percentile	75th percentile	Sig	Ref Control	Conditions	Screen
ARD screens										
N2	21.93	-	35	21	19	23	-	-	AL + FUDR	1
R2	34.85	59	46	38	30	39	<0.0001	N2	AL + FUDR	1
R6	28.97	32	42	29	24	31	<0.0001	N2	AL + FUDR	1
R12	32.28	47	44	31	26	35	<0.0001	N2	AL + FUDR	1
R29	27.02	23	38	27	22	29	0.0001	N2	AL + FUDR	1
R35	31.82	45	60	34	22	39	<0.0001	N2	AL + FUDR	1
R37	27.52	25	41	27	22	29	<0.0001	N2	AL + FUDR	1
N2	21.78	-		20	19	22	-	-	AL + FUDR	1
R39	23.71	9	60	25	18	29	0.6169	N2	AL + FUDR	1
R43	25.52	17	34	27	21	27	0.0111	N2	AL + FUDR	1
R46	31.09	43	41	34	27	34	<0.0001	N2	AL + FUDR	1
R55	31.01	42	50	50	23	40	<0.0001	N2	AL + FUDR	1
R60	26.79	23	41	27	21	32	0.0281	N2	AL + FUDR	1
R62	24.26	11	34	27	21	27	0.5469	N2	AL + FUDR	1
daf-16(mgDf50)	10.33	-	21	12	12	16	-	-	AL + FUDR	2
S4	13.42	30	29	13	13	18	p = 0.000000	*daf-16(mgDf50)*	AL + FUDR	2
S22	13.38	30	28	13	13	18	p = 0.000000	*daf-16(mgDf50)*	AL + FUDR	2
S23	13.77	34	28	18	13	18	p = 0.000000	*daf-16(mgDf50)*	AL + FUDR	2
S24	12.63	22	30	13	13	18	p = 0.000000	*daf-16(mgDf50)*	AL + FUDR	2
S25	12.21	18	33	13	13	18	p = 0.000000	*daf-16(mgDf50)*	AL + FUDR	2
S26	13.67	32	33	18	13	18	p = 0.000000	*daf-16(mgDf50)*	AL + FUDR	2
S30	14.25	38	35	18	13	18	p = 0.000000	*daf-16(mgDf50)*	AL + FUDR	2
S32	12.30	19	31	13	13	18	p = 0.000000	*daf-16(mgDf50)*	AL + FUDR	2
S33	13.17	27	30	18	13	18	p = 0.000000	*daf-16(mgDf50)*	AL + FUDR	2
S47	14.27	38	30	18	13	18	p = 0.000000	*daf-16(mgDf50)*	AL + FUDR	2
S48	14.91	44	26	18	13	18	p = 0.000009	*daf-16(mgDf50)*	AL + FUDR	2
N2	17.74	-	38	23	23	23	-	-	AL + FUDR	3
D3	16.67	-6	38	23	23	23	p = 0.293720	N2	AL + FUDR	3
D20	18.1	2	38	23	23	30	p = 0.428384	N2	AL + FUDR	3
D22	17.06	-4	50	25	25	25	p = 0.379440	N2	AL + FUDR	3
D35	18.59	5	38	23	23	30	p = 0.000098	N2	AL + FUDR	3
D42	17.16	-3	44	23	23	23	p = 0.024437	N2	AL + FUDR	3
J9	15.82	-11	34	21	21	29	p = 0.078096	N2	AL + FUDR	3
J16	17.18	-3	47	20	20	29	p = 0.000001	N2	AL + FUDR	3
J32	18.17	2	40	21	21	34	p = 0.000001	N2	AL + FUDR	3
N2	20.42	-	34	23	18	29	-	-	AL + FUDR	4
M20	23.18	20	40	23	18	29	p = 0.000519	N2	AL + FUDR	4
N2	21.3	-	37	25	17	25	-	-	AL + FUDR	4
M40	24.98	30	40	25	20	30	p = 0.000011	N2	AL + FUDR	4
M154	24.88	29	44	25	25	30	p = 0.000021	N2	AL + FUDR	4
N2	19.65	-	33	23	19	23	-	-	AL + FUDR	4
M1	23.08	20	37	23	19	28	p = 0.000005	N2	AL + FUDR	4
M44	22.49	17	40	23	19	28	p = 0.000008	N2	AL + FUDR	4
M123	23.53	22	47	23	19	30	p = 0.000000	N2	AL + FUDR	4
N2	19.48	-	29	20	20	23	-	-	AL + FUDR	4
M26	20.07	4	35	20	16	26	p = 0.100813	N2	AL + FUDR	4
M41	22.27	16	40	23	20	28	p = 0.000000	N2	AL + FUDR	4
M58	20.54	7	35	35	16	26	p = 0.010375	N2	AL + FUDR	4
M99	19.7	2	36	20	16	26	p = 0.318822	N2	AL + FUDR	4
M116	20.44	6	30	23	16	26	p = 0.003225	N2	AL + FUDR	4
M132	21.87	13	35	23	20	26	p = 0.000019	N2	AL + FUDR	4
M153	20.29	5	33	20	20	26	p = 0.084267	N2	AL + FUDR	4

Strain/Treatment	Mean lifespan	Mean % change	Max lifespan	Median	25th percentile	75th percentile	Sig	Ref Control	Conditions	Screen
N2	19.36	-	43	18	11	27	-	-	AL	1
R2	21.79	13	53	19	18	29	p = 0.078346	N2	AL	1
R29	18.19	-6	34	18	11	27	p = 0.162582	N2	AL	1
R34	22.75	18	43	25	13	32	p = 0.003396	N2	AL	1
N2	23.24	-	45	24	18	28	-	-	AL	1
R2	25.04	8	45	24	17	34	p = 0.004233	N2	AL	1
R29	15.96	-31	36	14	7	24	p = 0.000000	N2	AL	1
R34	24.06	4	48	24	17	34	p = 0.068343	N2	AL	1
N2	17.66	-	33	16	14	23	-	-	AL	1
R2	23.17	31	51	21	14	33	p = 0.000019	N2	AL	1
R29	21.26	20	37	21	14	30	p = 0.032285	N2	AL	1
R34	22.73	29	47	26	14	30	p = 0.000001	N2	AL	1
daf-16(mgDf50)	12.97	-	40	12	9	14	-	-	AL	2
S50	17.2	33	34	19	12	23	p = 0.000002	*daf-16(mgDf50)*	AL	2
daf-16(mgDf50)	12.7	-	34	11	9	20	-	-	AL	2
S50	18.01	42	27	20	18	22	p = 0.018415	*daf-16(mgDf50)*	AL	2
daf-16(mgDf50)	13.35	-	29	12	10	19	-	-	AL	2
S50	19.02	42	29	21	16	24	p = 0.002639	*daf-16(mgDf50)*	AL	2
N2	20.5	-	33	26	24	29	-	-	AL	3
D3	23.15	13	36	26	21	29	p = 0.006553	N2	AL	3
J16	20.44	0	36	22	19	27	p = 0.018270	N2	AL	3
J32	24.74	21	42	29	19	31	p = 0.000001	N2	AL	3
N2	22.49	-	37	25	16	29	-	-	AL	3
D3	22.51	0	37	25	18	29	p = 0.633490	N2	AL	3
J16	23.47	4	45	28	16	31	p = 0.056197	N2	AL	3
J32	22.78	1	45	23	16	33	p = 0.135071	N2	AL	3
N2	20.52	-	38	22	13	29	-	-	AL	3
D3	24.57	20	44	27	20	31	p = 0.001814	N2	AL	3
J16	23.00	12	42	27	14	29	p = 0.009206	N2	AL	3
J32	23.18	13	42	27	13	34	p = 0.004914	N2	AL	3
N2	20.5	-	34	21	16	29	-	-	AL	
M154	24.4	19	42	29	19	31	p = 0.000000	N2	AL	4
N2	19.35	-	34	20	14	27	-	-	AL	
M154	25.49	32	48	29	14	36	p = 0.000001	N2	AL	4
N2	16.96	-	36	22	15	27	-	-	AL	
M154	18.55	9	46	22	15	27	p = 0.495153	N2	AL	4

Strain/Treatment	Mean lifespan	Mean % change	Max lifespan	Median	25th percentile	75th percentile	Sig	Ref Control	Conditions	Screen
Candidate RNAi										
N2 luci	21.25	-	31	22	15	26	-	-	AL	
N2 aakg-2i	18.05	-15	31	19	15	22	p = 0.000009	N2 luci	AL	1 (R29)
N2 T24H7.2i	21.76	2	37	22	19	29	p = 0.059222	N2 luci	AL	1 (R34)
N2 kcc-3i	20.17	-5	37	22	15	29	p = 0.366445	N2 luci	AL	1 (R2)
N2 rsr-2i	15.87	-25	32	15	15	19	p = 0.000000	N2 luci	AL	1 (R34)
N2 C27A12.9i	20.35	-4	37	22	15	26	p = 0.702041	N2 luci	AL	1 (R29)
N2 cdh-3i	19.22	-10	35	19	15	24	p = 0.097160	N2 luci	AL	1 (R34)
N2 egl-8i	21.54	1	31	24	19	26	p = 0.598904	N2 luci	AL	1 (R29)
N2 che-3i	23.67	11	35	26	19	29	p = 0.000108	N2 luci	AL	1 (R34)
N2 tbb-4i	16.26	-23	26	15	15	19	p = 0.000000	N2 luci	AL	3 (J32)
N2 emb-9i	18.86	-11	29	19	15	24	p = 0.031330	N2 luci	AL	1 (R29)
N2 luci	19.88	-	31	21	15	28	-	-	AL	
N2 fat-3i	18.98	-5	32	21	15	25	p = 0.479481	N2 luci	AL	1 (R2)
N2 sdc-2i	13.13	-34	21	15	11	15	p = 0.000000	N2 luci	AL	1 (R34)
N2 marc-6i	21.78	10	34	23	18	28	p = 0.077141	N2 luci	AL	2 (S50)
N2 Y8A9A.2i	19.52	-2	34	21	15	25	p = 0.740807	N2 luci	AL	1 (R34)
N2 C30A5.3i	19.77	-1	37	23	15	28	p = 0.082063	N2 luci	AL	1 (R2)
N2 cdc-25.4i	19.18	-4	34	21	15	25	p = 0.233707	N2 luci	AL	1 (R34)
N2 cogc-1i	12.45	-37	21	15	11	15	p = 0.000000	N2 luci	AL	1 (R29)
N2 unc-52i	13.38	-33	21	15	15	15	p = 0.000000	N2 luci	AL	1 (R34)
N2 png-1i	16.74	-16	30	18	15	21	p = 0.000013	N2 luci	AL	1 (R2)
N2 F13B12.2i	20.21	2	34	21	15	28	p = 0.524694	N2 luci	AL	1 (R2)
N2 F39C12.1i	20.39	3	34	21	15	25	p = 0.573232	N2 luci	AL	1 (R34)
N2 twk-31i	20.85	5	34	23	15	28	p = 0.203845	N2 luci	AL	1 (R29)
N2 luci	18.34	-	32	16	15	27	-	-	AL	
N2 elpc-2i	24.15	32	39	27	18	29	p = 0.000014	N2 luci	AL	3 (J32)
N2 B0495.5i	21.47	17	34	22	15	25	p = 0.980975	N2 luci	AL	1 (R2)
N2 epg-6i	19.67	7	36	25	15	27	p = 0.008417	N2 luci	AL	3 (J32)
N2 ogdh-1i	27.58	50	40	24	20	33	p = 0.768242	N2 luci	AL	4 (M154)
N2 ceh-20i	17.64	-4	27	18	15	25	p = 0.054632	N2 luci	AL	3 (J32)
N2 aars-2i	19.01	4	25	18	18	22	p = 0.015988	N2 luci	AL	1 (R2)
CRISPR candidates										
N2	15.92	-	28	19	13	26	-	-	AL	
marc-6 18.6	13.65	-14	28	21	13	26	p = 0.184155	N2	AL	
marc-6 32.1	15.10	-5	28	19	13	21	p = 0.021926	N2	AL	
N2	16.02	-	35	21	12	26	-	-	AL	
marc-6 18.6	18.33	14	35	23	19	26	p = 0.027903	N2	AL	
marc-6 32.1	18.14	13	33	21	14	26	p = 0.674688	N2	AL	
N2	16.69	-	36	22	15	27	-	-	AL	
marc-6 18.6	13.79	-17	34	20	15	27	p = 0.759238	N2	AL	
marc-6 32.1	15.2	-9	34	20	15	2	p = 0.057046	N2	AL	
daf-16(mgDf50)	11.04	-	22	13	8	16	-	-	AL	
marc-6;daf-16 18.6	10.08	-9	24	13	8	14	p = 0.951235	*daf-16*	AL	
marc-6;daf-16 32.1	14.66	33	26	14	15	22	p = 0.000000	*daf-16*	AL	
daf-16(mgDf50)	10.4	-	21	13	8	16	-	-	AL	
marc-6;daf-16 18.6	9.08	-13	23	13	8	14	p = 0.994711	*daf-16*	AL	
marc-6;daf-16 32.1	13.09	26	26	14	13	19	p = 0.003104	*daf-16*	AL	
daf-16(mgDf50)	11.16	-	26	12	10	17	-	-	AL	
marc-6;daf-16 18.6	11.41	2	26	12	10	17	p = 0.949690	*daf-16*	AL	
marc-6;daf-16 32.1	15.28	37	26	19	15	22	p = 0.000000	*daf-16*	AL	

Strain/Treatment	Mean lifespan	Mean % change	Max lifespan	Median	25th percentile	75th percentile	Sig	Ref Control	Conditions
N2	16.72	-	29	19	15	24	-	-	AL
ogdh-1	18.18	9	36	22	15	24	p = 0.174197	N2	AL
elpc-2 50.6A	15.16	-9	36	20	13	27	p = 0.053485	N2	AL
elpc-2 50.2 H	16.59	-1	36	22	15	27	p = 0.803594	N2	AL
png-1	14.7	-12	29	17	12	22	p = 0.074041	N2	AL
N2	16.96	-	36	22	15	27	-	-	AL
ogdh-1	16.63	-1	32	20	13	27	p = 0.010456	N2	AL
elpc-2 50.6A	14.99	-12	34	21	14	26	p = 0.063149	N2	AL
elpc-2 50.2 H	15.64	-8	35	22	14	27	p = 0.259761	N2	AL
png-1	15.98	-6	28	15	11	23	p = 0.061247		AL
N2	16.72	-	29	19	15	24	-	-	AL
ogdh-1	17.65	6	30	19	13	22	p = 0.133298	N2	AL
elpc-2 50.6A	13.45	-20	33	19	14	23	p = 0.006235	N2	AL
elpc-2 50.2 H	15.98	-4	31	20	13	24	p = 0.027968	N2	AL
png-1	15.21	-9	28	16	11	21	p = 0.071368	N2	AL
ARD CRISPR mutants									
N2	16.86	-	33	19	12	24	-	-	AL
alg-4(syb635)	17.21	2	36	19	15	24	p = 0.722714	N2	AL
xpb-1(sy682)	17.47	4	36	19	12	26	p = 0.604601	N2	AL
anoh-1(syb742)	17.87	6	36	22	15	26	p = 0.077211	N2	AL
upp-1(sy569)	18.33	9	36	22	15	26	p = 0.089568	N2	AL
ZC581.7(syb662)	18.68	11	33	22	15	29	p = 0.015618	N2	AL
piki-1(syb658)	17.92	6	36	22	15	24	p = 0.093066	N2	AL
prp-21(syb755)	17.76	5	38	22	15	24	p = 0.007501	N2	AL
vps-18(syb773)	17.45	3	31	22	15	24	p = 0.199332	N2	AL
Y55F3BR.1(syb657)	17.87	6	36	19	15	24	p = 0.024904	N2	AL
alg-1(syb656)	18.38	9	36	22	15	26	p = 0.002767	N2	AL
ptr-10(syb633)	16.47	-2	33	22	15	24	p = 0.059973	N2	AL
N2	16.39	-	33	22	12	24	-	-	AL
alg-4(syb635)	16.32	0	35	20	14	23	p = 0.879033	N2	AL
xpb-1(sy682)	17.98	10	35	20	12	26	p = 0.789872	N2	AL
anoh-1(syb742)	18.49	13	36	19	15	25	p = 0.078333	N2	AL
upp-1(sy569)	21.3	30	39	23	19	29	p = 0.000346	N2	AL
ZC581.7(syb662)	19.21	17	35	21	14	28	p = 0.021479	N2	AL
piki-1(syb658)	18.08	10	37	21	15	24	p = 0.081364	N2	AL
prp-21(syb755)	20.15	23	39	23	19	27	p = 0.006445	N2	AL
vps-18(syb773)	17.43	6	32	20	15	24	p = 0.231487	N2	AL
Y55F3BR.1(syb657)	18.12	11	36	21	15	25	p = 0.035478	N2	AL
alg-1(syb656)	18.99	16	35	22	14	26	p = 0.002987	N2	AL
ptr-10(syb633)	17.72	8	34	22	15	24	p = 0.060012	N2	AL

Strain/Treatment	Mean lifespan	Mean % change	Max lifespan	Median	Sig	Ref Control	Conditions
ARD CRISPR lifespans							
N2	50.93	-	76	49	-	-	ARD (starvation)
anoh-1(syb742)	50.913	0	76	49	p = 0.2852	N2	ARD (starvation)
F55F3BR.1(syb657)	54.36	7	73	52	p = 0.0061	N2	ARD (starvation)
prp-21(syb755)	54.43	7	99	49	p = 0.0189	N2	ARD (starvation)
upp-1(syb659)	57.027	12	115	51.5	p = 0.0009	N2	ARD (starvation)
N2	63.34	-	87	69	-	-	ARD (starvation)
anoh-1(syb742)	62.326	-2	85	62	p = 0.1368	N2	ARD (starvation)
F55F3BR.1(syb657)	59.71	-6	82	63	p = 0.00812	N2	ARD (starvation)
prp-21(syb755)	59.72	-6	90	55	p = 0.118	N2	ARD (starvation)
upp-1(syb659)	70.56	11	111	65	p = 0.0009	N2	ARD (starvation)
N2	55.32	-	82	56	-	-	ARD (starvation)
anoh-1(syb742)	56.14	1	81	50	p = 0.2450	N2	ARD (starvation)
F55F3BR.1(syb657)	56.9	1	77	49	p = 0.3611	N2	ARD (starvation)
prp-21(syb755)	58.14	2	94	50	p = 0.0923	N2	ARD (starvation)
upp-1(syb659)	64.32	11	113	53	p = 0.0008	N2	ARD (starvation)
N2	64.77	-	88	56	-	-	ARD (starvation)
upp-1(syb2043	74.37	15	112	72	p = <0.0001	N2	ARD (starvation)
N2	60.34	-	78	62	-	-	ARD (starvation)
upp-1(syb2043	70.65	17	115	69	p = <0.0001	N2	ARD (starvation)
N2	58.19	-	75	52	-	-	ARD (starvation)
upp-1(syb2043	69.32	19	109	65	p = <0.0001	N2	ARD (starvation)
Supplementation ARD lifespans							
N2	60.21	-	79	58	-	-	ARD (starvation)
N2 0.5mM Uridine	63.62	6	100	62	p = <0.0001	N2	ARD (starvation)
N2 1mM Uridine	62.96	5	86	63.5	p = 0.0001	N2	ARD (starvation)
N2 0.5mM Thymine	62.72	4	104	62	p = 0.0014	N2	ARD (starvation)
N2 1mM Thymine	66.96	11	117	69	p = <0.0001	N2	ARD (starvation)
upp-1 (syb659)	61.51	-	104	58	-	-	ARD (starvation)
upp-1 (syb659) 0.5mM Uridine	64.15	4	125	62	p = 0.0176	*upp-1(syb659)*	ARD (starvation)
upp-1(syb659) 1mM Uridine	63.6	3	121	62	p = 0.0921	*upp-1(syb659)*	ARD (starvation)
upp-1(syb659) 0.5mM Thymine	64.33	5	117	62	p = 0.0070	*upp-1(syb659)*	ARD (starvation)
upp-1(syb659) 1mM Thymine	63.94	4	107	62	p = 0.0308	*upp-1(syb659)*	ARD (starvation)
N2	60.56	-	81	59	-	-	ARD (starvation)
N2 0.5mM Uridine	62.14	3	98	62	p = <0.0001	N2	ARD (starvation)
N2 1mM Uridine	63.28	4	87	63	p = 0.0056	N2	ARD (starvation)
N2 0.5mM Thymine	63.97	6	108	62	p = 0.0007	N2	ARD (starvation)
N2 1mM Thymine	66.31	9	120	70	p = <0.0001	N2	ARD (starvation)
upp-1 (syb659)	62.48	-	116	60	-	-	ARD (starvation)
upp-1 (syb659) 0.5mM Uridine	65.47	5	124	63	p = 0.0313	*upp-1(syb659)*	ARD (starvation)
upp-1(syb659) 1mM Uridine	63.01	1	120	63	p = 0.099	*upp-1(syb659)*	ARD (starvation)
upp-1(syb659) 0.5mM Thymine	63.98	2	123	63	p = 0.0912	*upp-1(syb659)*	ARD (starvation)
upp-1(syb659) 1mM Thymine	64.85	4	110	63	p = 0.0146	*upp-1(syb659)*	ARD (starvation)

Strain/Treatment	Mean lifespan	Mean % change	Max lifespan	Median	Sig	Ref Control	Conditions
TGF-β and IIS ARD lifespans							
N2	58.46	-	82	49	-	-	ARD (starvation)
hlh-30(tm1978)	7.77	-	13	8	-	-	ARD (starvation)
daf-1(m40)	67.58	16	143	68	p = <0.0001	*N2*	ARD (starvation)
daf-1(m40);hlh-3-(tm1978)	29.87	284	53	30	p = <0.0001	*hlh-30(tm1978)*	ARD (starvation)
daf-2(e1368)	62.13	6	116	61	p = <0.0001	N2	ARD (starvation)
daf-2(e1368);hlh-30(tm1978)	27.55	255	40	27	p = <0.0001	*hlh-30(tm1978)*	ARD (starvation)
daf-7(e1372)	63.82	9	136	61	p = <0.0001	*N2*	ARD (starvation)
daf-7(e1372);hlh-30(tm1978)	23.02	196	34	22	p = <0.0001	*hlh-30(tm1978)*	ARD (starvation)
pdk-1(sa680)	60.32	3	110	58	p = 0.00036	*N2*	ARD (starvation)
pdk-1(sa680);hlh-30(tm1978)	31.35	303	48	32	p = <0.0001	*hlh-30(tm1978)*	ARD (starvation)
N2	55.36	-	76	49	-	-	ARD (starvation)
hlh-30(tm1978)	5.18	-	10	6	-	-	ARD (starvation)
daf-1(m40)	60.23	9	130	59	p = <0.0001	*N2*	ARD (starvation)
daf-1(m40);hlh-3-(tm1978)	24.08	365	38	24	p = <0.0001	*hlh-30(tm1978)*	ARD (starvation)
daf-2(e1368)	68.43	24	124	68	p = <0.0001	N2	ARD (starvation)
daf-2(e1368);hlh-30(tm1978)	8.94	73	12	8	p = <0.0001	*hlh-30(tm1978)*	ARD (starvation)
daf-7(e1372)	64.12	16	128	60	p = <0.0001	*N2*	ARD (starvation)
daf-7(e1372);hlh-30(tm1978)	18.43	256	22	20	p = <0.0001	*hlh-30(tm1978)*	ARD (starvation)
pdk-1(sa680)	58.36	5	104	54	p = 0.00187	*N2*	ARD (starvation)
pdk-1(sa680);hlh-30(tm1978)	23.11	346	43	27	p = <0.0001	*hlh-30(tm1978)*	ARD (starvation)
N2	58.14	-	81	50	-	-	ARD (starvation)
hlh-30(tm1978)	5.75	-	10	6	-	-	ARD (starvation)
daf-1(m40)	63.08	8	134	64	p = <0.0001	*N2*	ARD (starvation)
daf-1(m40);hlh-3-(tm1978)	19.35	237	32	18	p = <0.0001	*hlh-30(tm1978)*	ARD (starvation)
daf-2(e1368)	70.53	21	131	70	p = <0.0001	N2	ARD (starvation)
daf-2(e1368);hlh-30(tm1978)	9.81	71	16	10	p = <0.0001	*hlh-30(tm1978)*	ARD (starvation)
daf-7(e1372)	62.73	8	127	59	p = <0.0001	*N2*	ARD (starvation)
daf-7(e1372);hlh-30(tm1978)	18.18	216	26	20	p = <0.0001	*hlh-30(tm1978)*	ARD (starvation)
pdk-1(sa680)	62.78	8	111	55	p = 0.00053	*N2*	ARD (starvation)
pdk-1(sa680);hlh-30(tm1978)	19.18	234	38	20	p = <0.0001	*hlh-30(tm1978)*	ARD (starvation)
Triple mutant lifespans							
N2	59.04	-	78	43	-	-	ARD (starvation)
hlh-30(tm1978)	5.82	-	8	6	-	-	ARD (starvation)
daf-1(m40)	68.32	16	139	61	p = <0.0001	N2	ARD (starvation)
daf-3(e1376)	49.05	-17	53	51	p = 0.88414	N2	ARD (starvation)
daf-5(e1386)	58.42	-1	78	45	p = 0.3642	N2	ARD (starvation)
daf-16(mgDf50)	25.87	-56	42	31	p = <0.0001	N2	ARD (starvation)
daf-1(m40);hlh-30(tm1978)	25.19	333	40	28	p = <0.0001	*hlh-30(tm1978)*	ARD (starvation)
daf-3(e1376);daf-5(e1386)	70.12	19	99	58	p = <0.0001	N2	ARD (starvation)
daf-1(m40);hlh-30(tm1978); daf-3(e1376)	6.06	4	10	6	p = >0.9999	*hlh-30(tm1978)*	ARD (starvation)
daf-1(m40);hlh-30(tm1978); daf-5(e1386)	5.87	1	9	6	p = >0.9999	*hlh-30(tm1978)*	ARD (starvation)
daf-1(m40);hlh-30(tm1978); daf-16(mgDf50)	8.65	49	10	8	p = <0.0001	*hlh-30(tm1978)*	ARD (starvation)
N2	57.8	-	88	56	-	-	ARD (starvation)
hlh-30(tm1978)	6.08	-	10	6	-	-	ARD (starvation)
daf-1(m40)	64.01	11	135	57	p = <0.0001	N2	ARD (starvation)
daf-3(e1376)	55.07	-5	75	60	p = 0.6085	N2	ARD (starvation)
daf-5(e1386)	61.61	7	81	49	p = 0.29864	N2	ARD (starvation)
daf-16(mgDf50)	21.49	-63	40	30	p = <0.0001	N2	ARD (starvation)
daf-3(e1376);daf-5(e1386)	68.23	18	90	52	p = <0.0001	N2	ARD (starvation)
daf-1(m40);hlh-30(tm1978)	23.78	291	36	27	p = <0.0001	*hlh-30(tm1978)*	ARD (starvation)
daf-1(m40);hlh-30(tm1978); daf-3(e1376)	5.90	-3	9	6	p = >0.9999	*hlh-30(tm1978)*	ARD (starvation)
daf-1(m40);hlh-30(tm1978); daf-5(e1386)	5.81	-4	6	6	p = >0.9999	*hlh-30(tm1978)*	ARD (starvation)
daf-1(m40);hlh-30(tm1978); daf-16(mgDf50)	7.32	20	10	8	p = >0.9999	*hlh-30(tm1978)*	ARD (starvation)

12 ACKNOWLEDGEMENTS

I would like to express my deepest gratitude to Prof. Adam Antebi for allowing me the opportunity to perform my doctoral research in his laboratory. Your guidance, patience and endless passion for science is incredibly motivating and inspiring, which always encouraged me to be a better scientist. Additionally, I would like to thank Prof Thorsten Hoppe and Prof Jan Riemer for agreeing to evaluate my thesis and participate in my defence.

I would also like to extend my gratefulness to Dr Birgit Gerisch for being my supervisor. I am extremely appreciative for your support throughout this project and suggestions for my thesis. I will always value your enthusiasm for science, willingness to help and I will never forget your patience during this project. I also want to thank Dr Wenming Huang for his knowledge and input for this project and Dr Orsoyla Symmons for her support and encouragement.

Of course, I want to thank the entire A-team and the Denzel lab for being such great lab members and providing supportive input to my project during lab meetings and PhD meeting. I feel very blessed to work in an incredibly friendly and sociable environment, where every lab member is willing to help in times of need. I personally want to thank Dr Rebecca Tharyan, Dr Isabelle Schiffer, Dr Andrea Annibal, Dr Tilly van Oepen-Popkes, Dr Gabriel Gurrero and Raymond Laboy for becoming such great friends and making me laugh when times were tough. Completing a PhD project is a tough challenge and I wouldn't have got through it without your support.

I want to thank my incredibly family for their love and encouragement thought my PhD especially my parents for sending me care food packages of all the things I missed from home and my wonderful school friends (Magic 9) for their craziness, you girls are so inspiring and I feel so blessed you're in my life.

Last but not least, a special thanks to Marc Franzke for being there during the frustrating times in the lab and taking me climbing; and my best friend Louise Palmer. You have continuously been there for me and I couldn't imagine a world without you.

13 WORK CONTRIBUTION

All the experiments described in this thesis were performed by myself, with the exception of ARD lifespans and ARD recovery experiments, which were performed with the help of Dr Birgit Gerisch. Additionally, I had assistance from summer interns Dylan Aidlen and Logan Rance in performing the second *hlh-30* suppressor screen. RNA seq analysis was performed at Max-Plank Genomic Center, Koeln. Transcriptomic data wad performed by Dr. Jorge Bouças and Dr Franziske Metge at the bioinformatics core facility at Max-Plank for Biology of ageing.

14 ERKLÄRUNG ZUR DISSERTATION

gemäß der Promotionsordnung vom 12. März 2020

Diese Erklärung muss in der Dissertation enthalten sein.
(This version must be included in the doctoral thesis)

„Hiermit versichere ich an Eides statt, dass ich die vorliegende Dissertation selbstständig und ohne die Benutzung anderer als der angegebenen Hilfsmittel und Literatur angefertigt habe. Alle Stellen, die wörtlich oder sinngemäß aus veröffentlichten und nicht veröffentlichten Werken dem Wortlaut oder dem Sinn nach entnommen wurden, sind als solche kenntlich gemacht. Ich versichere an Eides statt, dass diese Dissertation noch keiner anderen Fakultät oder Universität zur Prüfung vorgelegen hat; dass sie - abgesehen von unten angegebenen Teilpublikationen und eingebundenen Artikeln und Manuskripten - noch nicht veröffentlicht worden ist sowie, dass ich eine Veröffentlichung der Dissertation vor Abschluss der Promotion nicht ohne Genehmigung des Promotionsausschusses vornehmen werde. Die Bestimmungen dieser Ordnung sind mir bekannt. Darüber hinaus erkläre ich hiermit, dass ich die Ordnung zur Sicherung guter wissenschaftlicher Praxis und zum Umgang mit wissenschaftlichem Fehlverhalten der Universität zu Köln gelesen und sie bei der Durchführung der Dissertation zugrundeliegenden Arbeiten und der schriftlich verfassten Dissertation beachtet habe und verpflichte mich hiermit, die dort genannten Vorgaben bei allen wissenschaftlichen Tätigkeiten zu beachten und umzusetzen. Ich versichere, dass die eingereichte elektronische Fassung der eingereichten Druckfassung vollständig entspricht."

Teilpublikationen:

September 2020, Koeln, JENNIFER MAK

15 CURRICULUM VITAE

MISS JENNIFER MAK
Vogelsanger Str 298, Cologne, 50825, Germany
Mob: +4917681467717
E-mail: jennifer.mak@age.mpg.de

PERSONAL PROFILE

- Bachelors degree from the University of Liverpool in Pharmacology.
- Masters from Aston University in pharmacology
- Volunteered in the neurophysiology research laboratory at the University of Birmingham.
- Worked as an honorary intern worker for the West Midlands Regional Genetics Laboratory.
- MRes Biomedical Science and Translational Medicine course at the University of Liverpool.
- PhD student at the Max Planck Institute for the Biology of Ageing.

EDUCATION & QUALIFICATIONS

Nov 2014 – Nov 2020	**Max Planck Institute for the Biology of Ageing** PhD Molecular Genetics of Ageing
Sept 2013 – Sept 2015	**University of Liverpool** Mres Biomedical Science and Translational Medicine (Distinction)
Sept 2009 – Sept 2010	**Aston University** MSc Pharmacology (Merit)
Sept 2006 –July 2009	**University of Liverpool** BSc (Hons) Pharmacology (2.2)
Sept 1999 – July 2006	**Sutton Coldfield Grammar School for Girls** A level Biology (C), Chemistry (C), Maths (C)

RESEARCH EXPERIENCE AND SKILLS

Max Planck Institute for the Biology of Ageing – PhD Molecular Genetics of Ageing

- Direct genetic screen for novel regulators of lifespan regulation of adult reproductive diapause (ARD) in *C. elegans* longevity supervised by Prof. Dr. Adam Antebi.
- Gained analytical skills using Galaxy to analyse sequencing data.

University of Liverpool – Mres Biomedical Science and Translational Medicine

- This project aimed to evaluate the CRISPR-CAS9 system for editing the genome of *C.elegans*. *unc-18* and *dnj-14* genes were targeted using CRISPR.
- Gained skills in molecular biology procedures including site directed mutagenesis, Gibson assembly and restriction digests. Also gained experience in gel electrophoresis, PCR, the maintenance of *C. elegans*, behavioural assays for *C.*

elegans, western blot, gel extraction and purification and mini preparation of plasmid DNA.

University of Birmingham – Volunteer Research Assistant

- This pilot study investigated the effect of ketamine on kainic acid and carbachol induced gamma oscillations in methlyazomethanol acetate (MAM) treated rats

Aston University – MSc Pharmacology

- This project aimed to investigate the effects of dopamine agonists and antagonists on kainic acid induced gamma oscillations in the entorhinal cortex of the rat brain.
- Gained experience in setting up holding chamber and recording chambers for entorhinal cortex/hippocampal slices as well as maintaining the flow of artificial cerebral spinal fluid through the recording chamber to allow preservation of the slice. Pulled and applied electrode to specific areas to measure gamma activity.

University of Liverpool – BSc Pharmacology

- Investigating the inhibition of protein tyrosine phosphatases (PTP) in immune cell function.
- Gained experience in the generation of bone marrow derived dendritic cells, DC proliferation, T-cell proliferation and MHC II/CD40 expression. These involved extracting bone marrow and spleen from a mice model, counting and culturing cells in a 96 well U-bottomed plate, harvesting cell onto filter mats using the cell harvester, using a scintillation counter to observe proliferation and using a flow cytometer to measure MHC II/CD40 expression

OTHER SKILLS

- Strong communication/ presentation skills: Presented data clearly and confidently in powerpoint and poster presentations to small and large groups.
- Interpersonal skills: Collaborated with other scientists, outlining methods and conclusions on different projects.
- Time management and organisational skills: managed several projects in parallel, planned the work to achieve goals and targets on time.
- IT: extensive knowledge of Microsoft office, Abode Illustrator, Photoshop and Prism.
- Efficient, organised, reliable, fast leaner and highly motivated.

EMPLOYMENT HISTORY

July 2012 – Sept 2014	**The Greenhouse** Front of house staff
Oct 2012 – Feb 2013	**West Midlands Regional Genetics Laboratory** Honorary Intern Worker
July 2012 – Sept 2012	**University of Birmingham** Volunteer Research Assistant
Dec 2011 – Apr 2012	**Mountain Heaven** Ski/Chalet Host